Sedimentological facies analyses of Clinothem 8C (Eocene), Battfjellet Formation, Brogniartfjella, Svalbard

Karoline Thu Skjærpe

Thesis for the degree of Master of Science

In Sedimentology / Petroleum Geology

November 2017

Department of Earth Science
University of Bergen

Abstract

The Eocene Battfjellet Formation in Van Keulenfjorden, Spitsbergen, Svalbard, has been investigated on the basis of a logged section at eastern Brogniartfjella. A comprehensive study of clinothem 8C, with focus on facies distribution, sandbody geometry and masterbedding architecture has been fulfilled. The sedimentary structures revealed influence from unidirectional and bidirectional currents. The studied clinothem 8C demonstrate a clear dichotomy both in internal structures and the external architecture. The proximal part of the unit presents progradational delta front lobe deposits deposited at the shelf, which display a high degree of wave reworking, characterised by an external tabular architecture. The succession can be laterally traced into the downslope subaqueous channel infill deposits, dominating the shelf-edge- to upper slope segment of the studied succession. The abundance of multiple local erosional surfaces, the dominance of current generated structures as well as the widespread distribution of soft-sediment deformed units imply deposition in a dynamic environment, supplied with sediments from the rising hinterland. Rip-up mud conglomerates, coal fragments, coal conglomerates (coffee ground) and the low degree of bioturbation substantiates this notion.

The clinoforms at the Brogniartfjella corresponds to an overall falling shelf-edge trajectory. The evolution of clinothem 8C can be explained by deposition of a prograding wave dominated delta front during high relative sea-level, followed by relative sea level fall succeeded by multiple erosional subaqueous channelized units, presenting turbiditic and hyperpycnal erosion and deposition. The clinothem is bounded by marine deposits of the transgressive system tract. The combination of highstand, forced regression, lowstand wedge and transgressive system tracts summarize the studied clinothem. The study confirms the general notion of a foreland basin dominated by high supply of sediments. The tectonically active hinterland provided high sedimentation rates, whereas the narrow shelf in concert with a warm climate represent ideal conditions for establishment of shelf-edge deltas, slope wedges and associated deep water deposition. The succession represents deposition during an overall regression, which resulted in the final infill of the Central Basin.

The study has improved the general understanding of the origin and development of shelf-edge clinoforms, and bears important information about the shelf-edge to- slope system which represents a key element in the understanding shallow to deep marine reservoirs.

Acknowledgments

This thesis was conducted at the Department of Earth Science at the University of Bergen during 2016-2017.

First, I would like to thank my supervisor, prof. William Helland-Hansen (UiB, Department of Earth Science) for providing me with an interesting and challenging project. Your guidance during the fieldwork and constructive feedback have been appreciated. I would also like to thank my co-supervisor Sten-Andreas Grundvåg (UiT, Department of Earth Science) for guidance and valuable discussions during the fieldwork. Dirk Knaust (Statoil ASA) are thanked for helpful guidance, recognition and interpretation of trace fossils during the 2017 field season.

Further on I want to thank the Research Council of Norway, whom generously funded parts of this research which was conducted in relation to the ARCEx project.

Additionally, I would like to thank the logistics department at UNIS for practiscalities and for providing all necessary equipment during the field seasons. Thanks to Ingvild Prestegård, Øystein Grasdal and Ranveig Halseth for being an excellent team during the 2016 field season.

Kristine Alvestad, Louise Poole, Marthe Førland, Tone Hetland Hansen, Kay Sørbø and Håvard Hallås Stubseid are thanked for proofreading the thesis and for constructive feedback. Many thanks to Ole Marius Solvang and Iselin Tjensvold for valuable discussions and brilliant company. Special thanks to Theodor Lien for support and for your willingness to always help. Last, but not least, I would like to thank my classmates for a memorable time at UiB.

Karoline Thu Skjærpe

Bergen, 20.11.2017

Table of Contents

1 Introduction

1.1 Aims and objectives

For many years, the remarkably well exposed clinothems within the Battfjellet Formation have been a popular location for geological fieldtrips and industry excursions. The clinothems are of Eocene age and exposed at mountainsides among others on the northern side of Van Keulenfjorden and in Reindalen at Spitsbergen, Svalbard. The Central Basin (CB) (Figure 1.1) is one of few basins in the world with nicely preserved seismic scale shelf-edge-to-slope systems (Kellogg, 1975; Helland-Hansen, 1992; Plink-Björklund, 2005). Despite the many published articles from these exposures (e.g., Helland-Hansen, 1990; Steel et al., 2000; Mellere et al., 2002; Mellere et al., 2003; Johannessen and Steel, 2005; Plink-Björklund and Steel, 2005; Uroza and Steel, 2008; Helland-Hansen, 2009; Pontén and Plink-Björklund, 2009), some units within the succession are still not well understood. Clinothem 8C is one of them, exposed at the Brogniartfjella (Figure 1.2). This thesis aims to document and improve the understanding of clinothem 8C. This was mainly achieved by sedimentological field work comprehended and literature research. The specific objectives of this thesis are:

1. Establish a facies framework for clinothem 8C.
2. Study the sandbody geometry and the masterbedding architecture of clinothem 8C to distinguish the different architectural elements.
3. Reconstruct the palaeogeography and develop a depositional model for clinothem 8C.

1.2 Previous work

The well preserved geological record together with the well-exposed outcrops has drawn geologists to Svalbard for many years. Svalbard represents a unique onshore analogue for the sedimentary rocks found in the subsurface of the Barents Sea Shelf.

The cliff-forming Battfjellet Formation is easy to recognize and distinguish from the underlying offshore mudstone of the Frysjaodden Formation, as well as from the overlying terrestrial shales and sandstones of the Aspelintoppen Formation (Figure 1.2). The formation

was first described in the early part of the 20th century by Nathorst (1910); Ljutkevic (1937); and Orvin (1940). This is the earliest geological work on the Cenozoic succession on Spitsbergen, which includes the establishment of the Battfjellet Formation as a recognizable stratigraphic unit. The name Battfjellet Formation was first used by Major and Nagy (1964). The name originates from the mountain Battfjellet located northwest of Sveagruva in the central parts of Nordenskiöld Land. Most of the early geological fieldwork and mapping was carried out with the aim of finding minerals and coal; therefore few studies were carried out in the Battfjellet Formation.

The Battfjellet Formation has later been included in regional stratigraphic and structural works of the Central Spitsbergen (e.g., Major and Nagy, 1964; Major and Nagy, 1972; Kellogg, 1975; Dalland, 1976; Steel, 1977). During the last decades the Central Basin including the Battfjellet Formation has been illuminated in many sedimentological studies, with the development of clinoforms and the associated basin-floor fans as one of the focus areas. Helland-Hansen (1985) performed a comprehensive investigation in Nordenskiöld Land, were the palaeoenvironmental and palaeogeographic framework of the formation was established. The development of clinoforms, their position relative to the shelf-edge and their possibility of being a bypass zone have been the main topics in several papers (Steel, 1977; Steel and Olsen, 2002; Mellere et al., 2003; Crabaugh and Steel, 2004; Plink-Björklund and Steel, 2004; Johannessen and Steel, 2005; Clark and Steel, 2006; Petter and Steel, 2006; Uroza and Steel, 2008).

Due to the well-exposed outcrops along the Van Keulenfjorden transect, the area is perfect to study the transportation of sediment from shallow to deep marine environments. The outcrops are of seismic scale, and it is accordingly of interest as an analogue to use in the petroleum industry. Many articles have been written from the area, focusing on aspects like sequence stratigraphy, shoreline trajectories and parasequence stacking patterns (Helland-Hansen, 1990, 1992; Mellere et al., 2002; Mellere et al., 2003; Plink-Björklund and Steel, 2004; Johannessen and Steel, 2005; Plink-Björklund and Steel, 2005; Helland-Hansen, 2009; Grundvåg et al., 2014a).

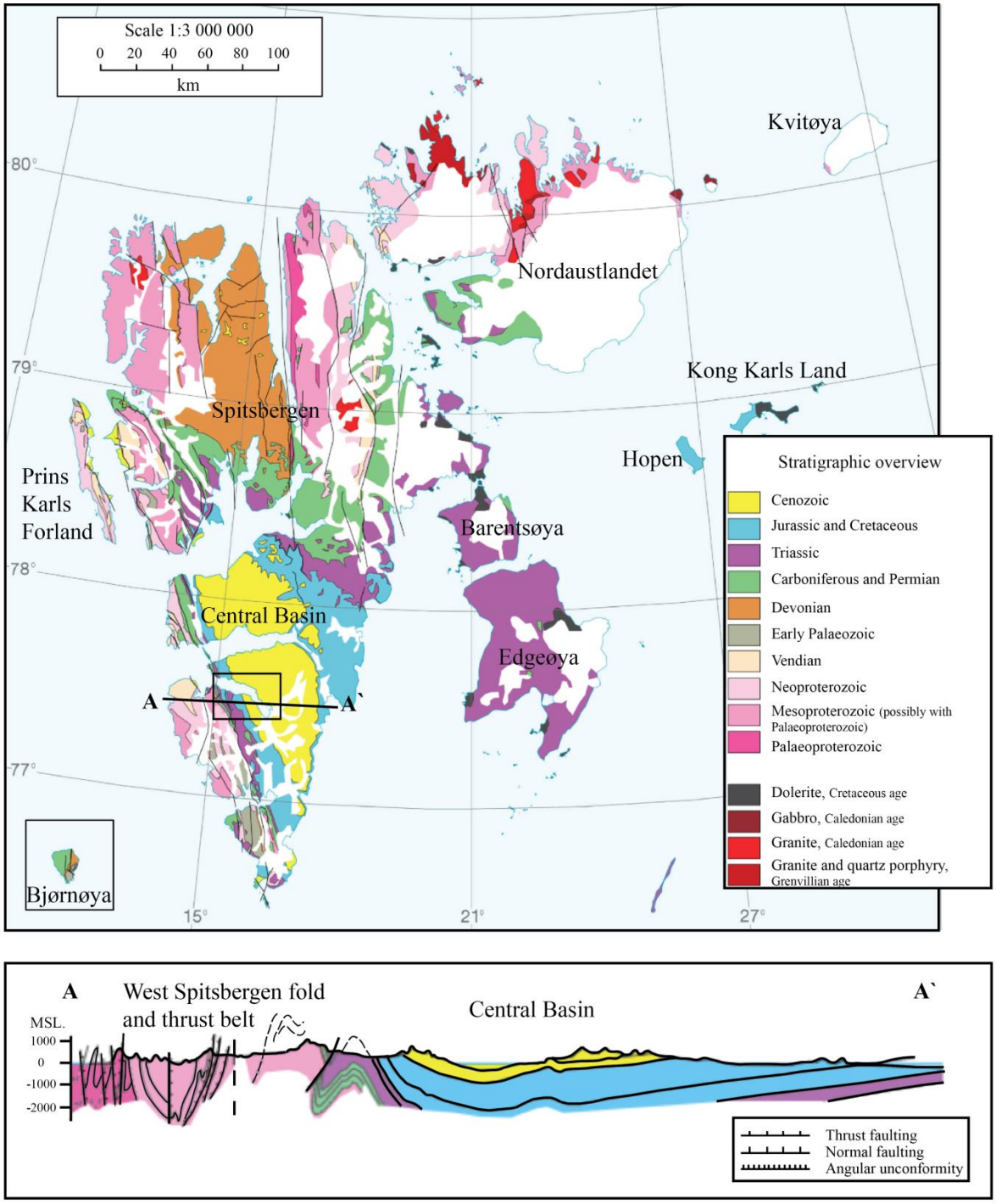

Figure 1.1 Geological map of Svalbard. The black rectangle marks up the study area. Profile A-A` presents the section from Dunderbukta to Kvalvågen, slightly modified from (Dallmann, 1999).

1.3 Study area

Spitsbergen is the largest island of the archipelago of Svalbard, located in the north-western part of the Barents Sea (Figure 1.1). The sediments in the Central Basin cover the central and southern parts of the island (Figure 1.1). The study area is located in the south-western part of

the basin, on the northern side of Van Keulenfjorden. The outcrops were reached by tracking from the field camp in Davisdalen, located 5km west of the study area (Figure 1.2).

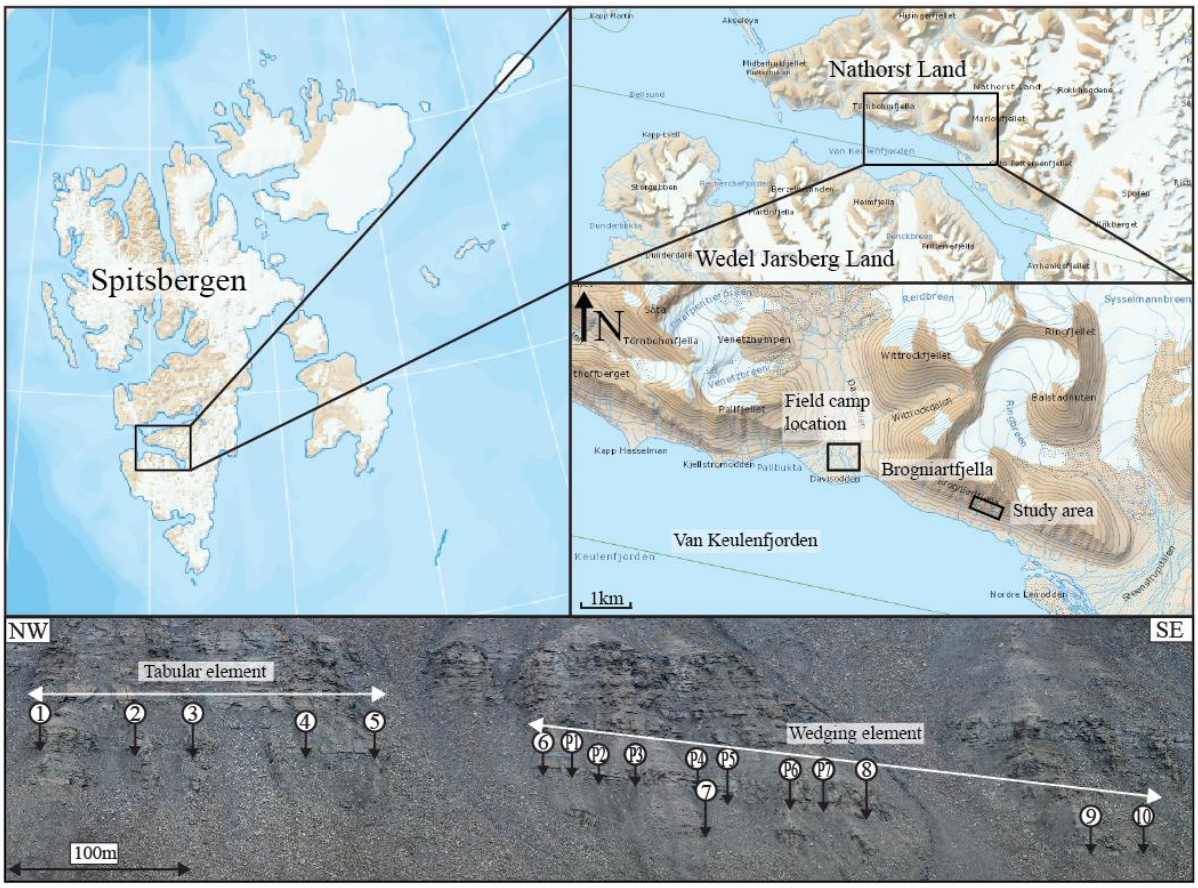

Figure 1.2: Overview maps of the study area and photo of the logged section. The logs are indicated by numbers and black vertical arrows. The white arrows mark up the two comprising elements of studied clinothem 8C. The cliff-forming units distinguish Battfjellet Formation from the underlying mudstones of Frysjaodden Formation and the overlying terrestrial shales and sandstones of Aspelintoppen Formation. (Map: Norsk Polarinstitutt, photo taken by Øystein Grasdal.)

1.4 Terminology and background theory

Clinothem 8C is one of approximately twenty clinothems exposed within the Battfjellet Formation along the Van Keulenfjorden transect (Steel and Olsen, 2002) (Figure 1.3). Clinothem 8 constitutes parasequences 8A, 8B and 8C. The studied succession of parasequence 8C can be separated into two different elements based on the external sandbody geometry. Clinothem 8C is characterized by a tabular package in its proximal part which develops into a sloping or wedging element in the distal part (Figure 1.2).

Each clinothem is estimated to have been deposited during a time interval of approximately 100ky (4^{th}-order sequences) (Steel and Olsen, 2002; Petter and Steel, 2006). Rich (1951) first used the term clinoform to address the sloping part of a depositional surface. However, the

term has lately been used by scientists in a broader sense, as a description for the entire sigmoidal surface from the shallow dipping topsets to the bottomsets (Steel and Olsen, 2002) (Figure 1.3). Based on this terminology, a clinoform presents the morphological profile from the shelf to the slope and into the basin-floor. A clinothem is the accompanying rock unit bounded by the clinoforms (Helland-Hansen, 1992; Johannessen and Steel, 2005).

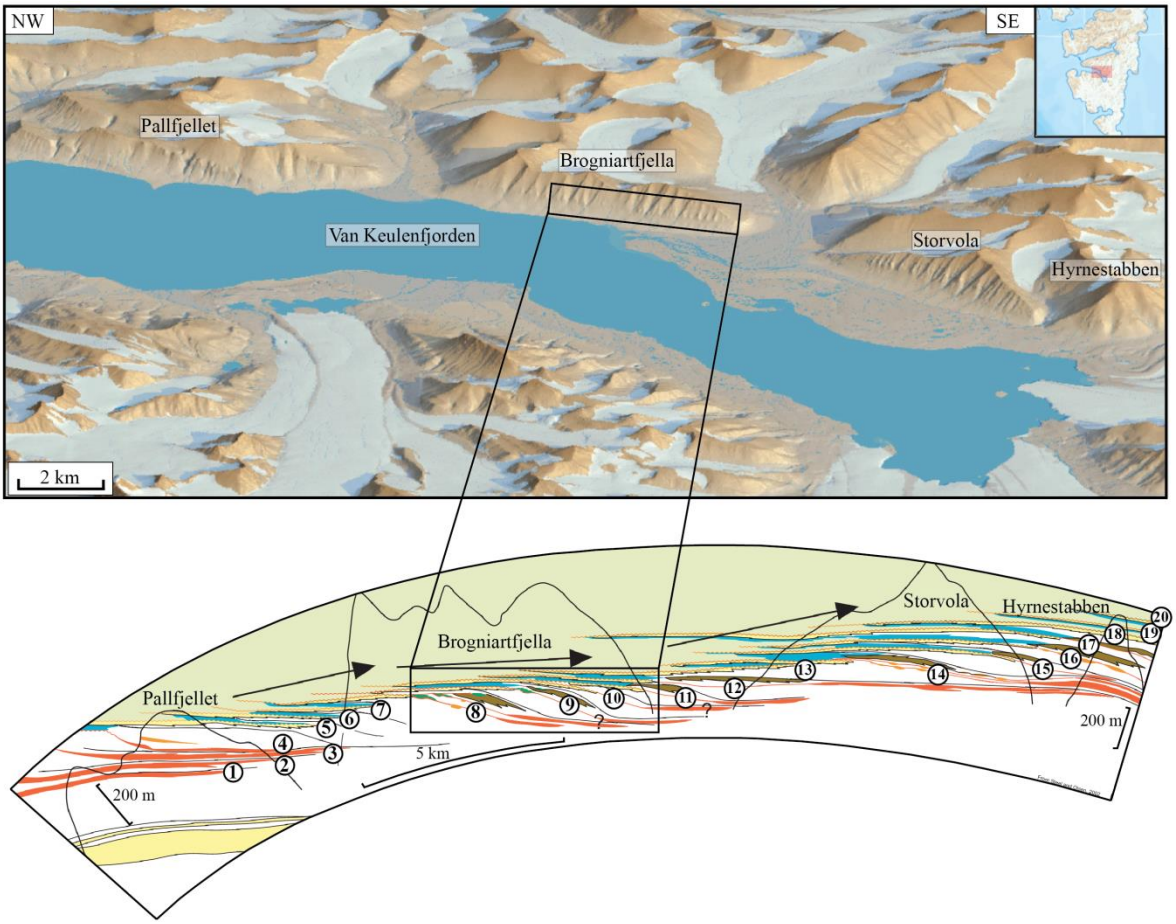

Figure 1.3: Simple 3D map from the northern side of Van Keulenfjorden, from Norsk Polarinstitutt. Below is a flattened transect of the Van Keulenfjorden section (after Steel and Olsen (2002)) with outcropping 4th-order clinothems at Pallfjellet, Brogniartfjella, Storvola and Hyrnestabben. The Brogniartfjella with the studied clinothem 8C is in the middle of the transect. The black arrows indicate the overall shelf-edge trajectory. Green=coastal plain, yellow/blue = shelf, brown/white = slope, white/red = basin-floor.

The terms shelf and slope have been used to refer to the topsets and foresets of the basin-margin clinoforms along the section. The terms are therefore not restricted to clinoforms along passive continental margins, which commonly are an order of magnitude larger than the foreland basin clinoforms (Swift and Thorne, 1991). In this study, the terms are justified by the relief of the facing slope (>100m) (cf. Porebski and Steel, 2006; Helland-Hansen, 2009). Furthermore, the issue of scale is also important to illuminate to avoid confusion with the deltaic clinoforms, which are an order of magnitude smaller in height than the studied clinoforms (Porębski and Steel, 2003) (Figure 1.4).

The sediments at Brogniartfjella were scoured from the fold-and-thrust belt, located west of the basin (Plink-Björklund, 2005) (Figure 1.1). The clinoforms reflect an overall progradation from west to east of a shelf-edge-to-slope system (Steel et al., 1985; Helland-Hansen, 1990), and are interpreted to represent an ancient wave dominated and fluvial influenced deltaic system (Helland-Hansen, 1990). The clinothems within Battfjellet Formation have an easterly dip and wedge out in the shales of Frysjaodden Formation in a basinward direction (Helland-Hansen, 1992). In the text, the northwest (hinterland) is referred to as landward, and the south-eastern direction is referred to as basinward. The clinoforms along the Van Keulenfjorden transect are several hundred meters in height and are characterized to be sigmoidal to concave-up in profile; connecting the shelf and slope with the basin-floor (Figure 1.4).

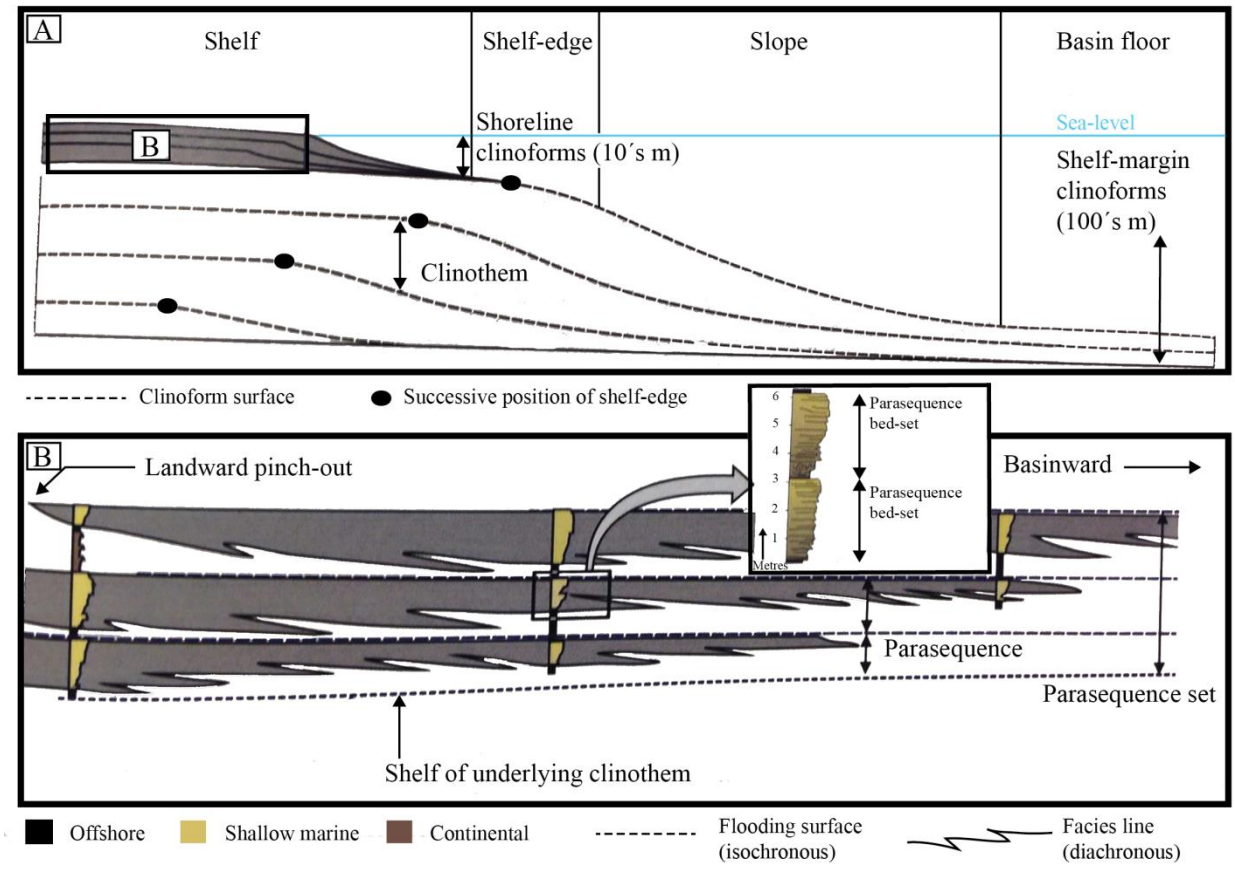

Figure 1.4: Schematic cartoons illustrating the different terminology used in this thesis. **A:** All sediment bodies which are prograding into a standing body of water will produce clinoforms. The scale of the clinoforms varies from 10`s meters to 1000`s meters in height. The clinoforms along the Van Keulenfjorden transect are 100`s of metre in scale. Therefore, shelf-margin clinoforms are the main focus of this thesis. **B:** Schematic diagram illustrating the following terms; a parasequence, a parasequence bedset and a parasequence set as used in the main text in this study. Cartoons slightly modified from (Grundvåg, 2012).

The increasing interest in studying shelf-edge deltas is primary because; (1) they are located at the boundary between major facies at shelf-edges (and basins with other types of margins) (Porębski and Steel, 2003); (2) they may potentially both store sediments and bypass sand onto the basin-floor (e.g., Curray and Moore, 1964; Winker and Edwards, 1983; Suter and Berryhill, 1985; Mayall et al., 1992; Sydow and Roberts, 1994; Morton and Suter, 1996); (3) they normally display great hydrocarbon reservoir potential (cf. Mayall et al., 1992; Hart et al., 1997; Skorstad et al., 2008).

The driving mechanism for the deltas to reach the shelf-edge along the Van Keulenfjorden transect has been discussed in several studies (e.g., Porebski and Steel, 2006; Carvajal and Steel, 2009; Sømme et al., 2009a; Henriksen et al., 2010; Grundvåg et al., 2014a). A progradational to aggradational deltaic system is driven by high rates of sediment supply in combination with the available accommodation space, the latter being controlled by sea level variations and shelf-width (e.g., a narrow shelf may force a delta to prograde to the shelf-edge).

Shelf and slope sediments are studied in this thesis. The studied succession can be classified as an infill of a foreland basin (e.g., Steel et al., 1985; Helland-Hansen, 1990; Müller and Spielhagen, 1990; Bruhn and Steel, 2003). The infill succession comprises a 2500m thick regressive megasequence ranging from offshore and slope shales to continental deposits (Helland-Hansen et al., 2012). The shelf can be classified as a sedimentary shelf formed by sedimentary nucleation and basinward propagation of the break in slope from the shoreline or subaqueous delta slopes (Mortimer et al., 2005) to full-scale deep water slopes (Helland-Hansen et al., 2012). Sediments are supplied in sufficient amounts to prograde the margin which episodically leads to shelf-edge collapse and oversteepening of the slope (Helland-Hansen et al., 2012). The shelf-edge trajectory is a function of bathymetry, sediment supply, eustatic sea-level changes and subsidence, including subsidence from compaction and loading (Helland-Hansen and Martinsen, 1996; Kim et al., 2006).

2 Methods

2.1 Field work

The present study is based on the observations and interpretations obtained from sedimentological investigation of clinothem 8C at Brogniartfjella (Figure 1.2). The data were predominantly collected by logging with emphasis on observable features such as grain size, sedimentary structures, boundaries, geometry, thickness, textures, color, bioturbation and mineralogy. The large-scale geometry of the studied section was documented by observations and photographs captured from a ship. A 25-meter-long "selfie stick" and associated camera lens were used to document the inaccessible parts of the unit. By usage of the "selfie stick" and camera lens, continuous shooting was performed from the top to the base of the units at selected positions. Other necessary equipment used to obtain the results in the field were grain size identification sheet, shovel, GPS, hand lens, hammer and yardstick. A geological compass was used to measure palaeocurrents. A dish brush was necessary to "clean" the exposure to bring out the sedimentary structures. The location of the logs along the clinothem was carefully picked based on the vertical extent and accessibility.

Some units were covered by debris. Consequently, these beds were therefore traced laterally to complement the logs. The logs presented in this study are in a 1:50 scale. A ship was used for transportation to get to the study area during both field seasons.

2.2 Post- field work

Post-field work included further examination of the collected data from the field. Sedimentary logs from the field were redrawn digitally in Adobe Illustrator CS6. The photos taken by the "selfie stick" was put together to develop continuous vertical photologs. The lower, reachable meters of the succession were logged ordinarily and assembled together with the photologs. Pseudologs (combinational logs from the sedimentary logs and photos) were generated in Adobe Illustrator CS6. Adobe Illustrator CS6 was also used for further correlation of the logs along the 2D-transect, and later on, used to fix photos and to complete the pseudologs.

3 Geological framework

3.1 Introduction

Svalbard is an archipelago which comprises all islands between 74-81° N latitude and 10-35° E longitude (Figure 1.1). Spitsbergen constitutes the main island and it is situated in the north-western part of the Barents Shelf. Svalbard presents an uplifted part of the shelf, and the archipelago has almost a complete geological record from Precambrian to Palaeogene (Figure 3.1). The geology of Svalbard is divided into several geological provinces based on the age of the rock units. The oldest rocks are located in the north-eastern part and along the west coast. This includes metamorphic rocks of Precambrian to Early Silurian age. The uplift of the shelf was most extensive in the north-eastern and western parts; the latter was also exposed to the pressure of the West Spitsbergen fold-and-thrust belt of Svalbard (Steel et al., 1985; Friend et al., 1997; Dallmann, 1999). Hence, the oldest rocks are located in these areas (Figure 1.1). The geological record from Precambrian to Early Silurian show evidence from several tectonic events. The orogenic development of the Grenvillian (Late Mesoproterozoic), the Caledonian (Ordovician-Silurian), and the Ellesmerian (Late Devonian) are most significant (Dallmann, 1999). Devonian grabens are situated in the north, Late Paleozoic and Mesozoic platform sediments are located in the central and eastern areas, while Paleogene strata dominate the western and the central parts of Spitsbergen. Exposed basement and the fold-and-thrust belt are dominating along the west coast of Spitsbergen (Steel et al., 1985; Harland et al., 1997; Dallmann, 1999) (Figure 1.1).

Svalbard is famous for the wide range of sedimentary depositional environments. The different environments indicate Svalbards palaeoposition through time. It reflects the different climatic changes from the arid southern position in Early Devonian to the present arctic position, as the Eurasian plate moved northward (Worsley, 2008).

The studied Clinothem 8C is of Eocene age; the Cenozoic development of Svalbard will therefore be the main focus of this introduction. Chapter 3.2 gives a brief introduction to the pre-Cenozoic geological history, while chapter 3.3 gives a more thorough description of the Cenozoic development.

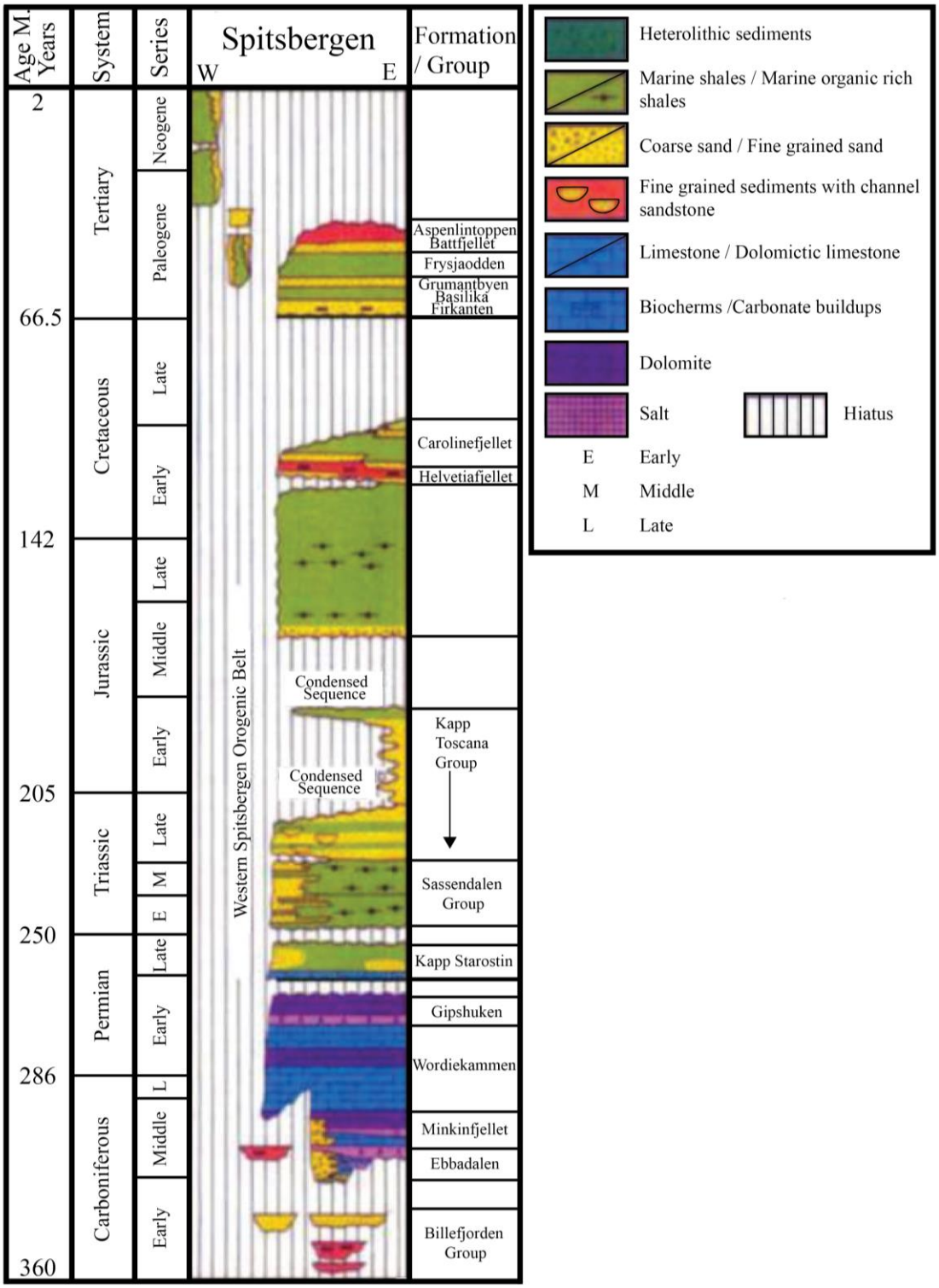

Figure 3.1: The stratigraphy of Spitsbergen, form Nøttvedt et al. (1992), slightly modified from Gjelberg (2010).

3.2 Pre-Cenozoic history of Svalbard

The Proterozoic and Paleozoic Eras

The basement rocks ranging from Precambrian to Silurian ages are defined as "Hecla Hoek." These rocks are intensively folded and faulted due to several tectonic events, the latest one being the Caledonian Orogeny. The Laurentian and the Fennoscandinavian plates collided during the Late Silurian causing the main deformation phase of Spitsbergen, leading to the metamorphism of the "Hecla Hoek" rocks (Harland, 1969; Friend et al., 1997; Harland et al., 1997). Several NNW-SSE trending lineaments developed or reactivated during this tectonically active period. The lineaments have proven to be an important feature that controls the sedimentation in the western parts of Spitsbergen (Steel and Worsley, 1984; Friend et al., 1997). Caledonian rocks are exposed at several localities on Svalbard; along the northern and western coast of Spitsbergen and Nordaustlandet, on a small area at Bjørnøya and on Prins Karls Forland (Dallmann, 1999) (Figure 1.1). The overall regional Caledonian (Ordovician-Silurian) structures have been hard to recognize and identify due to the disconfiguration created by the major faulting (e.g., Birkenmajer, 1975; Harland et al., 1997; Dallmann, 1999).

The Devonian sediments are time equivalent to the Old Red Sandstone in Northwest Europe and were derived from the newly formed Caledonian mountains. The Devonian strata constitute sandstones, siltstones, conglomerates with intercalations of smaller amounts of limestones and carbonates. The Late Silurian/Devonian succession predominantly present post-orogenic molasses deposits. The lowermost part of Devonian is presented by The Old Red Sandstones which was down-faulted within the thin north-south trending zones during the Haakonian deformation phase. A major unconformity separates the clastic fluvial red-beds and the interbedded conglomerates of Andrée Land Group with the succeeding Billefjorden Group (Friend and Moody-Stuart, 1972). Sinistral strike-slip movement between Spitsbergen and Greenland formed the unconformity, which spans the Devonian-Carboniferous Boundary. The tectonic phase presents the last stage of the Caledonian deformation, referred to as the Svalbardian phase. The Devonian depositional basins were formed due to the completed horizontal convergence and extension related to the collapse of the Caledonian Orogeny (Harland et al., 1997). A shift from red to grey sandstone takes place in the Middle Devonian. During the Devonian, Svalbard moved northwards from the southern, arid zone to the subtropics (30-20°N). The humidity and precipitation increased at

Svalbard, which is revealed in the rock record by the red-grey transition (Worsley et al., 1986).

Svalbard continued moving north, and during the Late Carboniferous Svalbard was located around 35° north, at the northern margin of Pangea (Worsley and Aga, 1984; Worsley, 2008). Terrestrial, fluvial, alluvial and coal deposits of Early Carboniferous Period forms up the Billefjorden Group (Gjelberg and Steel, 1981; Worsley, 2008). These deposits indicate a warm and humid climate, which was ideal for the spreading of lush vegetation on Svalbard. Svalbard moved further north towards semi-arid to arid environment during the period. This resulted in a change in the depositional environment, presented by the sabkha and the marine carbonates of the Gipsdalen Group (Gjelberg and Steel, 1981; Worsley, 2008). Gjelberg and Steel (1981) suggested that the marine carbonates of Gipsdalen Group reflect a long-term regional sea level rise. Three syn-rift half-grabens control the Gipsdalen Group and the succeeding, post-rift Dickson Land subgroup (Dallmann, 1999). Svalbard continued to move north and entered temperate climate in the Permian, which lasted through the Mezosoic (Steel and Worsley, 1984). The Late Permian can be identified by the sudden shift to cold and the deep water fine clastic recorded in the rock unit (Worsley, 2008).

The Mesozoic Era

The tectonic and climatic environment was generally stable during the Mezosoic, except the rifting initiating the opening of the Arctic and the North Atlantic Ocean at the end of Jurassic. The magmatic activity increased and sills of doloritic composition and basaltic lavas formed due to the vertical movements along the Billefjorden fault zone (Steel and Worsley, 1984). The first signs of the separation between Greenland and Europe documented at Svalbard are the dolerite sills and the basaltic lavas (Dallmann, 1999). Delta deposits and shallow shelf sediments, deposited in an open marine shelf area, dominates the Triassic to the Early Jurassic succession (Dallmann, 1999). A regional transgression followed in Mid-Jurassic causing the deep water to get anoxic, as a result, organic rich shales was consequently deposited (Worsley, 2008).

Svalbard reached 65° N latitude by the Early Cretaceous. Fluvial deposits of Early Cretaceous age overly the thick mudstones and shales of the Jurassic and Cretaceous succession (Gjelberg and Steel, 1995). The Barents Shelf was uplifted and exposed to erosion

during the Late Cretaceous. As a result, no upper Cretaceous rocks are found in Spitsbergen. The Cenozoic rocks are therefore deposited directly above the sandstones and shales of Carolinefjellet Formation of lower Cretaceous age (Harland, 1969; Steel and Worsley, 1984).

3.3 Introduction to the Cenozoic

The Cenozoic sedimentary system

Most of the Cenozoic sediments at Spitsbergen are located south of Isfjorden in the central areas of the island. The Cenozoic succession mainly consists of clastic rocks, deposited in the basin that is occupying a NNW-SSE trending syncline extending along the West Spitsbergen fold-and-thrust belt. The basin has preserved sediments from Paleogene time. Originally the succession was interpreted to range up to lower Oligocene, but this can be questioned since a large thickness of strata has later been eroded away (Dallmann and Elvevold, 2015). During the Late Cretaceous-Paleogene, the opening of the Norwegian-Greenland Sea occurred (Figure 3.2), forcing the North American plate to pass the Eurasian plate along the transform Hornsund-Senja Fault Zone (HSFZ) (Myhre et al., 1982; Eldholm et al., 1984). The western parts of Spitsbergen experienced extensive basement uplift and thin to thick-skinned tectonics related to the shearing and transpression along the HSFZ. The event resulted in the formation of a 300km long NNW-SSE trending fold-and-thrust belt (Bergh and Andresen, 1990; Braathen et al., 1999). Regional subsidence dominated east of the fold-and-thrust belt, and the large (ca. 60km) Central Basin developed on top of the Caledonian basement (Birkenmajer, 1981). The Paleocene sediments derived predominantly from the east, while the Eocene sediments entered the basin from a western source (Kellogg, 1975; Steel et al., 1981; Steel et al., 1985; Helland-Hansen, 1990; Bruhn and Steel, 2003).

The Central Basin comprises seven different formations (Harland, 1969; Harland et al., 1997). The deposits range from Late Paleocene to Late Eocene/Earliest Oligocene age (Paech, 1999). The succession consists of mixed marine and continental sediments, generally deposited on a wave to tidal dominated, river influenced delta system or on a coastal plain (Steel et al., 1981). The sedimentary succession ranging from Late Paleocene to Late Eocene/Earliest Oligocene age (Paech, 1999) is approximately 1.5km thick in the west and 600m thick in the east (Helland-Hansen, 1990; Uroza and Steel, 2008). Lithostratigraphically the succession comprises the Frysjaodden (deep water slope and basin floor), the Battfjellet

(shoreline and shelf) and the Aspelintoppen (coastal plain) formations (Uroza and Steel, 2008) (Figure 3.1).

The formation of the West Spitsbergen Orogeny and the Central Basin.

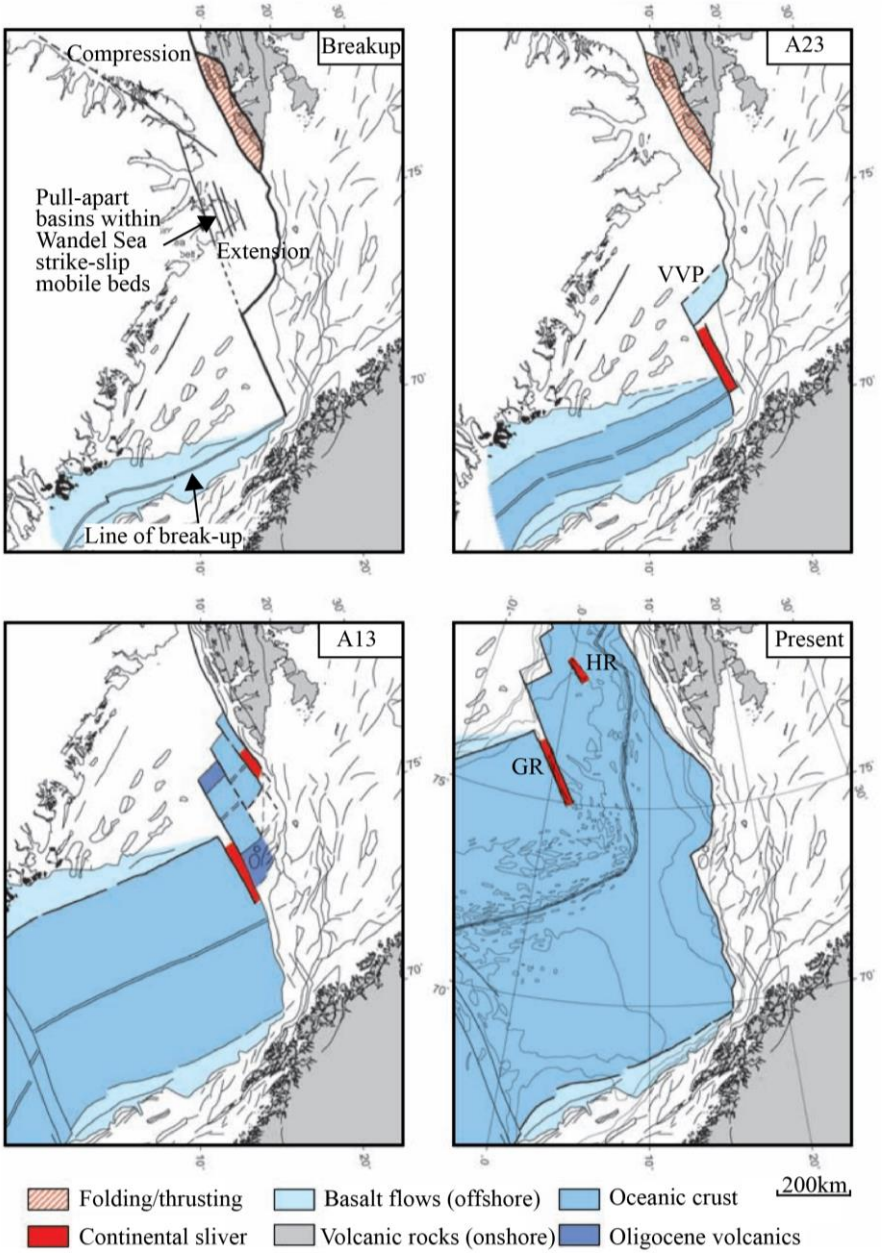

Figure 3.2: Cenozoic platetectonic evolution of the opening of the Atlantic Ocean. GR: Greenland Ridge, HR: Hovgård Ridge, VVP: Vestbakken Volcanic Basin (Faleide et al., 2008).

The opening of the North Atlantic Ocean took place in the Late Cretaceous-Early Cenozoic (Braathen et al., 1999). Continued sea-floor spreading forced the midoceanic-spreading ridge to migrate northwards. The Eurasian plate and the North American plate were separated by intracontinental rifting along the dextral transform Hornsund fault zone (Harland, 1969; Braathen et al., 1999). At this time Greenland acted as a separate plate and slid past Svalbard

resulting in a phase of dextral transpression. Consequently, a 300m long and 100-200km wide fold-and-thrust belt formed along the western part of Spitsbergen referred to as the West Spitsbergen Orogeny (Harland, 1969; Braathen et al., 1999; Dallmann and Elvevold, 2015). The fold-and-thrust belt were divided by Bergh et al. (1997); Braathen et al. (1999) into five different structural zones (Figure 3.1). The subdivisions are as following (Figure 3.3):

1. The first structural area was formed during the Late Cretaceous-Early Paleocene. The area consists of a western basement hinterland, which proves marks of a complex deformation history, including normal faulting and thrusting. The uplift of the Barents Shelf leads to a north-south contraction oriented obliquely to the orogeny (Roest and Srivastava, 1989; Braathen et al., 1999). The compression in the north together with the crustal shortening lead to the growth of a low-taper critical-supercritical wedge (Braathen et al., 1999).

2. Uplift and shortening of the crust in an ENE-WSW direction continued during the Early to Middle-Paleocene. Thick-skinned trusting and rotation of pre-existing thrusts in the basement dominated this stage. Piggy-back thrusting was formed due to thrust progradation in the central zones of the fold-and-thrust belt, while the eastern foreland segments were prone to layer parallel shortening and decollement thrusting. The Svartfjellet-Eidenbukta-Daudamannsodden lineament formed as a result of the movements in the hinterland (Braathen et al., 1999).

3. The contraction continued making the crust thicker in the form of basin inversion and thrust uplift. An unstable supercritical wedge of basement rocks continued to form in the central parts while shortening and thrusting continued in the eastern foreland province. The increased eastward thrusting has been explained by the thickening of the hinterland due to the strike-slip duplexing (Braathen et al., 1999).

4. During the fourth stage, shortening proceeded in a northeast-southwest direction, representing a temporal change in the direction of the tectonic movement. The unstable supercritical wedge stabilized during this stage as the eastwards progradation and lengthening continued. Out-of-sequence thrusts are recognized in the central and the foreland provinces, executing pre-existing faults. Large-scale monoclines were generated as a result of reverse reactivation of pre-existing faults. The hinterland

lineaments were prone to a dextral strike-slip movement. Simultaneously, a local transtensive setting most likely started the development of the Forlandsundet Graben (Braathen et al., 1999).

5. During the Late-Eocene-Oligocene the area experienced an east-northeast to west-southwest extension. The extension eventually caused collapse and the formation of a huge asymmetric depression known as the Central Basin (Braathen et al., 1999).

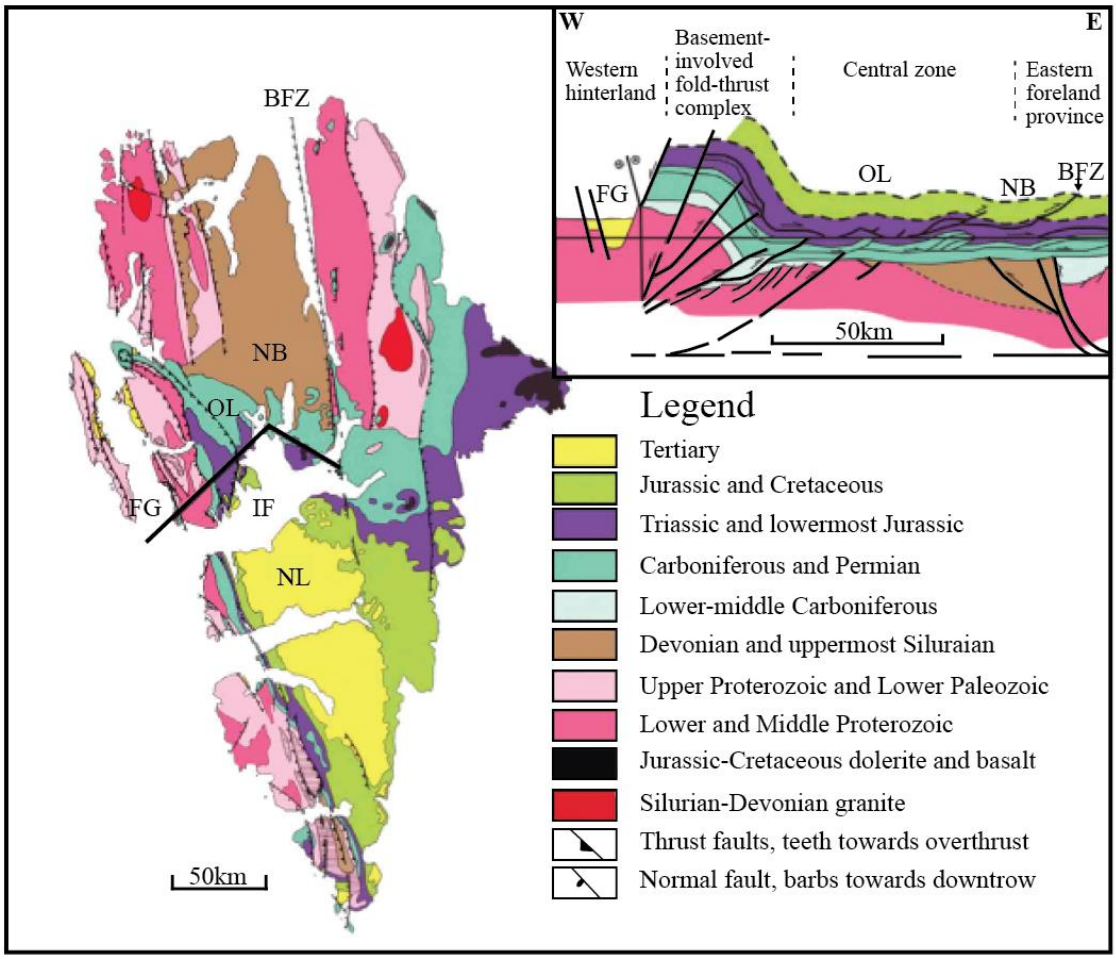

Figure 3.3: Map of Spitsbergen and cross-section of the structural zones of the Cenozoic fold-and-thrust belt. BFZ=Billefjorden Fault Zone, NB=Nordfjorden block, OL=Oscar II Land, IF=Isfjorden, FG= Forlandsundet Graben, NL= Nordenskiöld Land (Blinova et al., 2012).

3.4 Basin fill of the Central Basin

The Central Basin was classified as a foreland basin formed during the period of active thrusting in the West Spitsbergen fold-and-thrust belt (Steel et al., 1985; Helland-Hansen, 1990; Müller and Spielhagen, 1990; Bruhn and Steel, 2003). However, Blythe and Kleinspehn (1998) suggested a piggy-back basin development. The near location of the fold-and-thrust belt (Figure 1.1), the syndepositional tilting of the succession towards the orogeny

and the integration of the orogenic belt into the deformation indicate a foreland basin (Dickinson and Yarborough, 1979; Helland-Hansen, 1990). This basin was the result of a transpressional rather than a compressional regime, which is uncommon in the formation of a foreland basin (Helland-Hansen, 1990).

Steel et al. (1981) divided the stratigraphy of the infilling succession of the Central Basin into three main stages; the division is based on the large-scale transgressive and regressive trends. The Van Mijenfjorden Group comprises six formations described in this chapter (Figure 3.4).

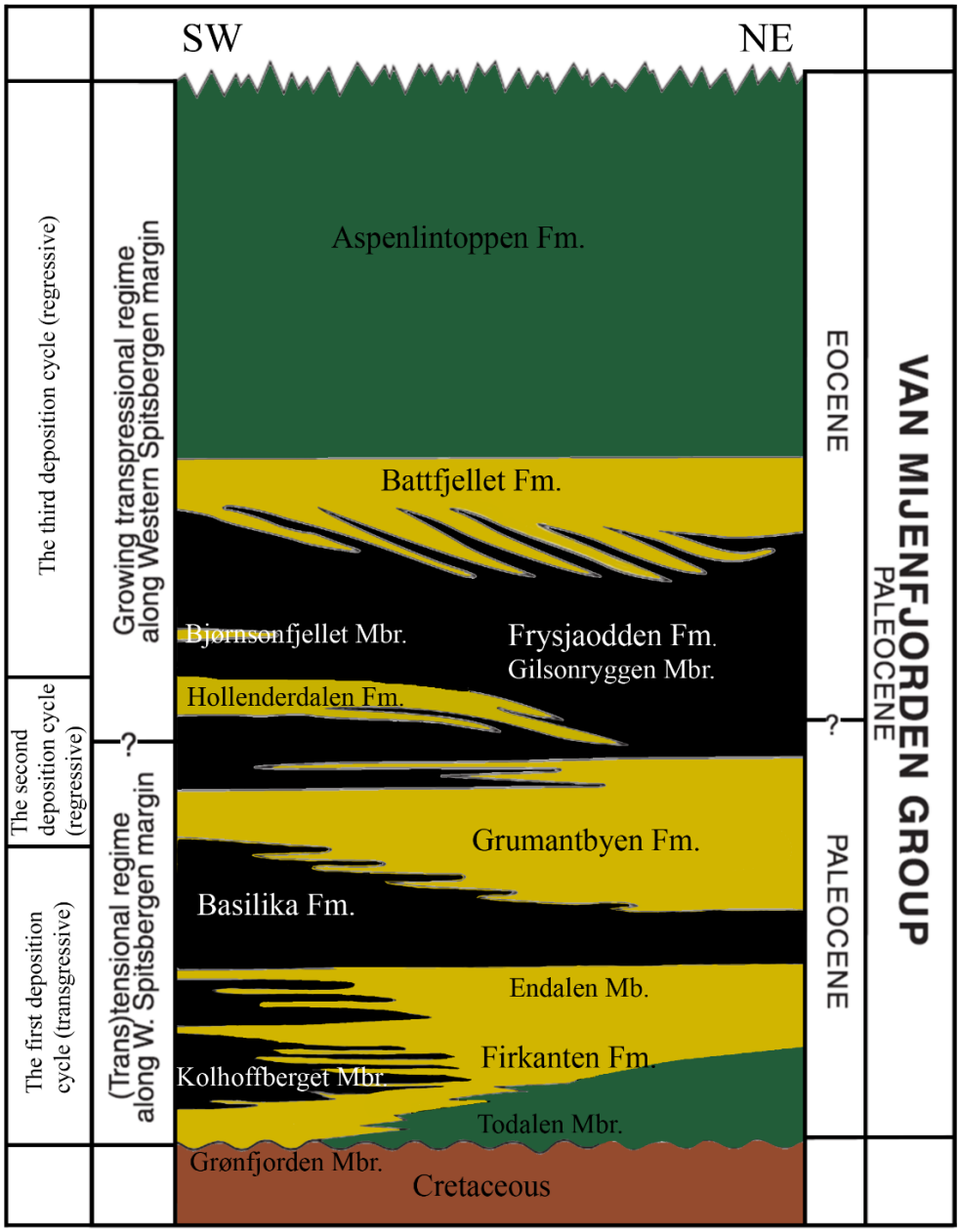

Figure 3.4 The three depositional cycles of the Van Mijenfjorden Group, with the formations and members from Paleocene and Eocene. Green: terrestrial, yellow: shallow marine, black: offshore and brown: Cretaceous (offshore deposits), modified from Steel et al. (1985).

The Firkanten and Basilika Formations; the first depositional cycle (transgressive)

The Firkanten Formation constitutes the lowermost unit of the Van Mijenfjorden Group (Figure 3.4), the formation is of lower to mid-Paleocene age. A Selendian age was established by Nagy et al. (2000) based on foraminifera analysis performed in the Kalthoffberget Member in the Basilikaelva. Blythe and Kleinspehn (1998) and Bruhn and Steel (2003) established a slightly younger age (Danian) based on fission tracks in apatite grains from the Endalen and Todalen Members. The Firkanten Formation represents the first depositional cycle of the infilling of the Central Basin. The sediments from the Firkanten and the Basilika formations are of Early Paleocene age and originated from the west, north and east (Dallmann, 1999). Nøttvedt (1982) argued that the delta regime and distribution of coal within Firkanten Formation mainly was controlled by tectonics. An approximately 32My hiatus separates the Firkanten Formation from the underlying Carolinefjellet Formation (Dallmann, 1999). Grønfjorden, Todalen, Kolthoffberget and Endalen members are the different members comprising the Firkanten Formation. The Firkanten Formation thickens towards the west from 80 to 200m (Bruhn and Steel, 2003). Braided river deposits constitute the Grønfjorden Member with its thin, irregular basal conglomerates. Overlying the Grønfjorden Member three to five sequences of shale-siltstone-sandstone-coal comprises the Todalen Member. These deposits represent delta-plain deposits, which can be traced laterally into delta front sandstones (Bruhn and Steel, 2003). The uppermost unit of the delta front sandstone constitutes the basin-wide Endalen Member. The shaly prodelta deposits of the Kalhoffberget Member interfingers with the Endalen Member in the south-western part of the basin. These deposits reflect an overall transgressive nature of the Firkanten Formation (Harland et al., 1997). Although the overall trend is transgressive, several smaller regressive phases occur. An example of a regressive phase is the transition from shallow marine to continental deposits in the Endalen Member (Harland et al., 1997).

Thick, dark offshore to outer shelf shales of Basilika Formation are deposited above the Firkanten Formation. The shales constitute the dominant lithology of the formation. Well-rounded pebbles of chert and quartzite and interbedded siltstones and sandstones are found at the base of the formation (Harland et al., 1997) and are likely to be ice-rafted (Dalland, 1976). The formation is thickest in the southwest in the basinal regions; the silt and sand layers thicknesses vary from approximately 20m in the northeast to 350m in the southwest (Steel et al., 1981; Harland et al., 1997). The ice-rafted evidence indicates Svalbard's arctic location in the Paleogene (Dalland, 1976).

The Grumantbyen and Hollendardalen Formations; the second depositional cycle (regressive)

The Grumantbyen Formation constitutes lower part of the second depositional cycle. The transition between the underlying Basilika Formation and the Grumantbyen Formation is gradual. The Grumantbyen Formation can be distinguished from the underlying formation with its highly bioturbated greenish (glauconite) sandstones (Harland et al., 1997). Steel et al. (1981) suggested that the Grumantbyen Formation is a part of a prograding inner shelf sand complex (offshore bar), but the depositional environment is still poorly understood due to the massive character and the high degree of bioturbation. The formation is approximately 450m thick in the north-eastern part of the basin and thins to approximately 200m thick in the south-western part of the basin (Dallmann, 1999).

The Hollendendalen Formation constitutes the upper part of the regressive cycle and the formation is intercalated with the lower part of the succeeding Frysjaodden Formation. The Hollendendalen Formation presents the first sediments derived from the rising Western Spitsbergen fold-and-thrust belt. The formation comprises several shallow marine sandstone wedges created by tidally influenced deltas. The sandstone wedges reach up to 150m in total thickness in the western part of the basin and thin out into the shales of the Frysjaodden Formation (Dalland, 1976; Dallmann, 1999).

The transition from shelf deposits of the Basilika Formation to the offshore sandstones of the Grumantbyen Formation and to the tidally influenced deltaic deposits of the Hollendendalen Formation indicates an overall regressional cycle (Steel et al., 1981; Steel et al., 1985). As figure 3.4 illustrates Grumantbyen Formation and Hollendendalen Formation is separated by a major flooding surface (represented by the Marstrandbreen Member). It will therefore be more reasonable to separate the second depositional cycle into two minor regressive divisions.

The Frysjaodden, Battfjellet and Aspelintoppen Formations; the third depositional cycle (regressive)

The third depositional cycle comprises the Frysjaodden, the Battfjellet and the Aspelintoppen Formation. Together, these formations are approximately 1.5km thick and range from latest Paleocene through Eocene/Early Oligocene (Steel et al., 1985). The shales of the Frysjaodden

Formation follow the drowning episode of the Grumantbyen Formation. The formation is predominantly comprised of shales, but there are sandstone wedges of approximately 15-20m in thickness in the western part, thinning towards the center of the basin. The sandstone wedges are interpreted to be turbidite and slump deposits and are derived from the Bjørnsonfjellet Member (Steel et al., 1981). The turbidites and slumping occurred as a result of the rising orogenic belt in the west. The dark shales are interpreted to be of offshore to prodelta origin (Dallmann, 1999).

The boundary between the Frysjaodden Formation and the overall Battfjellet Formation is rather transitional. The Battfjellet Formation is present as a shallow marine coarsening upwards sandstone succession (Harland et al., 1997) predominantly comprised of very fine- and fine-grained sandstones (Steel et al., 1981). The development of the Battfjellet Formation will be the main focus of this thesis. Helland-Hansen (1990) suggested establishing the boundary between the two formations where the shales become subordinate relative to the sandstones. The sandstones of the Battfjellet Formation are divided into as many as seven coarsening upward shoreline sequences. These coarsening upwards shoreline sequences are separated by flooding surfaces making up parasequences. The parasequences vary in thickness from 10-30m (Helland-Hansen, 1990).

The Battfjellet Formation varies in thickness from 60-200m (Harland et al., 1997). The thinnest development of the formation is in the north-eastern part of the basin, and the thickest is in the south-western part of the basin (Dallmann, 1999). The sediments of the Battfjellet Formation are deposited in the entire Central Basin. An eastward progradational deltaic system is interpreted to be the source of the sediments (Steel et al., 1981; Steel et al., 1985; Helland-Hansen, 1990). Palaeocurrent measurements display a north-south oriented shoreline during the progradation of the delta with the hinterland located in the west (Helland-Hansen, 1990).

The presence of approximately 20 large-scale eastwards-sloping sand bodies is another important feature characterizing the Battfjellet Formation. The sand bodies comprise clinothems reflecting the build-out of the basin margin driven by the sediments derivated from the mountain belt to the west (Plink-Björklund, 2005). Each clinoform surface present a timeline beginning with the coastal plain deposits (the Aspelintoppen Formation), to the shallow marine shelf (the Battfjellet Formation) and down into the deep water slope and

basin floor environments (shales of Gilsonryggen Member) where they finally pinch out (Kellogg, 1975; Steel et al., 1985; Plink-Björklund, 2005). The Battfjellet Formation represents the last stage of the coastal progradation episode, which resulted in the final infill of the Central Basin (Steel et al., 1981; Steel et al., 1985; Helland-Hansen, 1990).

Based on the aggradational/progradational style, the sand distribution along the clinoforms and the degree of channel incision at the shelf-edge of the clinoforms cf. Steel et al. (2000); Steel and Olsen (2002); Deibert et al. (2003); Uroza and Steel (2008) distinguished between four main types of Eocene clinoforms along the mountainside on Spitsbergen. Type 4 (Figure 3.5) is the most common type of clinoforms and they develop by progradation of wave-dominated shorelines or by deltas, with sand deposition restricted to the inner shelf. These clinoforms are highly aggradational and shale prone (Deibert et al., 2003). Clinothem 8C display thick sandstone units across the entire shelf with channels bypassing sands onto the slope.

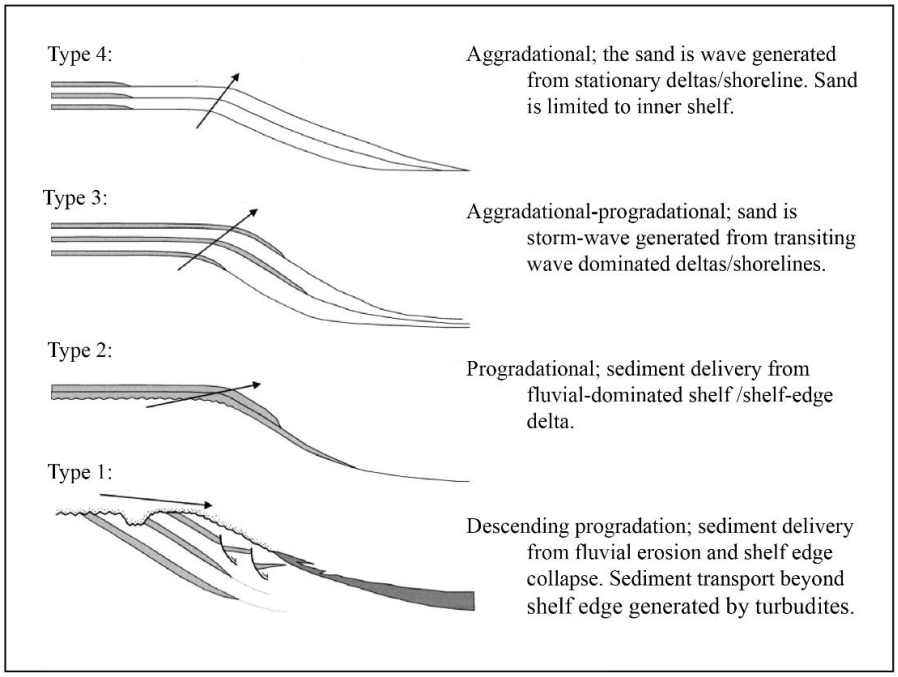

Figure 3.5: The four types of clinoforms along the Van Keulenfjorden transect. The clinoforms along Brogniartfjella is normally of type 1 and 2, slightly modified from Steel et al. (2000).

Stacked upward coarsening parasequences dominates the Battfjellet Formation in the Central Basin. The sandstones of the Battfjellet Formation are characterised by unsorted and texturally immature sand. The sandstones are predominantly comprised of lithic greywacke, revealing rapid deposition of the sand from the source area (Helland-Hansen, 1990, 2009). The poor porosity of the sandstones and the abundance of soft-sediment deformation supports

the statement. According to Helland-Hansen (1990), the grains of the sandstones are a mixture of fragments of sedimentary derived carbonates, siliciclastic and polycrystalline metamorphic quartz grains.

Above the Battfjellet Formation the time equivalent Aspelintoppen Formation is deposited. The formation is nearly 1000m thick and it represents the final infilling of the foreland basin. The Aspelintoppen Formation is interpreted to represent a coastal plain environment (Harland et al., 1997). The formation consists of alternating layers of poorly sorted sandstones, siltstones, shales and coals. The formation has a high content of organic material, and plant beds are widespread (Harland et al., 1997). The alternating layers are interpreted to present delta plain deposits (Steel et al., 1985) indicating fluvial channels, overbank deposits and bay fill sediments. In some of the hilltops in the central part of the basin soft-sediment deformation is widespread together with plant remains (Helland-Hansen, 1990; Harland et al., 1997).

The third and last stage of the basin infilling is clearly of a regressive nature, as evidenced by the transition from the deep water shales of the Frysjaodden Formation, through the shallow marine sandstones of the Battfjellet Formation and into the continental plain deposits of the Aspelintoppen Formation.

4 Sedimentary lithofacies, ichnology and facies associations

4.1 Introduction

To obtain a better understanding of the depositional environment and the palaeogeography of the Battfjellet Formation, the investigated sedimentary strata have been divided into ten sedimentary lithofacies. The usage of the term facies was first introduced by Gressly (1838) Gressly in 1838, but the term has been used in several different ways afterward. Facies association, as defined by Collinson (1969) is assemblages of spatially and genetically related facies, interpreted based on the different sedimentary systems or depositional palaeoenvironments. The facies in this thesis have been divided based on the bulk macroscopic characteristics of the rock. The section has been divided based on lithologic features such as grain size, sedimentary structures, boundary types, color and bioturbation. In the present work, the term hyperpycnal flow has been used as defined by Mulder and Syvitski (1995).

4.2 Sedimentary lithofacies

Table 4.1 provides an overview of lithofacies descriptions and interpretations, while a more extensive description and interpretation of each lithofacies is provided in chapter 4.2. The lithofacies in table 4.1 are listed according to grain size. The lithofacies are further grouped into three facies associations which are presented in chapter 4.3.

Table 4.1: Table of lithofacies ordered after increasing grain size.

Lithofacies	Lithofacies name	Grain size	Thickness (m)	Description	Interpretation
M_L	Mudstone	Mudstone	0.05-0.35 m thick units	Finely laminated silty mudstone with occasional very fine sand lenses and very fine, thin sand streaks.	Fallout from suspension from hyperpycnal plumes possibly ignited to low-density turbidite currents.
S_{SSD}	Soft-sediment deformed sandstone	Mixture of siltstone/mudstone and very fine-grained sandstone.	0.30-2.5 m thick units	Ball and pillow structures/ loading structures: Heterolithics with soft-sediment deformation.	Secondary structure developed due to high sedimentation rate and liquefaction of sediments.
S_{ARCL}	Asymmetrical ripple cross-laminated sandstone	Very fine- to fine-grained sandstone.	0.1-0.40 m thick units	Asymmetrical unidirectional ripple cross-laminated sandstone.	Tractional transport of sand by a unidirectional current in lower flow regime.
S_{SRCL}	Symmetrical ripple cross-laminated sandstone	Very fine- to fine-grained sandstone.	0.05-0.25 m thick units	Symmetrically rippled cross-laminated sandstone.	Deposition from oscillatory currents (symmetrical and combined). Combined flow ripples are a result of influence from a unidirectional current in addition to the oscillatory current.
S_{HCS}	Hummocky cross-stratified sandstone	Very fine- to fine-grained sandstone.	0.5-1m thick units	Amalgamated hummocky cross-stratification with varying wavelengths.	Forms in shallow water between fairweather and storm wave bases. Aggradation rates during storms are high enough to build up and preserve hummocks.
S_{PPS}	Plane parallel-stratified sandstone	Very fine- to medium-grained sandstone	0.1-1 m thick units	Plane parallel-stratified sandstone units.	Plane-bed transport of sand predominantly deposited by high-velocity unidirectional currents. Oscillatory currents are subordinate.

S_{LACS}	Low angle cross-stratified sandstone	Very fine- to medium-grained sandstone	0.2-2 m thick units	Normal graded low angle cross-stratified sandstone.	Tractional deposition from unidirectional current, possibly low-density turbidity currents.
S_{CS}	Cross-stratified sandstone	Very fine- to medium-grained sandstone.	0.2-1 m thick units	Irregular troughs were the internal bedset lamination is terminating against a trough-shaped lower boundary.	Tractional transport of sand from unidirectional currents.
S_{NG}	Normal graded sandstone	Very fine- to medium-grained sandstone.	0.25-5.3 m thick units	Massive, homogenous non-structured to weakly laminated normal graded sandstone.	Hyperpycnal flow deposits, most likely turbidites.
M_{CC}	Matrix-supported mud-clast conglomerate	Matrix of fine- to medium-grained sandstone.	0.3-1.6 m thick units	Normal graded sandstone units with rounded mud-clast conglomerates.	Turbidite channel lag-deposits from basal scouring.

Sedimentary lithofacies descriptions and interpretations

Lithofacies M_L: Mudstone

Description: This lithofacies comprises of finely laminated mudstones (Figure 4.1). Occasionally dark grey to brown colored very fine-grained sand lenses and thin very fine-grained sand streaks are recorded. Coal fragments and horizons rich in organic detritus are also documented within the facies. The lower boundary is unclear and the upper boundary is either unclear or erosive typically towards soft-sediment deformed sandstones (S_{SSD}).

Interpretation: Based on the fine grain size, the lamination and the occurrence of coal fragments the lithofacies is interpreted as formed by fallout from suspension, possibly by hyperpycnal plumes or low-density turbidite currents (Collinson et al., 2006).

Figure 4.1: Laminated mudstone succeeded by very fine-grained sandstone, from the lower reaches of log 2 (Figure 1.2).

Lithofacies S_{SSD}: Soft-sediment deformed sandstone

Description: Chaotic, heterolithic layers consisting of a mixture between siltstones, mudstones and very fine-grained sandstones characterize the lithofacies. Loading structures such as balls and pillows dominate along the outcrop, but convolute bedding, flame structures and dish structures are also found along the section (Figure 4.2). The top is commonly eroded, while the base is gradual to loaded. The ratio of mudstones, siltstones and sandstones is highly variable both internally in each bed and also in the lithofacies.

The balls and pillows range in size from 5-20cm and are composed of very fine-grained sandstone. Balls and pillows are typically capsulated in mudstones and siltstones. Ellipsoidal or lensoid shaped balls and pillows dominate, while some spherical shaped are also seen in

less deformed areas. Bigger balls and pillows up to 1m wide with preserved internal stratification occur along the section.

Irregular, wavy laminated anticlines and synclines of 5-15cm are recognized as convolute bedding. Dish structures are also found locally and can be distinguished as thin, flat to concave upwards clayey laminations; the structures are particularly nicely exposed in the fine-grained sandstone in the most proximal part of the wedging unit (log 6) (Figure 1.2). The structures are of a few millimeters thick and range from 5-30cm wide. The occurrence of rip-up mud conglomerates and coal clasts are common features in this stirred, chaotic lithofacies.

Interpretation: The interbedding of mudstones, siltstones and very fine-grained sandstones indicates fluctuating energy conditions. The widespread occurrence of soft-sediment deformed units implies stirring of the sediments during or right after deposition. The structures observed are a result of high sedimentation rates in combination with liquefaction of sediments, allowing the sediments to pack loosely. Both factors lead to instability within the layers, which permit the deformational structures to form. Most of the soft-sediment deformation along the studied succession is a result of liquefaction and remobilization of sediments, although sparse slumping could be present at the distal delta front. According to Rich (1950), slumping is a result of postdepositionally intra-stratal sliding.

Ball and pillow structures are generated by density differences between the different lithologies, generating a chaotic and stirred appearance. The ball and pillow structures, which normally comprises of sandstone sinks into the underlying unit, and becomes a part of the underlying mudstone/ siltstone layer.

Convolute bedding is commonly found in turbidite dominated successions, but such structures can also occur in intertidal-flat sediments, point-bar sediments and deltaic deposits (Middleton et al., 2003). The origin of convolute bedding is still questioned, but it is certainly a result of plastic deformation of partially liquefied sediments during or soon after deposition (Boggs, 2011).

Dish structures are also most commonly found in liquefied flows. The structures have however also been documented in sediments from deltaic, alluvial, lacustrine and volcanic ash layers (Nichols et al., 1994). Rapid deposition of the sandstone due to the escape of water

forms the structure (Lowe, 1975). The structures are normally identified in massive sandstones.

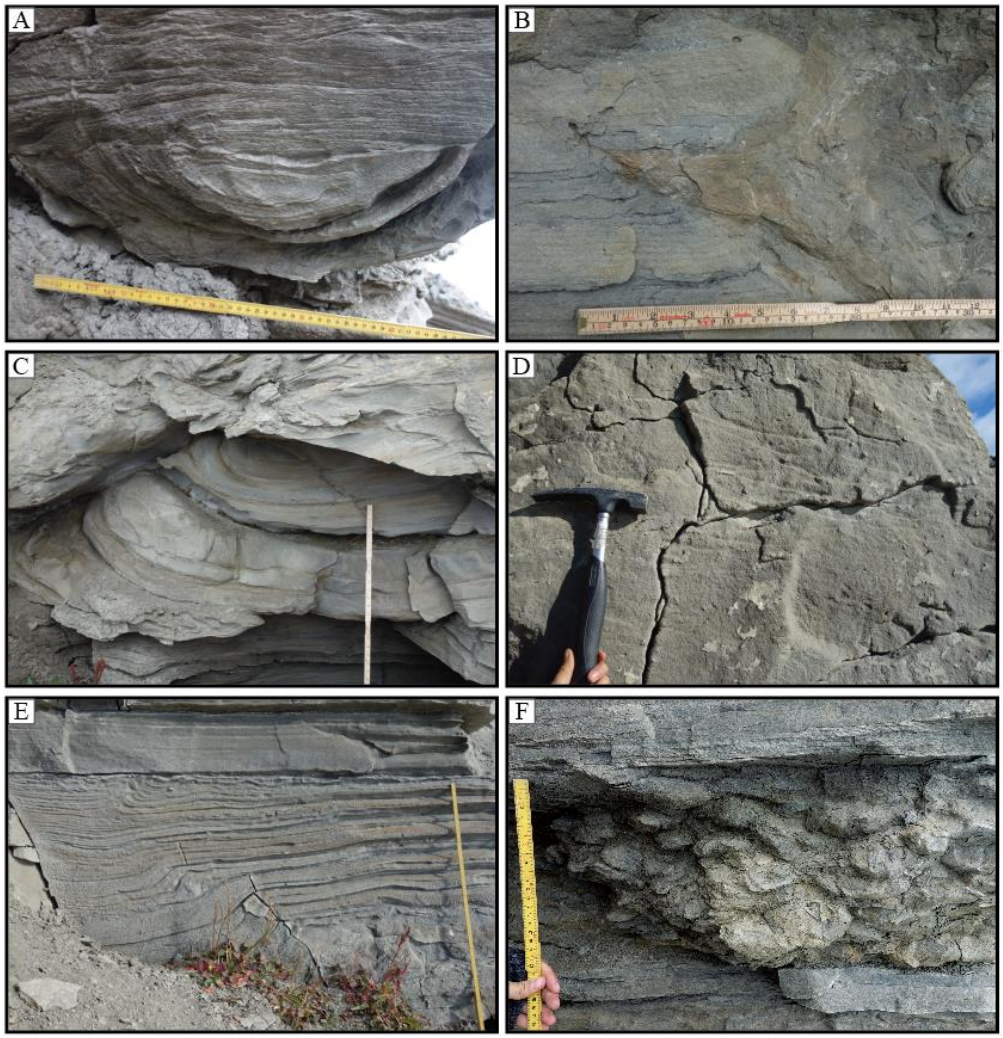

Figure 4.2: The diverse appearance of soft-sediment deformed sandstones. **A:** Truncated ball and pillow structure overlain by symmetrical ripple cross-laminated sandstone, scale in centimeters (log 1). **B:** Flame structure in centimeters scale located at the base of the channelized sandstone of FA3 (log 4). **C:** Ball and pillow structure, measure stick for scale are 22cm (log 4). **D:** Shallow concave-up dish structures in massive fine-grained sandstone (log 6). **E:** Convolute bedding, measure stick for scale is 90cm (log 6). **F:** Ball and pillow structure between thin very fine-grained plane parallel-stratified sandstones, scale in centimeters (log 3). Figure 1.2 demonstrate the locations of the sedimentary logs.

Lithofacies SARCL: Asymmetrical ripple cross-laminated sandstone

Description: Lithofacies SARCL is dominated by asymmetrical light grey to yellow-brown ripple cross-lamination in very fine- to fine-grained sandstone in 0.1-0.40m thick units (Figure 4.3A). The sandstone beds vary between sheeted and lenticular geometries with straight to erosive lower boundaries and straight to gradual upper boundaries. Rip-up mud conglomerates and coal fragments occur within the lithofacies. The ripples become up to 3cm in height. Climbing current ripple cross-lamination is also seen, predominantly along the wedging unit (Figure 4.3B.)

Interpretation: Asymmetrical ripple cross-lamination in sandstone are formed by tractional transport of sand by unidirectional currents in the lower part of lower flow regime (Allen, 1982). Climbing current ripples form in environments characterized by rapid fallout from suspension. The cross-lamination is produced by superpositioning of the migrating ripples (Collinson et al., 2006). Climbing current ripples are often associated with turbidity currents (Bouma, 1964).

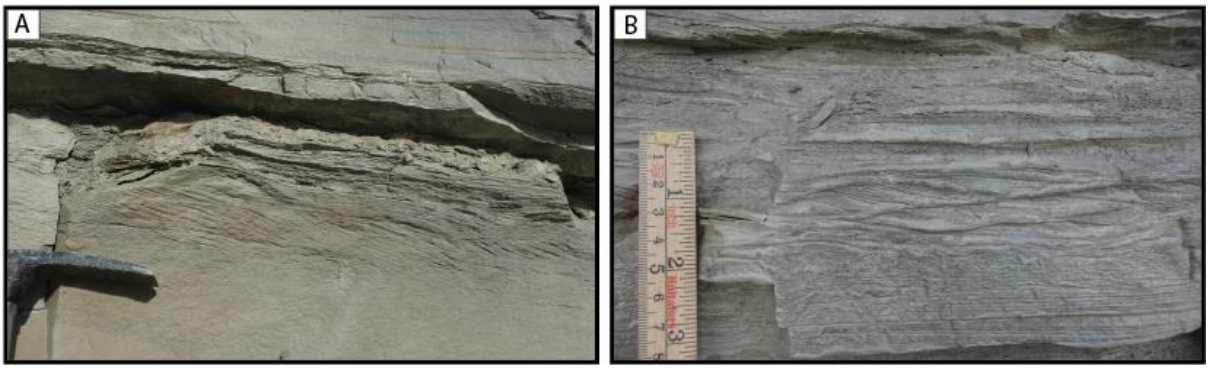

Figure 4.3: Current ripple cross-laminated sandstones. **A:** Current ripple cross-lamination in very fine-grained sandstone. The photo was taken between pseudolog 1 and 2. Geological hammer for scale. **B:** Climbing current ripple cross-lamination in fine-grained sandstone. Figure 1.2 demonstrates the locations of the pseudologs.

Lithofacies S_{SRCL}: Symmetrical ripple cross-laminated sandstone

Description: Symmetrically light grey ripple cross-laminated sandstone in 0.05-0.25 thick units dominates this lithofacies (Figure 4.4). Lithofacies S_{SRCL} often alternates with lithofacies S_{PPS}. Gradual, non-erosive upper and lower boundaries are typical for this lithofacies. The ripples are of 10-20cm in spacing and up to 3cm in height. The internal lamination is dipping towards NW and to SE. The sandstone units of this lithofacies have a sheeted to lenticular geometry. Some ripples have slightly asymmetrical crests; these are defined as combined flow ripples. The combined flow ripples are often alternating with sandstones of lithofacies plane parallel-stratified sandstone (S_{PPS}).

Interpretation: Symmetrical ripple cross-lamination forms by deposition from oscillatory currents in the lower part of lower flow regime (Allen, 1982). The oscillatory nature of the current gives rise to the development of cross-lamination in two different directions. Symmetrical ripples form in relatively shallow water and are most common above fair weather wave base in middle to lower shoreface settings. However, the lithofacies can be identified down to offshore transition zone associated with hummocky-cross stratification (Figure 4.5). The interaction of oscillatory and unidirectional currents may develop combined flow ripples. The deposits are believed to be a result of the interaction by longshore currents,

rip-currents and possibly by the erosion related to higher energy (storms) in a wave-dominated shoreface settings (e.g., Allen, 1982; Collinson et al., 2006).

Figure 4.4: Symmetrical ripple cross-laminated sandstones. **A:** Symmetrical ripple cross-laminated sandstone with a spacing of 10-15cm (log 2), scale in centimeters. **B:** Symmetrical ripple with preserved internal cross-lamination (log 1), scale in centimeters. Figure 1.2 demonstrates the locations of the sedimentary logs.

Lithofacies S_{HCS}: Hummocky cross-stratified sandstone

Description: The lithofacies is characterized by undulating sets of amalgamated cross-stratified very fine- to fine-grained sandstones, which are identified as hummocky cross-stratification (S_{HCS}). The color varies from grey to grey-brown (Figure 4.5). Some of the cross-strata are made up of convex-upward parallel stratification. The sets commonly occur in 0.5-1m thick units. The lower boundary is normally sharp and often noticeable by an erosional surface.

Interpretation: Hummocky cross-stratification is formed below fair weather wave base by the interaction of oscillatory waves and a unidirectional current (Dumas et al., 2005). The shape of the parallel stratified domes are known as "hummocks" (Walker, 1984; Collinson et al., 2006), and is determined by the relation between the orbital velocity and the strength of the unidirectional current (e.g., Dumas and Arnott, 2006; Cummings et al., 2009). The sedimentary structure is interpreted as a storm event deposit and is typically formed in upper shoreface to offshore transition zone in relatively shallow water depths (Greenwood and Sherman, 1986; Dumas and Arnott, 2006). In outcrop, hummocky cross-stratification (S_{HCS})

with long wavelength can easily be mixed up plane parallel (S_{PPS}) - and low angle cross-stratified sandstones (S_{LACS}).

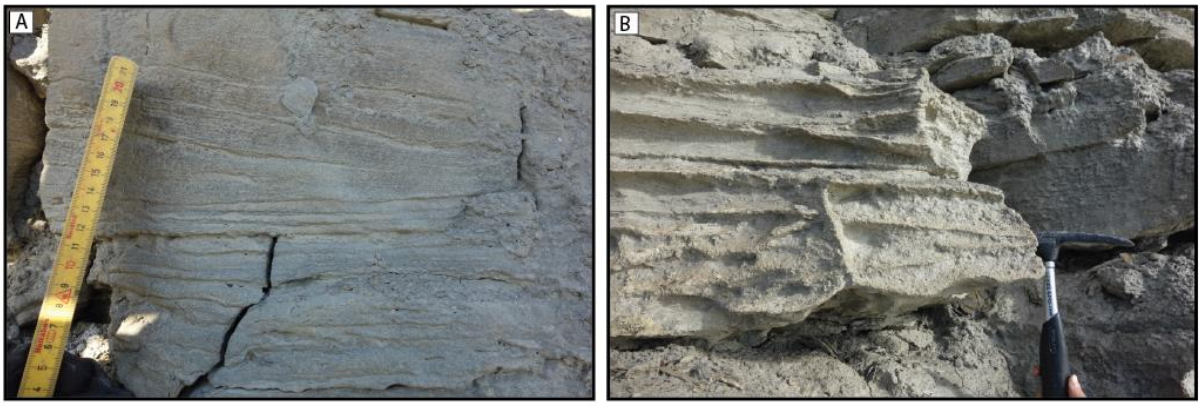

Figure 4.5: Hummocky cross-stratified sandstones**. A:** Hummocky cross-stratified sandstone from log 3, scale in centimeters. **B:** Hummocky cross-stratified sandstone from the upper reaches of log 2. Figure 1.2 displays the locations of the sedimentary logs.

Lithofacies S_{PPS}: Plane parallel-stratified sandstone

Description: Lithofacies S_{PPS} consists of plane parallel-stratified light grey- to grey sandstone in 0.1-m thick units (Figure 4.6). The grain size ranges from very fine- to medium-grained sand. The lithofacies is observed in the tabular and the wedging element. The laminae ranges from 0.5-2cm thick (average 1cm). The structure is seen as tabular lamination/stratification to slightly wedging within the units. Low-angle cross-stratified sandstones (S_{LACS}) are commonly seen alternating with sandstones of lithofacies plane parallel-stratified sandstones (S_{PPS}). The units have a sharp to gradual upper and lower boundaries. The lithofacies display a low rate of bioturbation along the studied succession.

Interpretation: The sandstones of lithofacies S_{PPS} are formed in the lower part of upper flow regime. Plane parallel-stratification form by rapid flows with continuous sediment transport (Collinson et al., 2006). The sedimentary structure is found at all depths; plane parallel-stratification is therefore not a good water depth indicator. However, the thickness of the strata can be used to predict flow velocity fluctuations and segregation and sorting of grains (Allen, 1982). The plane parallel-stratified beds of the tabular element have partly been reworked by oscillatory currents, implying deposition in shallow depths. The plane parallel-stratified sandstones within the wedging element are interpreted to present deposition from high-density turbidity currents, similar to T_b division of (Bouma, 1962).

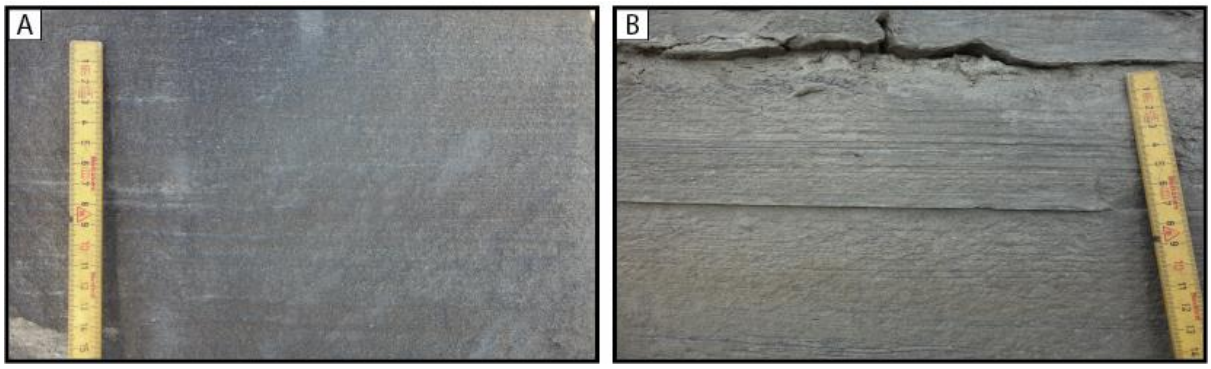

Figure 4.6: Plane parallel-stratified sandstones**. A:** Example of lithofacies S_{PPS} in medium-grained sandstone from log 8, scale in centimeters. **B:** Example of lithofacies S_{PPS} in very fine grained-sandstone from log 7, scale in centimeters. Figure 1.2 displays the locations of the logs.

Lithofacies S_{LACS}: Low angle cross-stratified sandstone:

Description: Low angle cross-stratified sandstone in 0.2-2m thick units dominates this lithofacies (Figure 4.7). The lithofacies are predominantly observed within the wedging element, although it is also present in the tabular element (Figure 1.2). The individual sandstone beds within the wedging element range from 0.5-2m in thicknesses, with an average thickness of approximately 1m. The low angle cross-stratified sandstones within the tabular element ranges from approximately 0.2-0.8m, with an average thickness of approximately 0.35m. The low angle cross-stratified sandstones of the tabular element are typically associated with undulating stratified sandstones and ripple cross-laminated sandstones. A typical stacking observed within the wedging element is normal graded and plane parallel stratified sandstones typically succeeded by low angle cross-stratified sandstone. The degree of bioturbation in the low angle cross-stratified sandstones in the tabular element is low, while bioturbation is absent in the low angle cross-stratified sandstones of the wedging element. The sandstones of this lithofacies have a tabular to wedge-shaped geometry. The base is normally planar or irregular and occasionally erosive, while the top is typically irregular or erosive.

Interpretation: The low angle cross-stratified sandstones within the wedging element are interpreted as deposits from tractional high-density turbidity currents. The low angle cross-stratified beds within the tabular element are deposited in the lower part of upper flow regime by unidirectional currents (Collinson et al., 2006), although the lithofacies is influenced by oscillatory currents.

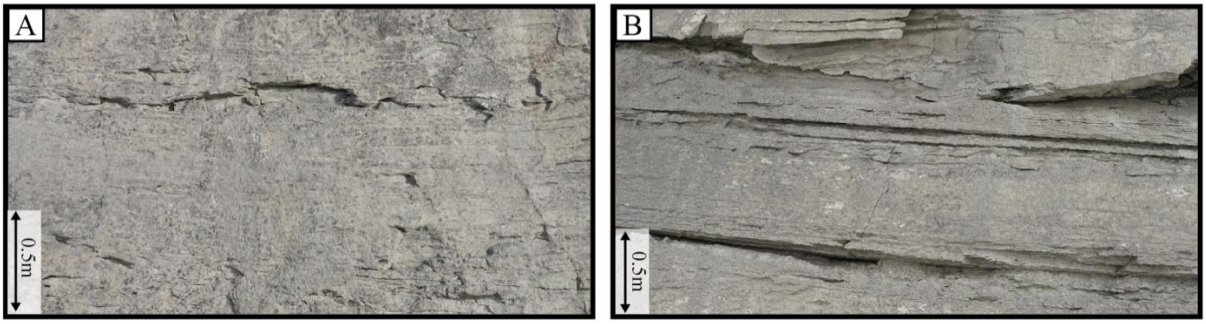

Figure 4.7: Low angle cross-stratified sandstones. **A:** Example of lithofacies S_{LACS} from the upper part of pseudolog 5. **B:** Example of lithofacies S_{LACS} from the upper part of pseudolog 4. Note that grain size measurements are lacking due to great highs. Figure 1.2 displays the locations of the pseudologs.

Lithofacies S_{CS}: Cross-stratified sandstone

Description: This facies consists of dark grey/brownish very fine- to medium-grained 0.2-1m thick sandstones. Amalgamated asymmetrical trough cross-stratification is the dominating structure, where the internal bedsets of the troughs downlap against the lower set surface (Figure 4.8). The troughs are isolated, irregular and become more than a meter in height and width. The trough cross-stratification sets are lenticular shaped. The lower surfaces are curved and erosive, while the upper boundaries are either erosive or gradual. Rip-up mud conglomerates and coal fragments are commonly observed within the facies, predominantly aligned along or near the base of the troughs. The low-angled cross-laminated sandstones are present in the early-stage deposits of the channel infill, while the plane parallel-stratified sandstones are observed in the late-stage deposits of the channel-infill.

Interpretation: The isolated and irregular troughs with erosional basal surfaces, suggests the development of scour and fill structures possibly establishing on channel bottoms or depressions. Erosion and fill from high energetic periods, such as storm and wave action are also capable of producing scour and fill structures (Reineck and Singh, 1980). Cross-stratified sandstones formed by migrating dunes are sparse along the studied succession. Few smaller tabular cross-stratified sandstones are possibly present within the tabular element. Due to the small scale, the structure can be easily mixed up with asymmetrical-ripple cross-laminated sandstones.

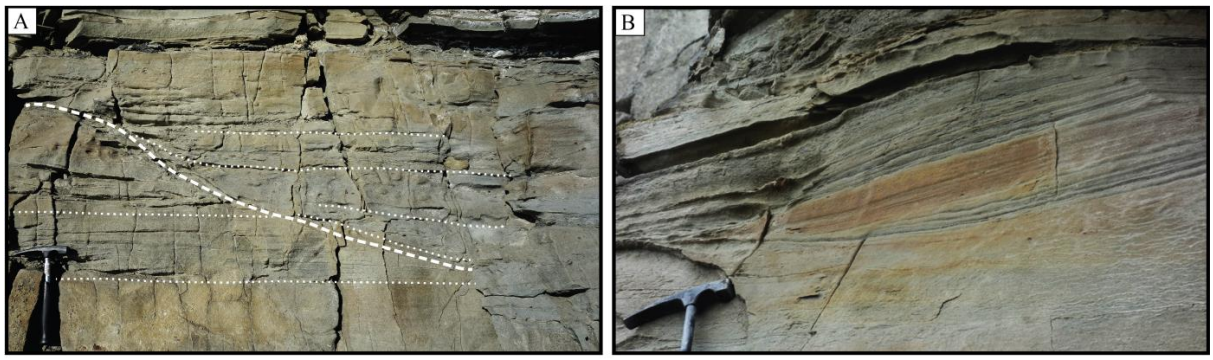

Figure 4.8*:* Scour and fill structures**. A:** The thick dashed line marks the erosive curved base of the scour and fill. The remaining lines mark up the stratification. Note that the tangential downlapping stratification changes into plane parallel to low- angle cross-stratification laterally and upwards within the succession, photo slightly proximal of pseudolog 1. **B:** Smaller scale scour and fill structure observed near pseudolog 5. Figure 1.2 demonstrates the locations of the logs.

Lithofacies S_{NG}: Normal graded sandstone

Description: Lithofacies S_{NG} is dominated by massive, homogenous, non-structured normal graded sandstone in 0.25- 5.3m thick units (Figure 4.9). The sandstones are moderately sorted and range from very fine- to medium in grain size. Intercalations of low angle cross-stratified sandstones (S_{LACS}) occur sporadically within the facies. The sandstones have an erosive base and gradual tops. The color is primarily grey and occasionally greyish-brown. Clasts of coal and siderite are common within the lithofacies.

Interpretation: Normal graded beds are a characteristic product of waning turbidity currents. The coal and rip-up mud conglomerates were transported within the turbidity current and settled out during the waning stage of the current (Bouma, 1962; Walker, 1967; Lowe, 1982; Middleton, 1993; Kneller, 1995).

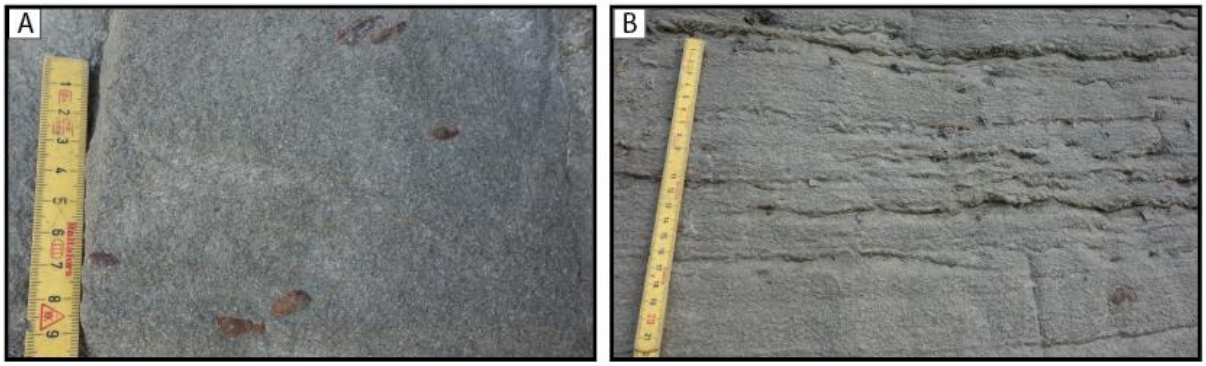

Figure 4.9: Normal graded sandstones **A**: Normal graded sandstone with massive appearance and rip-up mud conglomerates (log 9). Scale in centimeters. **B:** Normal graded sandstone with a massive appearance, which is weakly laminated (log 10). Scale in centimeters. Figure 1.2 displays the locations of the logs.

Lithofacies S_{MCC}: Matrix supported mud-clast conglomerate

Description: The lithofacies are located at the base of thicker normal graded sandstone beds of lithofacies S_{NG} (Figure 4.10). The matrix ranges from fine- to medium sandstone. The lithofacies have an erosional base and range from 0.3-1.6 m in thickness. The mudstone clasts are rounded and predominantly random oriented to occasionally display bed alignment and imbrication. The lithofacies are commonly succeeded by normal graded and plane parallel to low angle cross-stratified sandstones.

Interpretation: The mud-clast conglomerates located at the bases of normal thick bedded erosively based sandstones are interpreted to represent turbidity channel lag and deposition from basal scouring (Grundvåg et al., 2014b). The erosive lower base was scoured by high-density turbidity channels, similar to T_b division of Bouma (1962).

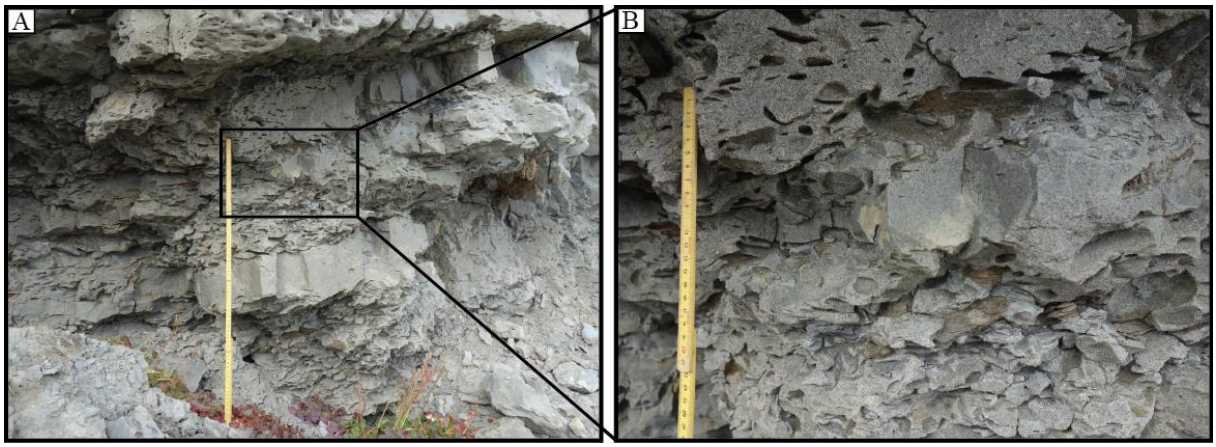

Figure 4.10: Matrix supported mud-clast conglomerate **A**: Matrix supported mud-clast conglomerate at the base of normal graded sandstone. **B:** Close up of the matrix-supported mud-clast conglomerate, scale in centimeters, (log 8). Location of the log is illustrated in Figure 1.2.

4.3 Ichnology

Introduction

The study of trace fossils along Clinothem 8C was performed and analyzed together with Dirk Knaust from Statoil ASA. Five different ichnotaxa were observed and recognized in the field. Most of the ichnotaxa were located in the scree-covered section under the base of clinothem 8C. The exact position of the blocks found in the scree-covered section is hard to determine. The blocks were normally a couple of centimeters thick, which makes it reasonable to believe that they were short transported. Nevertheless, the blocks could have been part of an originally larger block, or it could present scree-material from the overlying units. Trace fossils are used as an environmental indicator since the environmental conditions often constrain their behavior. However, most of the ichnotaxa are not in-situ, and they have therefore just been used as an additional indicator to verify the depositional environment. Below follows a description and interpretation of the different ichnotaxa documented in the study area.

Icnhotaxa

***Arenituba,* Stanley and Pickerill (1995) Previous named as *Micatuba,* Chamberlain (1971) (Figure 4.11)**

Description: Curved sand-filled tubes observed in dark grey fine-grained sandstone. The tubes are unbranched. The widths of the tubes vary from 0.3-0.5 cm and their lengths are up to 5cm.

Interpretation: The sand-filled tubes are interpreted to be traces of *Arenituba*. *Arenituba* represents feeding traces from clams. The traces are commonly found in shallow to marginal marine high energy environments. *Arenituba* is adaptable to brackish water conditions and is found in delta front deposits (Stanley and Pickerill, 1995).

Figure 4.11: Curved tube interpreted as an *Arenituba* trace. Found in a fine-grained sandstone block in the scree under Clinothem 8C.

Cylindrichnus, Howard (1966) (Figure 4.12)

Description: U-shaped burrows with unbranched morphology are observed. The dimensions range from a couple of centimeters to a decimetre in length while the width is a couple of centimeters. The traces are observed in the fine-grained grey and grey-brown sandstone blocks cemented with siderite.

Interpretation: *Cylindrichnus* are typical within the *Cruziana* ichnofacies, and is widespread in shelf settings to lower shoreface with low to moderate energy control (Knaust, 2017). *Cylindrichnus* is also a prevalent trace fossil found in sand dunes, storm deposits and shoals (Knaust, 2017). Deposit-feeding borrows from polychaete worms, or shrimps are interpreted as a suitable candidate for producing *Cylindrichnus*-like burrows (e.g., Gingras et al., 2008).

Figure 4.12: Siderite cemented *Cylindrichnus* burrow found in the scree-covered section under clinothem 8C.

***Diplocraterion,* Torell (1870) (Figure 4.13)**

Description: U-shaped burrows with unbranched morphology are observed in-situ in grey-brown very fine-grained sandstone. Two parallel tubes with narrow spacing and possible sperite development in between are observed.

Interpretation: The narrow tubes are interpreted as *Diplocraterion.* Most likely *D. habichi*. Nemerreans or Nereid Polychaetes are suitable candidates for producing *Diplocretarion*-like traces (Gingras et al., 2008). *Diplocraterion* is a common trace fossil of *Cruziana* ichnofacies (Knaust et al., 2012), and are commonly found in marginal marine settings (Gingras et al., 2008).

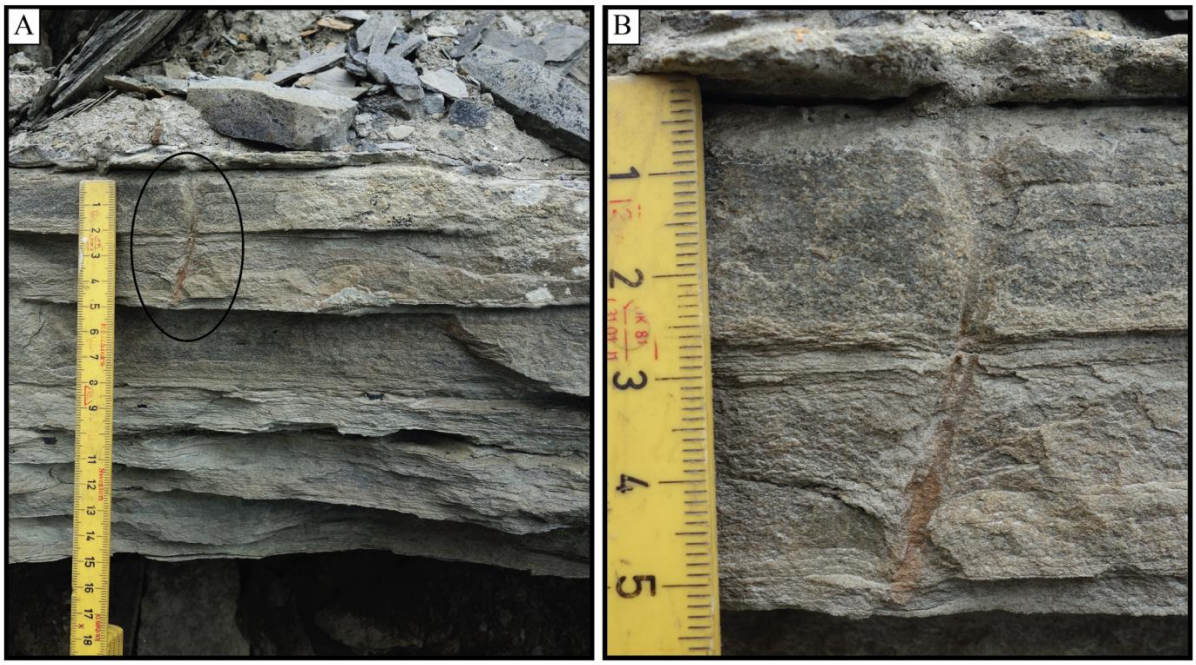

Figure 4.13: A-B: *Diplocraterion* indicated by the two parallel tubes creating a U-shaped burrow. The black circle marks up *Diplocraterion* on the photo to the left. Trace was found in-situ in log 1. Scale in centimeters on both photos. Location of log 1 is illustrated in figure 1.2.

***Kouphichnium*, Nopsca (1923) (Figure 4.14)**

Description: Straight lines with small footprints on both sides of the lines in very fine- and fine-grained grey to grey-brown sandstone blocks. The line of the trace fossil is 0.5cm wide and 20-30cm long. The footprints are 1cm in width and 1.5cm in length. The sandstone blocks were found in the scree-covered section under the clinothem, and are therefore not in-situ traces.

Interpretation: *Kouphichnium* occurs on sandy substrate and is of shallow marine origin. The traces are particularly widespread in beach and lake deposits. The traces are interpreted to originate from *Lumulids*. Rudloe (1981) identified *Limulids* on the eastern continental shelf of North America down to 30m depths. *Limulids* are predators, and the traces are interpreted to be locomotion traces.

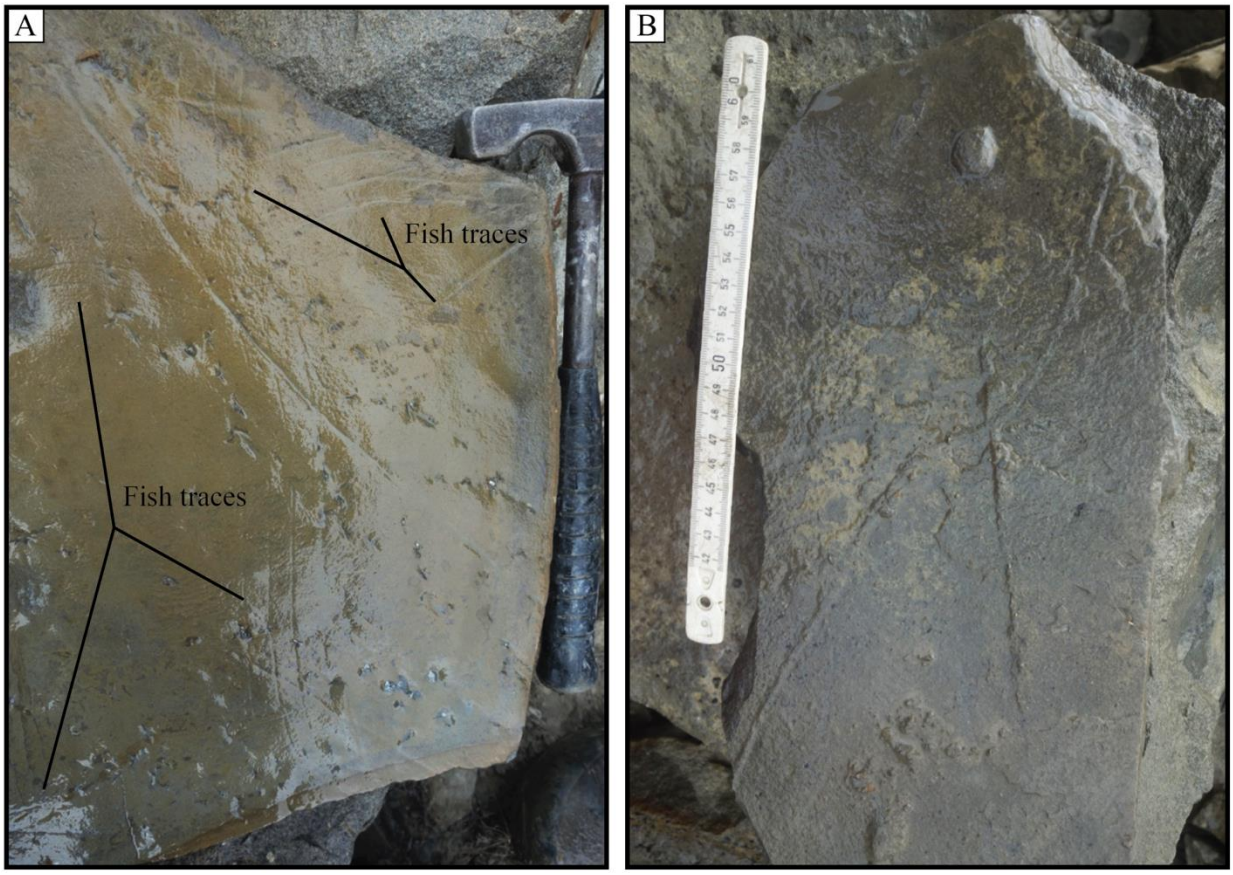

Figure 4.14: Fish traces and traces of *Limulids*. **A:** The black lines point towards fish traces. The traces of *Limulus* are observed in between the fish traces. The line represents the tail and the small traces along the line represents the footprints of the *Limulids.* Geological hammer for scale is 30cm long. **B:** Limulus is identified by the straight to slightly curved ridges. Scale in centimeters.

***Protovirgolaria,* M'Coy (1850) (Figure 4.15)**

Description: Straight to sinuous elongated ridges. The dimension of the ridges is approximately 0.5cm thick and the lengths vary from 2-30cm. The ridges are documented in fine-grained grey and grey-brown sandstone blocks in the scree.

Interpretation: *Protovirgolaria* is common in heterolithic marginal marine deposits, and is typically found in distal delta front to tide-influenced distal prodelta deposits (Carmona et al., 2009). The traces of *Protovirgolaria* are commonly found in nearshore environments that have been prone to stressed conditions with fluctuating salinity, sedimentation, turbidity and oxygen deficiency. Normally chevronate structures are associated with *Protovirgolaria,* representing the push-and-pull mechanism of a split-foot mollusk (protobranch bivalve or a scaphopod) (Carmona et al., 2010). Based on the type of morphology of the chevron pattern, the type of sediment and the sedimentary facies can be further classified. However, clear chevron structures were not observed in the sandstone blocks.

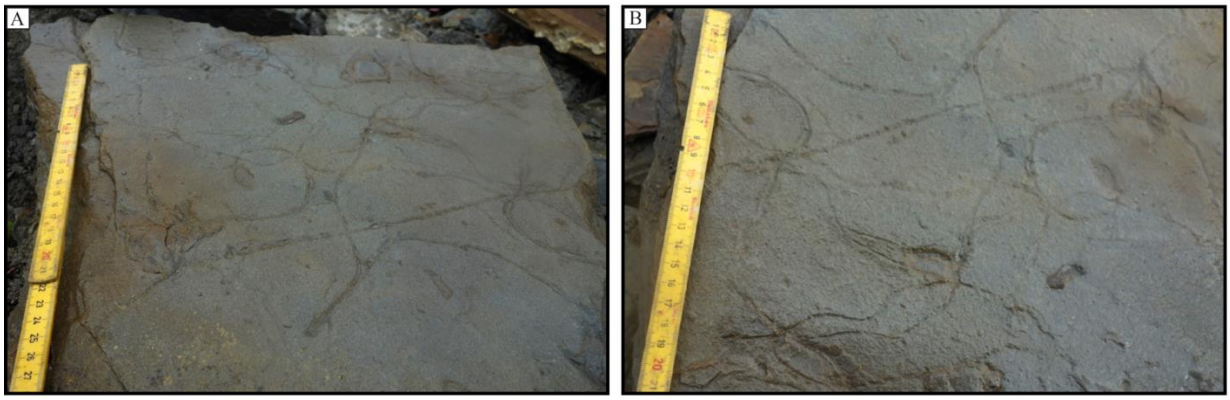

Figure 4.15: A-B: Straight to sinous elongated ridges in fine-grained sandstone indicating *Protovirgolaria* traces. Scale in centimeters on both photos.

Siphonichnus, Stanistreet et al. (1980) (Figure 4.16)

Description: Patches with a linear to bow-shaped morphology filled with fine-grained sandstone are identified. In cross-section, the trace fossils have a circular to oval core filled with fine-grained sandstone. The traces are observed in fine-grained grey sandstone blocks in the scree under log 3 (Figure 1.2).

Interpretation: *Siphonichnus* is a part of the *Skolithos* ichnofacies and is typical in shallow marine to marginal marine environments, often related to stressed environments with fluctuating salinity and fresh water influx (Knaust, 2015). *Siphonichnus* is distributed in offshore and shoreface to deltaic, estuarine and lagoonal environments, and it is highly tolerant against the influence of brackish water (Knaust, 2017). *Siphonichnus* is interpreted as a locomotion or feeding trace produced by clams.

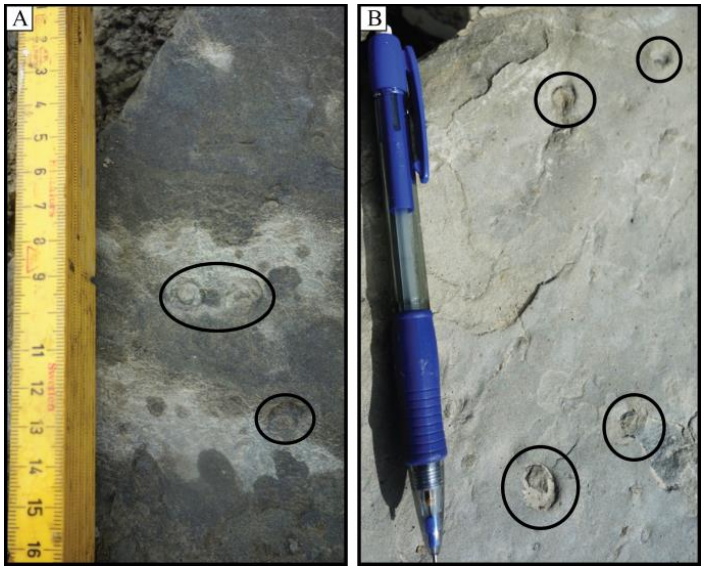

Figure 4.16: *Siphonichnus* in cross-section with filled core on fine-grained sandstone blocks (A-B). The black circles mark up the traces.

Implications for a depositional model

In total six different ichnotaxa were identified along the studied section. Only one was found in-situ (*Diplocraterion*), while the others were found in the scree-covered section under the clinothem. The low diversity and density of trace fossils in the area reflects stressed environmental conditions. Factors influencing the diversity of ichnotaxa can be related to the temperature, flow velocity, substrate, salinity, turbidity, rates of erosion, topography and the speed of the changes. The observations of coal fragments, rip-up conglomerates, soft-sediment deformed sandstones and the dirty unsorted sandstones support the notion of a stressed environment with frequent erosional events and turbulent flow. The ichnotaxa observed within the succession are grouped in the *Skolithos* and *Cruziana* ichnofacies, which are dominant in shallow to marginal marine environments. Traces from pioneers such as bivalves are identified several places along the section. Bivalves are a highly successful and adaptable class of invertebrates which thrive in fully marine conditions to brackish and estuarine waters. Figure 4.17 summarizes the different dominating ichnotaxa for a wave-and-fluvial dominated delta. Prodelta and the delta front are interpreted to be the habitats for the traces described. Burrows interpreted to be *Diplocraterion* were identified in-situ within the clinothem. By burrowing into the substrate, the species are protected from possible currents, turbulence, salinity changes and predators. This defense mechanism makes it possible for classes such as bivalves to survive and to colonize the stressful environments which the studied shelf-edge-to-slope system represents.

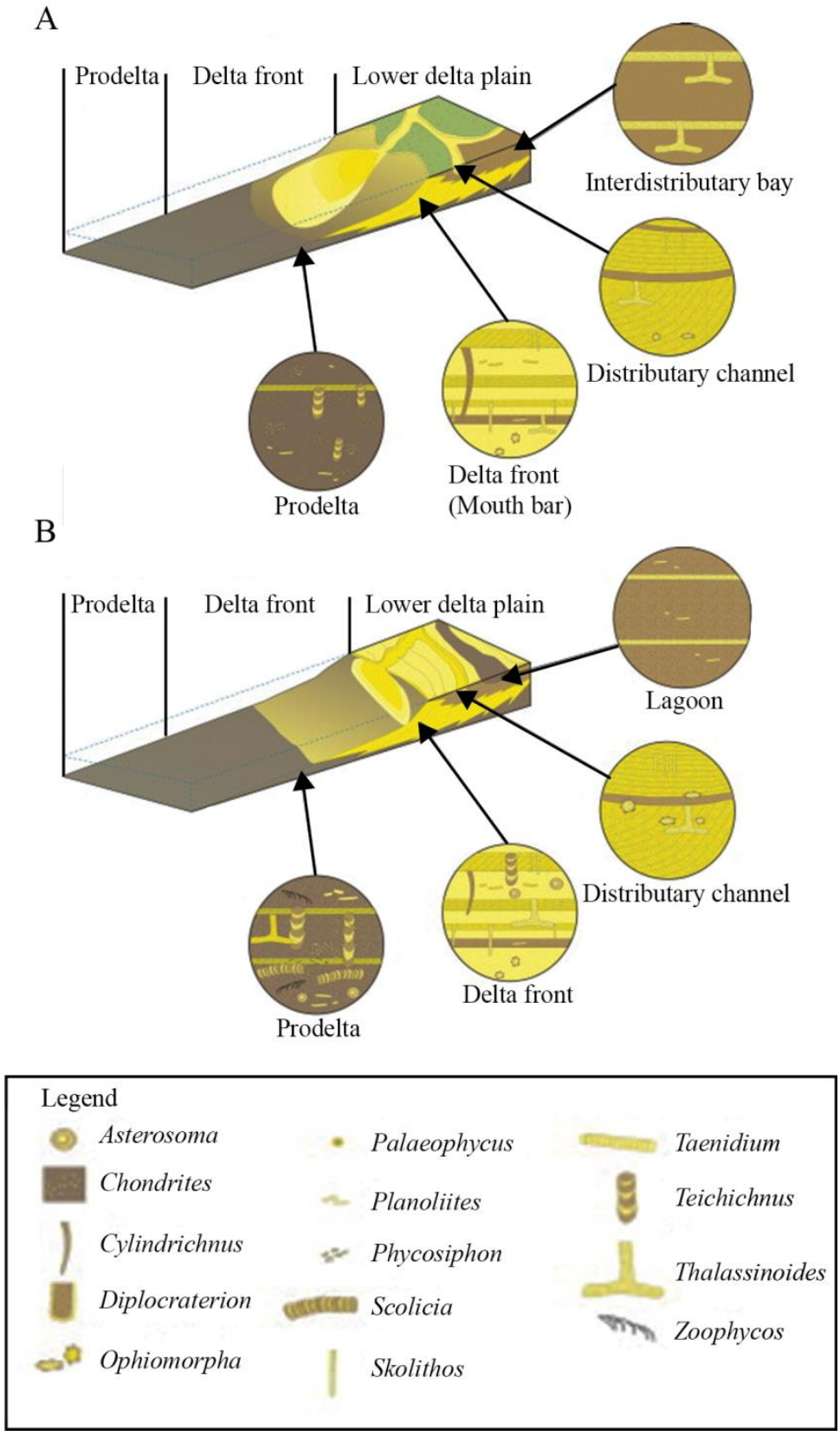

Figure 4.17: Diagram of the depositional environment with idealized illustrations of the corresponding ichnotaxa. Traces of *Cylidrichnus*, *Diplocraterion* and *Skolithos* can be identified in the diagram; these traces were also identified in this study. **A:** fluvial-dominated delta, **B:** wave-dominated delta. Note the high density and diversity at the delta front in the ideal wave-dominated delta, which contradicts with this study. Frequently bypassing turbulent sediment-laden currents are believed to explain the lower density and diversity in bioturbation of the studied succession. Diagram slightly modified from Allen (1970).

4.4 Facies associations

Introduction:

Based on detailed sedimentary analysis three facies associations has been distinguished, each representing a specific depositional environment. A brief description is provided in table 4.2, while complementary descriptions and interpretations of the individual facies associations are presented below. Figure 4.18 illustrates a simplified sketch with the general lateral distribution of the facies association from proximal to distal along clinothem 8C, while figure 4.19 gives an overview with the interpreted facies associations.

Table 4.2: Facies associations which clinothem 8C are grouped into.

	Facies Association	Component Lithofacies
FA1	Prodeltaic mudstones	Dominant: M_L Subordinate: S_{SSD}, S_{PPS}, S_{SRCL}
FA2	Wave reworked lobe deposits	Dominant: S_{PPS}, S_{SRCL}, S_{NG}, S_{LACS} Subordinate: S_{ARCL}, S_{CS}, S_{HCS}
FA3	Channel fill deposits	Dominant: S_{PPS}, S_{NG}, M_{CC}, S_{LACS} Subordinate: S_{SSD}, S_{HCS}, S_{SRCL}, S_{CS}, S_{ARCL}

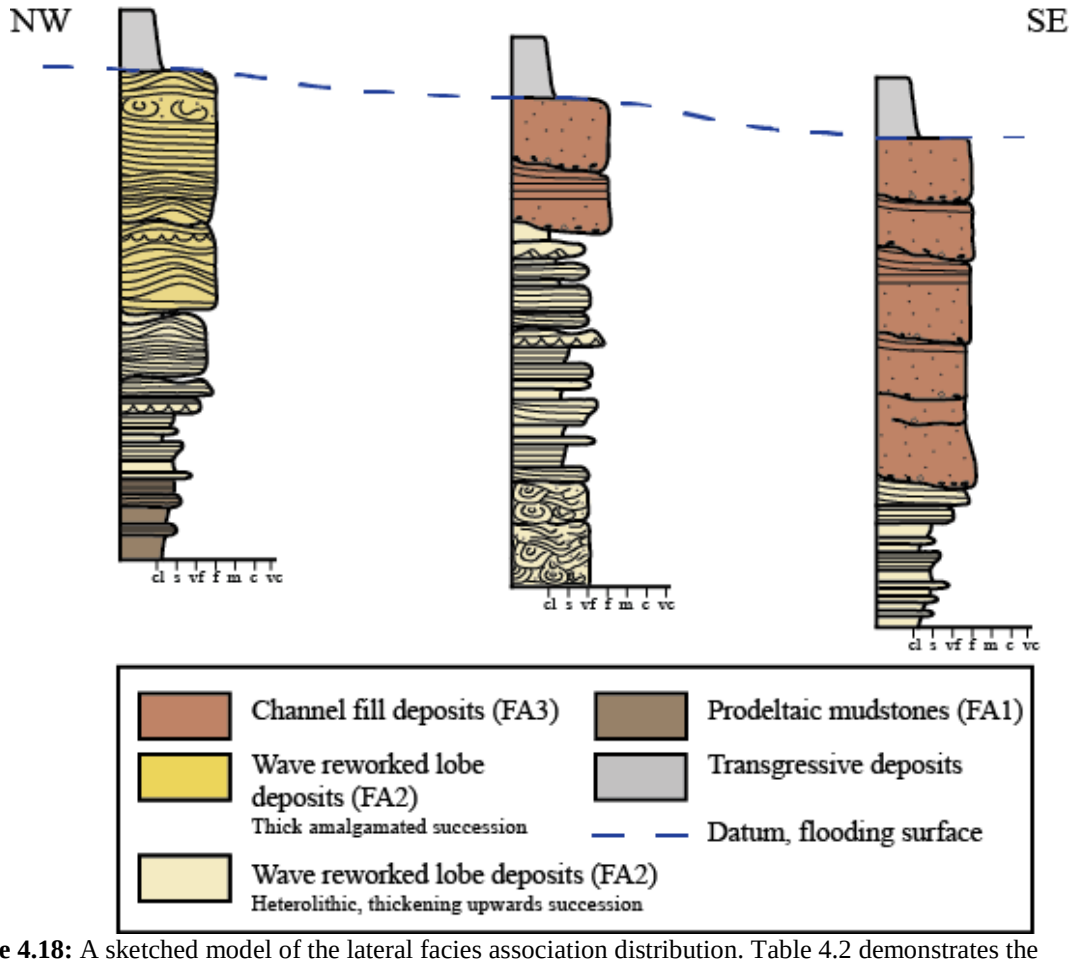

Figure 4.18: A sketched model of the lateral facies association distribution. Table 4.2 demonstrates the dominant and subordinate component lithofacies for the logged section. For complete legend, see Appendix.

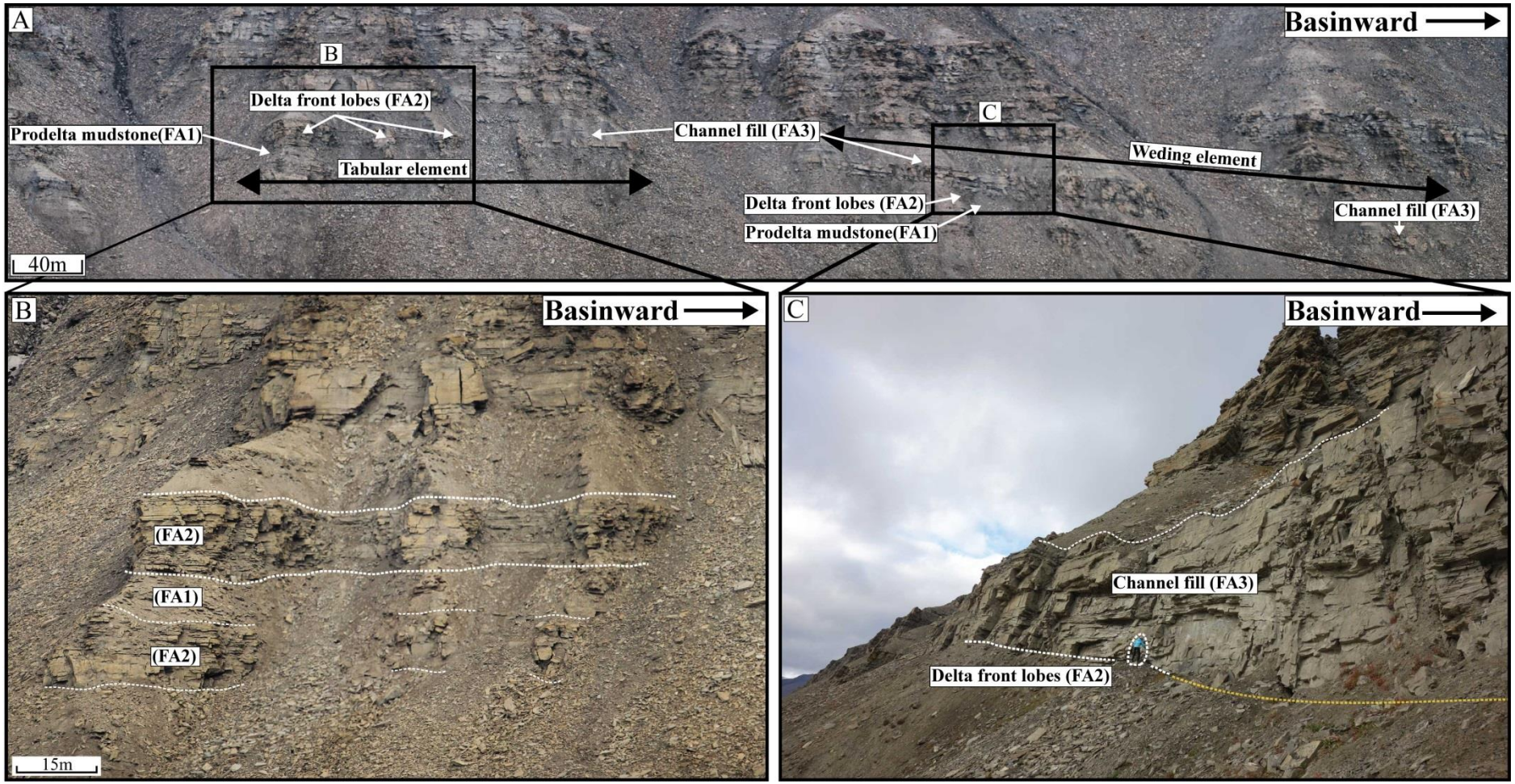

Figure 4.19: Identified facies associations in this study. **A:** Overview of the studied succession which comprises a tabular and a wedging element, the black rectangles indicates the location of photo B and C. **B:** Part of the tabular unit with delta front lobes (FA2) and prodelta mudstones (FA1).**C:** Middle part of the wedging unit with delta front lobes succeeded by channel fill deposits. The identified upper and lower boundary is marked with a white dashed line, while the yellow line presents the interpreted lower base of the wedging unit (scree-covered). The person for scale in the photo is 175cm. Note that the boundary between the prodeltaic mudstones and the lobe deposits are transitional.

Facies Association FA1: Prodeltaic mudstones

The section where FA1 is present has been prone to an extensive degree of weathering; as a result, most of FA1 is covered by scree in the study area. Few previous studies along the Van Keulenfjorden transect and in The Central Basin have focused on the thick muddy successions, which often are referred to as background sedimentation. The description of FA1 is therefore based on few field observations combined with descriptions made during previous work at Spitsbergen performed by Henriksen et al. (2010); Grundvåg et al. (2014a) and studies on the Cretaceous Seaway in North America performed by Bhattacharya and MacEachern (2009).

Description: This facies association is characterized by the black to dark grey color, monotonous to weakly laminated mudstone (M_L) (Figure 4.1) with the occurrence of an increasing amount of siltstones and very fine-grained sandstones upwards within the unit.

The mudstone is mostly massive and unstructured, occasionally comprising features such as weakly undulating non-continuous lamination, some organic material, a few rip-up mud conglomerates in the sandy intervals and a low index of bioturbation in the muddy intervals. Weakly undulating lamination, which may be undifferentiated ripples is sporadically seen in the coarser grained units of the lithofacies. Symmetrical ripple cross-laminated sandstone (S_{SRCL}) are recognized in the uppermost part of FA1.

Interpretation: Based on the general coarsening upwards succession, ranging from the dark lowermost mudstones to the uppermost siltstones and sandstone, the massive to non-consistent lamination and the presence of organics and rip-up mud conglomerates FA1 is suggested to reflect an overall shallowing upwards trend.

The traditional interpretation of how ancient shelf muds have been deposited commonly imply suspension fall-out and deposition in a calm, low-energy environment (Pettijohn, 1975; Bhattacharya and Walker, 1992; Prothero and Schwab, 2004; Boggs, 2006; Nichols, 2009). However, Rine and Ginsburg (1985) studied a high-energy prograding muddy shoreline and the corresponding inner shelf deposits along the modern Coast of Suriname. Recent studies of worldwide delta complexes show extensive mud-dominated coastlines and inner-shelf mud belts, which are commonly elongated downdrift of the river mouth (Bhattacharya and

MacEachern, 2009). The Mekong in Vietnam (Ta et al., 2005), the Po delta in the Adriatic (Cattaneo et al., 2003; Cattaneo et al., 2007) and the Atchafalaya in the Gulf of Mexico (Augustinus, 1989; Allison and Neill, 2003; Rotondo and Bentley Sr, 2004) are some modern examples.

We hypothesize that this facies association presents accumulated prodeltaic deposits deposited directly from hyperpycnal mud plumes (Figure 4.20). A hyperpycnal plume ignites when the river density exceeds the density of the receiving water body. Triggering factors for the development of hyperpycnal plumes may be related to inflated river discharge during flooding or storm waves (Mulder and Syvitski, 1995; Khan et al., 2005; Bhattacharya and MacEachern, 2009). According to Parsons et al. (2001), low sediment concentrated hyperpycnal plumes can rapidly evolve into hyperpycnal flows during expeditious flocculation of clay and fine-grained sediments. Small drainage basins with direct sediment input from dirty-sediment rich rivers near tectonically active mountains are favorable for producing hyperpycnal flows (Mulder and Syvitski, 1995). The Central Basin presented a small, restricted basin with high fluvial influx, which could suggest that the basin was prone to experience occasional increases in brackish water content, which also would favor the creation of hyperpycnal plumes.

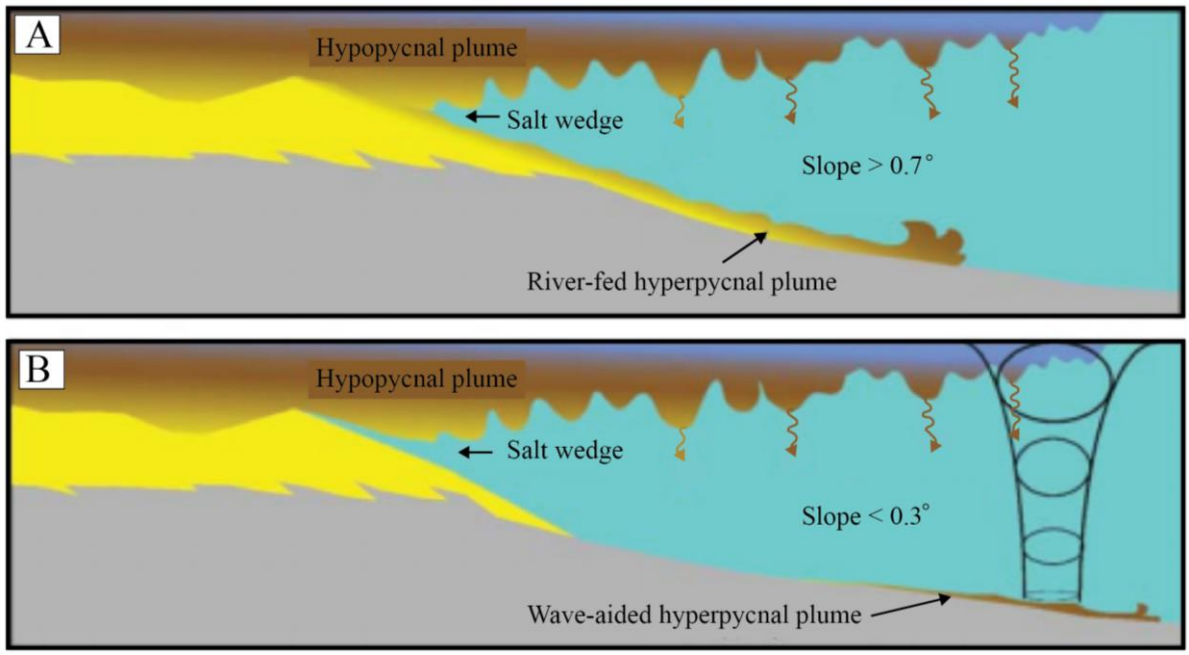

Figure 4.20: Slope control for hypopycnal and hyperpycnal plumes in river mouths. **A:** Fluvial-fed hyperpycnal plume form on slopes > 0.7°. **B:** Wave-aided or tide generated hyperpycnal plume dominates slopes < 0.3°. Note the difference in sediment thicknesses of the developed hyperpycnal plumes. The collapse of the hypopycnal plume may feed the hyperpycnal plumes. Cartoon slightly modified from Bhattacharya and MacEachern (2009).

During floods and the subsequent waning stage, distributary channels and mouth bars loses their capacity, resulting in rapid fall out and deposition of sand lenses and thin sand streaks. This interpretation indicates a fairly proximal setting with direct input of sediment from mouth bars. Henriksen et al. (2010) suggested that the mud layers might represent deposition as a result of clay flocculation from supersaturated rivers. Rapid accumulation of clay will provoke soft-sediment layers, which are prone to undergo sliding if overloading or disturbances follow (Henriksen et al., 2010). Seasonal climate changes with complementary storms and snow-and-ice melting may trigger the flooding of the rivers (Mulder et al., 2003). As an aftereffect, even in completely marine settings, the rivers may alternate between hyperpycnal and hypopycnal conditions (Mulder and Syvitski, 1995; Nemec, 1995; Parsons et al., 2001). The occurrence of ripple laminated sandstone, as well as small undulating lamination imply influence of currents, and possibly increasing proximity to the storm-wave base. The minimal to absence rate of bioturbation substantiates the notion of a lifeless, stressed environment with high sedimentation rates and limited time for biota to establish. Similar thin bedded muddy deposits were studied by Pontén and Plink-Björklund (2009) on the eastern side of Storvola and by Henriksen et al. (2010) on the eastern side of Hyrnestabben.

Facies Association FA2: Wave reworked lobe deposits:

The delta front deposits of FA2 constitutes the dominating succession of the tabular unit (Figure 4.19 and 4.22A). FA2 ranges from a couple of meters to 12 meters in vertical thickness. The facies association is coarsening upward from the heterolithic deposits to a sandstone dominated facies (Figure 4.21). The facies association is divided into heterolithic deposits and amalgamated sandstone deposits. In the lower reaches the deposits of FA2 are interfingering with the prodelta mudstones of FA1 (Figure 4.19).

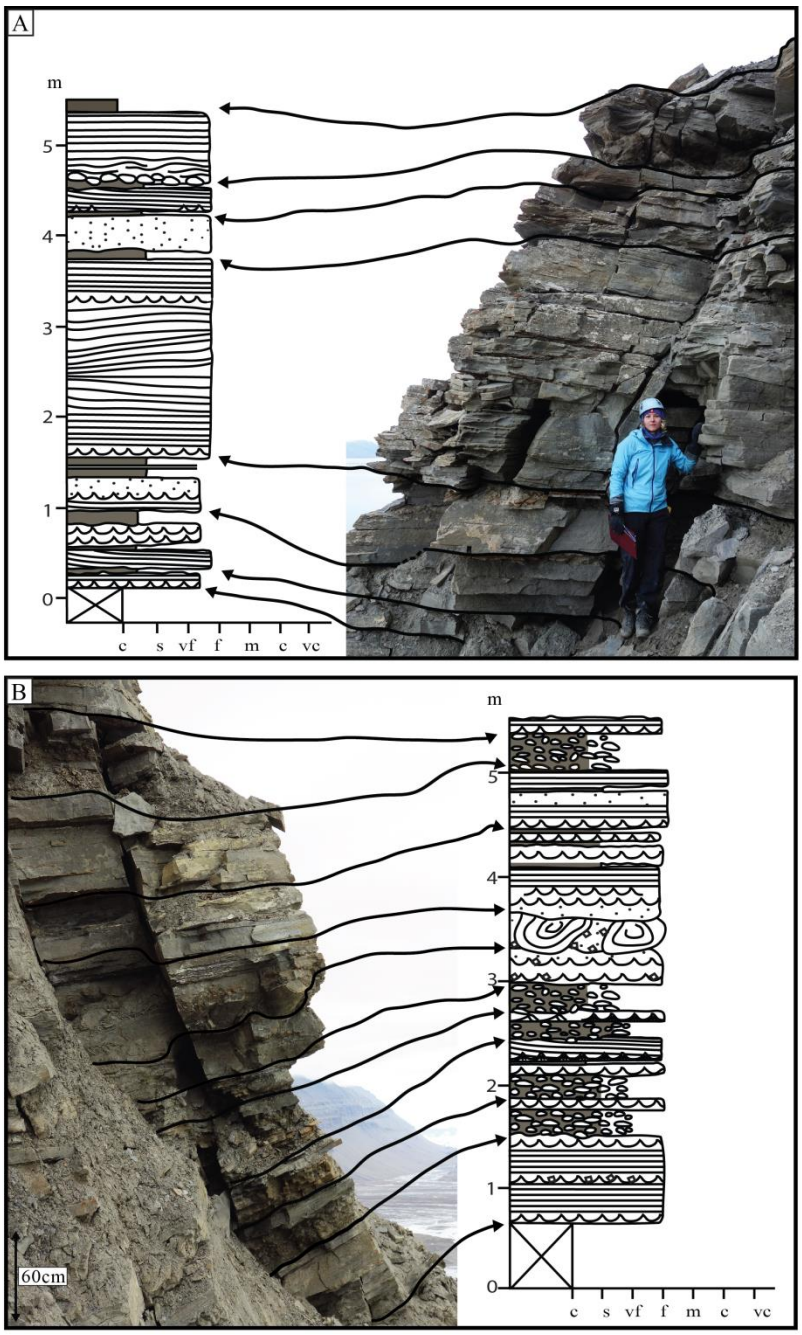

Figure 4.21: Delta front lobe deposits of FA2. **A:** The upper reaches of the lobe deposits comprises thick amalgamated sandstones, which are commonly wave reworked. The person for scale is 175cm. **B:** Lower reaches of the facies association is heterolithic, thickening upwards to the deposits of photo A. For legend, see Appendix.

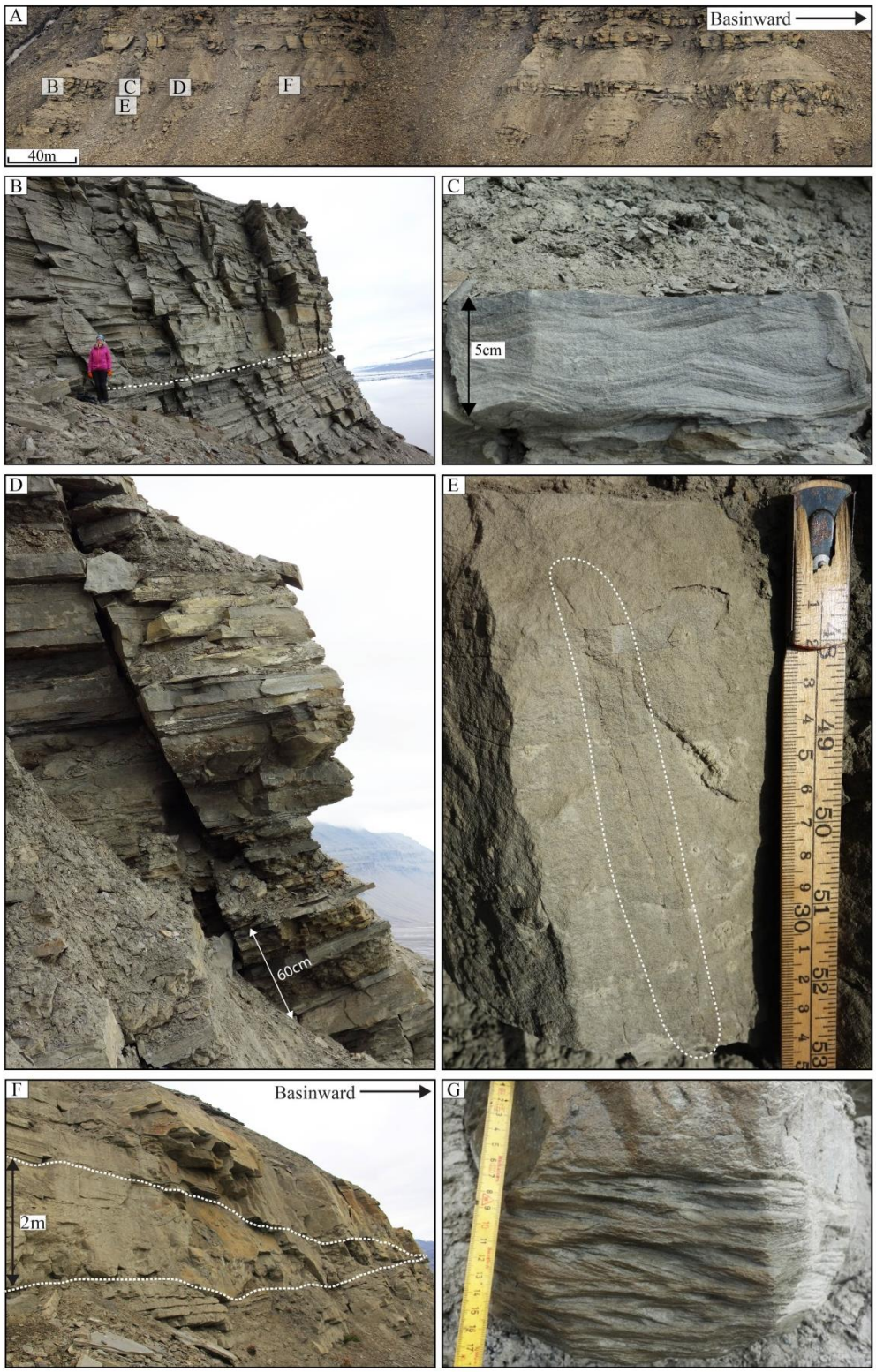

Figure 4.22: Photographs are demonstrating delta front deposits. **A:** Location of the studied delta front deposits (B-G). **B:** Overview of log 1, note the upwards thickening stacking pattern within the lobe deposits. The dashed white line separates the thin bedded heterolithic deposits from the succeeding thick bedded very fine-grained sandstones. The person for scale is 185cm. **C:** Wave ripple cross-laminated sandstones are abundant in the facies association, log 2. **D:** Alternating beds of soft-sediment deformed sandstone (S_{SSD}) and plane parallel-stratified sandstone (S_{PPS}), log 3 **E:** Burrow of *Diplocraterion* identified in-situ in the heterolithic section of log 2. **F:** Possible slumped unit, separating the delta front lobe deposits (FA2) from the channel fill deposits (FA3). The unit is pinching out in both directions (northwest and southeast). **G:** Climbing current ripple cross-laminated sandstones in log 8 scale in centimeters. Figure 4.19 illustrates the location of the logs.

Description:

Heterolithic deposits: Heterolithic deposits comprising alternating mudstones and very fine- to fine-grained sandstones dominate the lower units of FA2 (Figure 4.22B). A sheet-like geometry characterizes the beds. The mudstone units range from 5-40cm with an average thickness of 12cm. The sandstone units range from 5-50cm in thickness with an average thickness of 25cm and contain plane parallel to low-angle cross-lamination and soft-sediment deformed sandstones. The abundance and thicknesses of sandstones increase upwards within the deposits. An approximately 7m partly scree-covered section was documented above the soft-sediment deformed sandstones in log 7 (Figure 4.19). Intercalations of asymmetrical ripple cross-laminated sandstone (Figure 4.22G), symmetrical ripple cross-laminated sandstone (Figure 4.22C) and hummocky cross-stratified sandstone occur in intervals within the facies association. The abundance of soft-sediment deformed sandstones increases in a south-eastern direction within the heterolithic thickening upwards succession (Figure 4.22D). Flame structures, convolute bedding and ball and pillows in units from 30cm to 80cm are documented in log 1-3. Rip-up mud conglomerates and organic fragments are typically aligned within the low angle cross-stratified sandstones and are commonly identified within the soft-sediment deformed sandstone beds (S_{SSD}).

Thick amalgamated sandstones: Amalgamated wedged shaped very fine- to fine-grained sandstones dominate the topographically highest reaches of the facies association (Figure 4.22B). The units are slightly upward coarsening and consist of hummocky cross-stratified sandstone (S_{HCS}), symmetrical ripple cross-laminated sandstone (S_{SRCL}) and plane parallel-stratified sandstone (S_{PPS}). The base of the unit is either erosive or loaded (Figure 4.22B). The amalgamated very fine- to fine-grained hummocky cross-stratified sandstone (S_{HCS}) are commonly succeeded by very fine- to fine-grained sandstones containing alternating symmetrical ripple cross-laminated sandstone (S_{SRCL}) and plane parallel-stratified sandstone (S_{PPS}) to low angle cross-stratified sandstone (S_{LACS}). Thinner (5-15cm) laminated mudstone of lithofacies M_L occasionally separates the sandstones. The soft-sediment deformed units have a wedge-shaped geometry and the units tend to pinch out in both directions (northwest and southeast) (Figure 4.22F). The pinch-out distance is approximately 500m (see Grundvåg et al. (2014a)), while Mellere et al. (2003) identified the pinch out distance for the chaotic unit to be 300 meters. The units with soft-sediment deformation become up to 2m in thickness, where balls and pillows and flame structures dominate.

The degree of bioturbation of the sandstone beds is assessed to be of low degree. Traces of *Diplocraterion* (Figure 4.22E) were observed in-situ in the lower heterolithic deposits of the facies association. *Kouphichnium* (Figure 4.14), *Cylindrichnus* (Figure 4.12), *Arenituba* (Figure 4.11) and *Siphonichnus* (Figure 4.16) were interpreted traces identified in the sandstone blocks in the scree-covered section beneath the recognized delta front deposits (described in chapter 4.3).

In a landward direction, this facies association can be laterally traced into fluvial dominated mouth bars and distributary channels, which have not been a topic for this thesis (e.g., Plink-Björklund et al., 2001; Mellere et al., 2003; Plink-Björklund and Steel, 2004; Grundvåg et al., 2014a).

Interpretation:

Based on the internal lithofacies dominated by traction, wave and current generated structures, the upwards increase in sand and amalgamation rate, the stratigraphic position and the low internal degree of bioturbation, FA2 is interpreted to represent delta lobe progradation. According to Mellere et al. (2002); Petter and Steel (2006) the lobes were directly fed by the distributaries located on the shelf. The heterolithic deposits are interpreted to represent deposition from approaching lobes settled out on the lower delta front. The approximately 7m partly scree-covered section in log 7 (Figure 1.2) is assumed to be comprised of prodeltaic mudstones (FA1). The abrupt deepening is interpreted to represent a flooding surface. The flooding surface can be laterally traced to log 1. The flooding surface is interpreted to separate two different delta lobes (further described and interpreted in chapter 5.3).

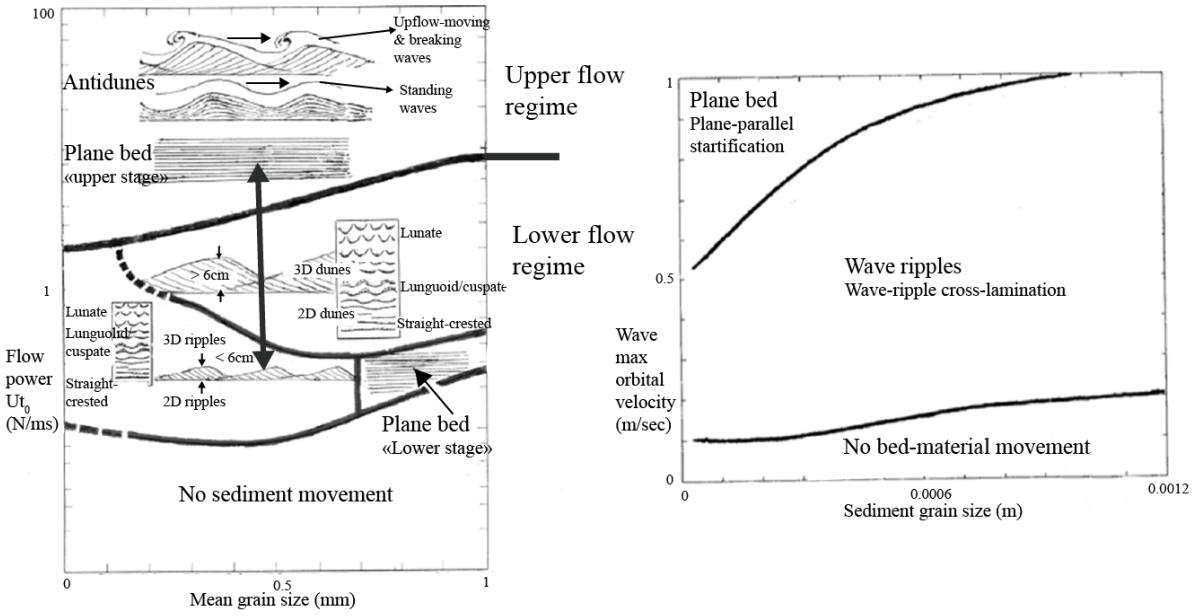

Figure 4.23: Bedforms in relation to hydraulic conditions. **A:** Flow regimes according to bedform phase produced in the lower and upper flow regimes; slightly modified from Allen (1982). The large arrow highlights the alternation of facies S_{SRCL} and S_{PPS}. **B:** Bedforms produced by waves; slightly modified from Komar and Miller (1975).

The alternation of symmetrical ripple cross-laminated sandstone (S_{SRCL}) and plane parallel-stratified sandstone (S_{PPS}) is common within the lobe deposits. The alternation and the absence of cross stratification produced by migrating dunes is explained by (Figure 4.23); (1) the grains size being too small (< 0.15mm), (2) the transition time being too short; (3) the water depth may being too shallow to enable creation of dunes (Allen, 1982). The two first mentioned factors are possible reasons for the alternation between symmetrical ripple cross-laminated sandstone (S_{SRCL}) and plane parallel-stratified sandstone (S_{PPS}) in the upwards coarsening section. In shorefaces dominated by waves and storms, the dunes tend to be obliterated by the high energy and replaced by plane parallel-stratified sandstone (S_{PPS}) or hummocky cross-stratified sandstone S_{HCS} (Greenwood and Sherman, 1986). The frequent shift of plane parallel-stratified sandstone (S_{PPS}), symmetrical ripple cross-laminated sandstone (S_{SRCL}) and hummocky cross-stratified sandstone (S_{HCS}) imply numerous stages of reworking by waves and occasional storm waves on the delta front.

Delta front lobe deposits are normally coarsening and thickening upward, where each lobe generates a parasequence (Bhattacharya, 2010). By comparison, the studied units are thickening upwards, and slightly coarsening upwards, although the trend is not very distinct. A reasonable suggestion for the relatively homogenous grain size could be that the coarser grained sediments settled out closer to the source, proximal of the studied succession,

resulting in a dilution and depletion of the sediments. Another suggestion might be that the majority of the available sandstones in the source area were initially fine-grained.

The soft-sediment deformed sandstones are most likely to be formed in-situ as a result of liquefaction and fluidization processes caused by the density differences between the sand, silt and mud. However, several studies along the Van Keulenfjorden transect (Figure 1.3) have identified slumping. Petter and Steel (2006) and Pontén and Plink-Björklund (2009) revealed slump deposits at Storvola in the gravitational process dominated delta front and shelf-edge deposits. The thick soft-sediment layers could possibly present slumped units. The slumping (Figure 4.22F) could be the product of a series of retrogressive slumps. The slump deposits are separating the fining-upward channelized deposits of FA3 from the underlying lobe deposits of FA2. Furthermore, slumped units located in the scree-covered section cannot be excluded.

The ichnodiversity and the density of the bioturbation are low, which imply a high degree of stress. The presence of amalgamated "hummocks", the soft-sediment deformed sandstones, the evidence of strong episodic influx of fresh water into the basin and the regional understanding of a supply-driven system (e.g., Maceachern et al. (2005) Porebski and Steel (2006); Li et al. (2011)) supports this notion.

Facies Association FA3: Channel fill deposits

FA3 dominates the distal upper reaches of the tabular element and predominates the wedging element (Figure 4.19). The deposits of FA3 are dominated by fine- to upper fine-grained sandstones; although medium-grained sandstones are also present (Figure 4.24). The base of the facies association is primarily covered by scree in the distal parts of clinothem 8C, hence the description of the base is from the middle part of clinothem 8C (Figure 4.19 and 4.25A).

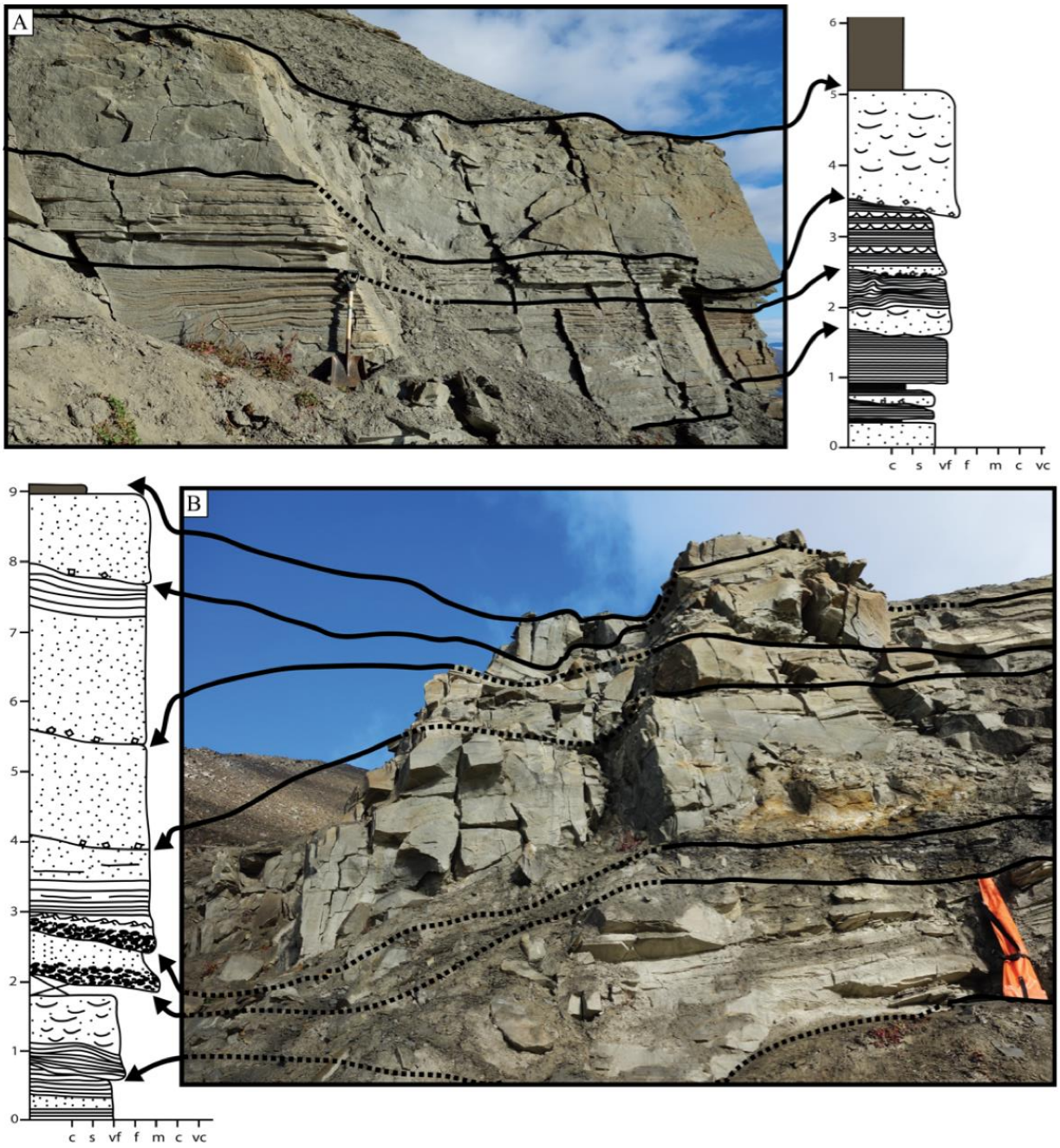

Figure 4.24: Photographs with corresponding sedimentary logs of the channel infill deposits of FA3. **A:** Thin-bedded turbidite succession erosively overlain by thick amalgamated turbidite deposits. Shovel for scale is 110cm high. **B:** Lobe deposits of FA2 (lower 2m) succeeded by thick bedded erosive turbidite deposits of FA3, rifle for scale is 100cm high. For legend, see Appendix.

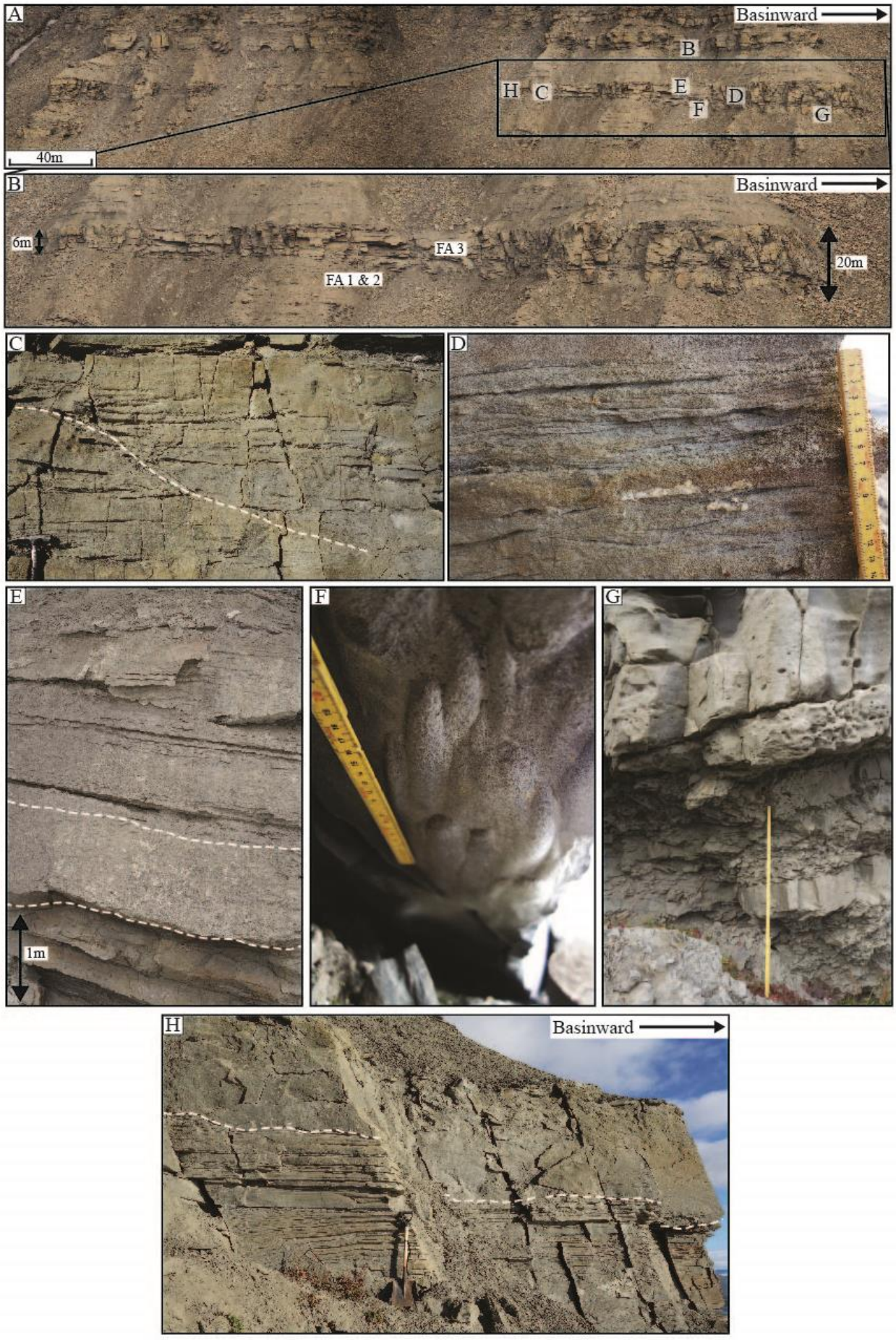
A
Basinward
B
H
C
E
F
D
G
40m
B
Basinward
6m
FA 3
FA 1 & 2
20m
C
D
E
1m
F
G
H
Basinward

Figure 4.25 (previous page): Photographs illustrating channel infill deposits of FA3 from the shelf-edge to the upper slope. **A:** Location of the studied channel fill deposits (B-G). **B:** Channel incision of FA3 cutting into lobe deposits (FA2) and prodelta mudstones (FA1). The unit is wedging in a basinward direction and thickens from 6 to 20 meters. **C:** Low-angle trough interpreted as a scour and fill structure, northwest of photolog 1. **D**: Alternation of plane parallel-lamination and ripple cross-lamination in fine-grained sandstone, slightly landward of photolog 6. **E:** Massive sandstones succeeded by plane parallel to low-angled cross-laminated sandstone characterize the thick bedded sandstones. The different lithofacies are separated by dashed lines. Sections of soft-sediment deformed sandstones are common (seen below the dashed line at the photo), although the prevalence decreases distally along the clinothem. Photo from the upper reaches of photolog 4. **F:** Flute marks from the base of the channelized sandstones. Photo from the channel base of photolog 5. **G:** Thick accumulations of rip-up mud conglomerates from the channel base. Photo from of log 7. **H:** Upwards fining channelized succession succeeded by a non-graded massive thick bedded turbidite with dish structures, possibly presenting Bouma T_a division. Figure 4.19 shows the location of the logs.

Description:

The facies association consists of grey/ brownish sandstones with grain sizes ranging from very fine- to medium. Fining upward successions from fine- to very fine-grained sandstones in 0.5-2.5m thick units are observed in the landward reaches within the facies association (log 4-6) (Figure 4.24A and 4.25H). The upper and lower boundaries are erosive. Downslope the fining-upward channelized units are replaced and eroded by the thick bedded normal graded sandstones.

Thick bedded poorly sorted sandstones ranging from upper stage very fine- to medium-grain size dominates the wedging unit from log 6 and basinward (Figure 4.24B). The basal unit of FA3 is characterized by a deeply scoured (relief of 3m) and very irregular contact (Figure 4.25G), while the top is erosive. The basal erosion surface cuts down into the deposits of the underlying prodeltaic mudstones of FA1 and lobe deposits of FA2 (Figure 4.25B). Multiple scouring surfaces or smaller scour and fill structures with coal and rip-up mud conglomerates along the erosive bases occur sporadically. The troughs are filled with upwards flattening low-angle cross-laminated very fine- to fine-grained sandstones (Figure 4.25C).

Flute marks were observed under the lower surface of the base along the wedging unit (Figure 4.25F). A series of stacked, erosively based thick bedded (2.5-5m) amalgamated very fine- to medium-grained sandstones follow the basal contact along the wedging unit. Amalgamated normal graded massive sandstones succeeded by plane parallel- to low-angle cross-laminated sandstones dominate the beds (Figure 4.25E). The subordinate intercalations of asymmetrical ripple cross-laminated sandstone (S_{ARCL}), soft-sediment deformed sandstone (S_{SSD}) and symmetrical ripple cross-laminated sandstone (S_{SRCL}) (Figure 4.24D) were observed in the lower part of the facies association. The abundance of these lithofacies decreases downslope and up-dip within the facies association. By investigating the photologs a few balls and

pillows (Figure 4.25E) and flame structures were identified in the upper reaches of the succession.

The ichnodiversity is low, but traces of *Kouphichnium* (Figure 4.14), *Cylindrichnus* (Figure 4.12), *Arenituba* (Figure 4.11) and *Siphonichnus* (Figure 4.16) were interpreted in the scree-covered section beneath the identified channel deposits. Fish traces (Figure 4.14) were identified in the scree- covered section under log 9 (Figure 1.2).

Interpretation:

Based on FA3`s stratigraphic position, the internal and basal erosive lower boundary with rip-up mud conglomerates, the external wedge-shaped geometry combined with the dominating lithofacies, FA3 are interpreted to represent channelized sandstone units, possibly representing channel infills deposited by hyperpycnites and turbidity currents. Stratigraphically the channelized deposits of FA3 are incising the delta front lobe deposits of FA2 on the shelf-edge and on the upper slope.

The erosively replacement of the fining upward channelized deposits reflect flows which did not accomplish to produce high-density turbidites (Mellere et al., 2003). Mellere et al. (2003); E.g., Clark and Steel (2006) interpreted smaller scale channel deposits at the upper slope as gullies. According to Mellere et al. (2002), the channelized deposits may present the distal reaches of a chain of shallow streams running on the delta front. Both channels, chutes and gullies share the same generating mechanism; the differences are the scale and the ability to ignite high-density turbidity currents. In the present work, the term channel has been used for both small and large-scale channelized deposits. The fining upwards channelized deposits are interpreted to present thinly bedded turbidite deposits. The multiple, local scourings within the succession are understood as scour and fill units which formed along the channel base.

The deposits of the thick bedded channelized succession are suggested to represent high-density turbidite deposits. Channelized deposits and turbidites reflect event sedimentation, therefore the deposits vary in appearance and in prevalence. Bouma (1962) turbidite facies model, known as the Bouma sequence is an example of an ideal turbidite sequence. However, most turbidites in outcrop deviate from the ideal Bouma sequence. Bouma divisions of T_{ab}, T_{acd}, and T_{bc} are present along the wedging element. The multiple stacking of lithofacies S_{NG} followed by lithofacies S_{PPS} and S_{LACS} in the upper reaches of the channels reflect deposition

from high-density turbidity currents (Figure 4.24B and 4.25E). The units are vertically stacked of Boumas T_{ab} divisions, separated by the erosional surfaces from the succeeding Bouma T_{ab} division. Coal and rip-up mud conglomerates are widespread along the erosional bases of the turbidite deposits. The ability to produce turbidity currents was perhaps aided by retrogressive slumping (Figure 4.22F). The observation of climbing current ripple cross-laminated sandstones in the distal reaches of the thick channelized plane parallel-stratified turbidites imply continuous traction and aggradation of sand within the streams which confirms the statement (Petter and Steel, 2006). Dzulynsky and Walton (1965) performed experiments producing flute marks by turbidity currents flowing over muddy substrates. Based on the experiments, they concluded that flutes form in strongly turbulent zones close to the point of discharge of turbidity currents.

According to Mellere et al. (2003), the channel fill deposits along the Brogniartfjella can be followed downdip for 2km before they eventually become covered by talus. Unfortunately, approximately only 550 metres of clinothem 8C is exposed, which makes it impossible for further investigation. However, Steel et al. (2000) investigated and laterally traced channel fill deposits at Storvola of clinothem 12 (located south-east of the Brogniartfjella), which demonstrated that the erosional pathways of the turbidites were continuing along the slope and into basin-floor fans (Steel et al., 2000; Clark and Steel, 2006). The observations of the moderately sorted and almost mud-free (5.6% according to Clark and Steel (2006)) sandstones, the high degree of amalgamation, the many internal scouring surfaces with rip-up mud conglomerates together with the dominance of tractional sedimentary structures indicate frequent by-pass of density currents which were primarily restricted within the channel walls (Mellere et al., 2003). Based on the listed arguments it is reasonable to believe that sand-rich basin-floor fans were formed downslope (Steel et al., 2000; e.g., Plink-Björklund and Steel, 2004; Johannessen and Steel, 2005; Clark and Steel, 2006; Grundvåg et al., 2014a). The forward stepping character of the infill, the evidence of periodic sediment by-pass through the channels and the nature of the channelized complex all supports the notion of the advancement of sand prone basin-floor fans (Steel et al., 2000).

5 Sandbody geometry and masterbedding architecture

5.1 Introduction

This chapter aims to present a correlation panel based on field observations and the obtained sedimentary logs, with corresponding surfaces and facies associations. The correlation panel was made based on sequence stratigraphic concepts. Hunt and Tucker (1992); Helland-Hansen and Martinsen (1996); Catuneanu (2002) four-fold subdivision of systems tract have been applied. Their sub-division consists of highstand (HST), falling stage (FSST), lowstand wedge (LST) and transgressive (TST) system tracts. Walther's law is violated when a facies association is abruptly overlain by a facies association of a much more basinward origin. This means that the gradual migration of facies belts both vertically and laterally are disordered. Violations of Walther's law causes unpredictable facies transitions and deviations from the ideal facies succession which a parasequence represent. Walther's law principles are the fundament for the correlation and the sequence stratigraphic investigation of the studied succession, although some additional principles for the correlation are as follows;

- The sands within a parasequence are thinning in concert with the increasing distances to the fold-belt-and thrust belt (Figure 1.4).
- Thick sands extend further compared with thin sands.
- Facies associations do not cross flooding surfaces.

5.2 Observations

The sandbody geometry and masterbedding architecture were studied in detail in the field, and from a distance at the beach and the ship. Clinothem 8 is one of 20 easterly dipping outcropping clinothems along the Van Keulenfjorden transect (Figure 1.3). Helland-Hansen (2009) suggested a lateral extent of the sandbodies ranging from a few kilometers up to ~10km. The dip of the clinothems normally decreases in their lower distal reaches (bottomset), reflected by a concave-up to sigmoid profile (Figure 1.3). The lack of outcrop makes it hard to contend the profile of the studied clinothem, although considering the overall depositional environment, the profile of the surrounding clinothems, the dip angles and the wedged shaped sandbodies a concave-up profile is most likely expected for clinothem 8C.

The studied succession is oriented very faintly oblique to the assumed depositional-dip profile of the Central Basin.

The parasequences at Brogniartfjella are vertically stacked, where clinothem 8C is one of the thickest and lowest positioned parasequences at the Brogniartfjella. Clinothem 9, 10 and 11 are succeeding clinothem 8. The vertical thicknesses of these parasequences thins upwards within the Battfjellet Formation. Helland-Hansen (2009) focused on the facies stacking patterns of the shelf-deltas within the Battfjellet Formation. He illuminated the connection between the water depths and the parasequence variability and stacking patterns. The deltas in the inner Van Keulenfjorden faced deep waters. He argued that the water depths decelerated the advancement of the system with repeated upbuilding of shelf-deltas, shelf-edge deltas, slope systems and occasionally, basin-floor fans. By time, the fronting depositional foundation became shallow enough for the deltas to further advance basinward at a faster rate (Helland-Hansen, 2009). According to Helland-Hansen (2009), the initial parasequences seem to be thicker than the sequences resting on top of another parasequence. This could be a result of higher compaction rates in the underlying mudstones of Frysjaodden Formation during the outbuilding of the first parasequence compared to the younger ones. The lowest positioned parasequences were probably exposed to heavier waves and storms (Helland-Hansen, 2009). As a consequence, the wave and storm weather wave bases became deeper for the first parasequences, which might expanded the offshore-transition and shoreface facies belts compared with the later deposited parasequences (Helland-Hansen, 2009). The parasequence variability and interpretation performed by Helland-Hansen (2009) concords well with the observed vertical stacking of the parasequences at Brogniartfjella.

Clinothem 8 comprise parasequences 8A, 8B and 8C (Figure 1.3), the succession consists of sand-prone, partly amalgamated units which are traceable from the delta plain to the middle slope. Parasequence 8A is located closest to the fold-and-thrust belt, followed by 8B and 8C. The studied succession of parasequence 8C can be separated into two different elements based on the external sandbody geometry. The proximal sandbodies are tabular, while the distal sandbody develop a wedged geometry (Figure 1.2). The sandstone cliffs of the tabular unit are dominated by the overall regressive lobe deposits, while the wedging unit is dominated by subaqueous channelized deposits (Figure 4.19).

Architectural components:

Based on the lateral and vertical organisation of the facies associations with corresponding boundaries, the internal architecture and the external sandbody geometry the clinothem can be divided into two different components; lobes (FA2) and channels (FA3) (Figure 5.1).

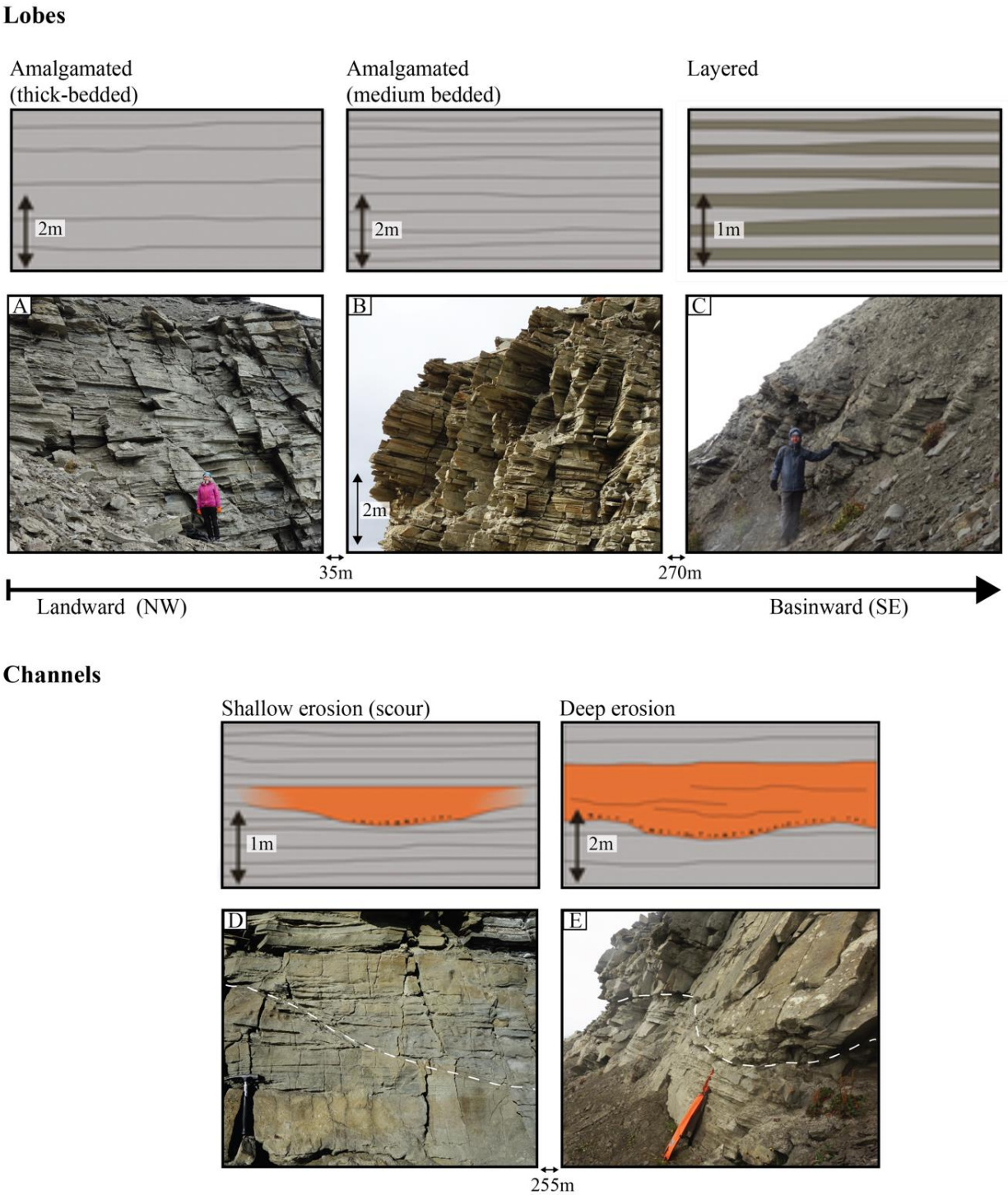

Figure 5.1: Schematic illustrations and outcrop photos from clinothem 8C which is dominated by the two different architectural elements: channels and lobes. The figure displays the different scales of the architectural components along the section; the erosional surfaces of the channels are marked with white dashed lines. See main text for further descriptions. Modified from figure 14 by Grundvåg et al. (2014b).

The architecture of the prograding lobes

The prograding lobes are characterized by a slightly coarsening and distinct thickening upwards trend. The lobes of FA2 dominates the tabular element of the studied succession (Figure 4.19). Based on the coarsening and thickening upwards trend (Figure 5.1C-A) together with the abrupt deepening marked by a flooding surface, two separate lobes were identified. Due to scree-covered sections, few outcrop descriptions were performed on the lowest positioned lobe. The description is therefore based on the observations of the upper positioned lobe, exposed from log 1-5 (Figure 1.2 and 4.19). The lobes consist of the thin bedded heterolithic prodelta deposits (FA1) (Figure 5.1C) succeeded by very fine-grained medium- to thick bedded sandstones of FA2 (Figure 5.1A-B). The coarsening and thickening succession are bounded by a marine flooding surface. The progradational style and the scale (10-15m) are characteristics of a parasequence as defined by (Van Wagoner et al., 1990).The constituting beds of the lobes display a tabular to slightly wedging geometry, and the grain size is fining basinward within the lobes (Figures 5.1A-C). Very fine-grained sandstones which are partly amalgamated dominate the upper reaches of log 1 (Figure 5.1A) before it fines downslope to layered and interbedded mudstones (log 7) (Figure 5.1C). The degree of amalgamation of the beds is accordingly decreasing basinward (Figure 5.1A-C). The vertical thickness of the lobes is expected to thin in concert with the increasing distance from the hinterland (sequence stratigraphic concepts mentioned in chapter 5.1).

The architecture of the slope channels

A slope channel complex which ranges in thickness from 6-20m dominates the wedging element of clinothem 8C. The slope channels can be laterally traced landward to the shelf (log 4-5). The channel complex is succeeded by transgressive marine mudstones. Each channel fill ranges from approximately 1m to 2.5, where the average infill thickness is approximately 2m (Figure 5.1E). The relief of the erosional channels is 1-3m. However, smaller scale internal shallow scours are observed within the lower proximal to the medial part of the erosional channels. The relief of the scours is approximately 0.5-1m (Figure 5.1D). The slope channels were identified by the observations of the four main characteristics as; (1) Thick bedded (>1m) erosively based sandstone units displaying a high degree of amalgamation. (2) Sandstone units displaying multiple horizons of rip-up mud conglomerates and organic fragments (e.g., Mattern, 2002) locally with amalgamated mudstone conglomerates (base of log 8) (Figure 4.25G). The erosion surface and accompanying channel infill unit at the base of the wedge can be demonstrated along parts of the outcrop (the red line in Figure 5.2).

5.3 Interpretation of correlation panel

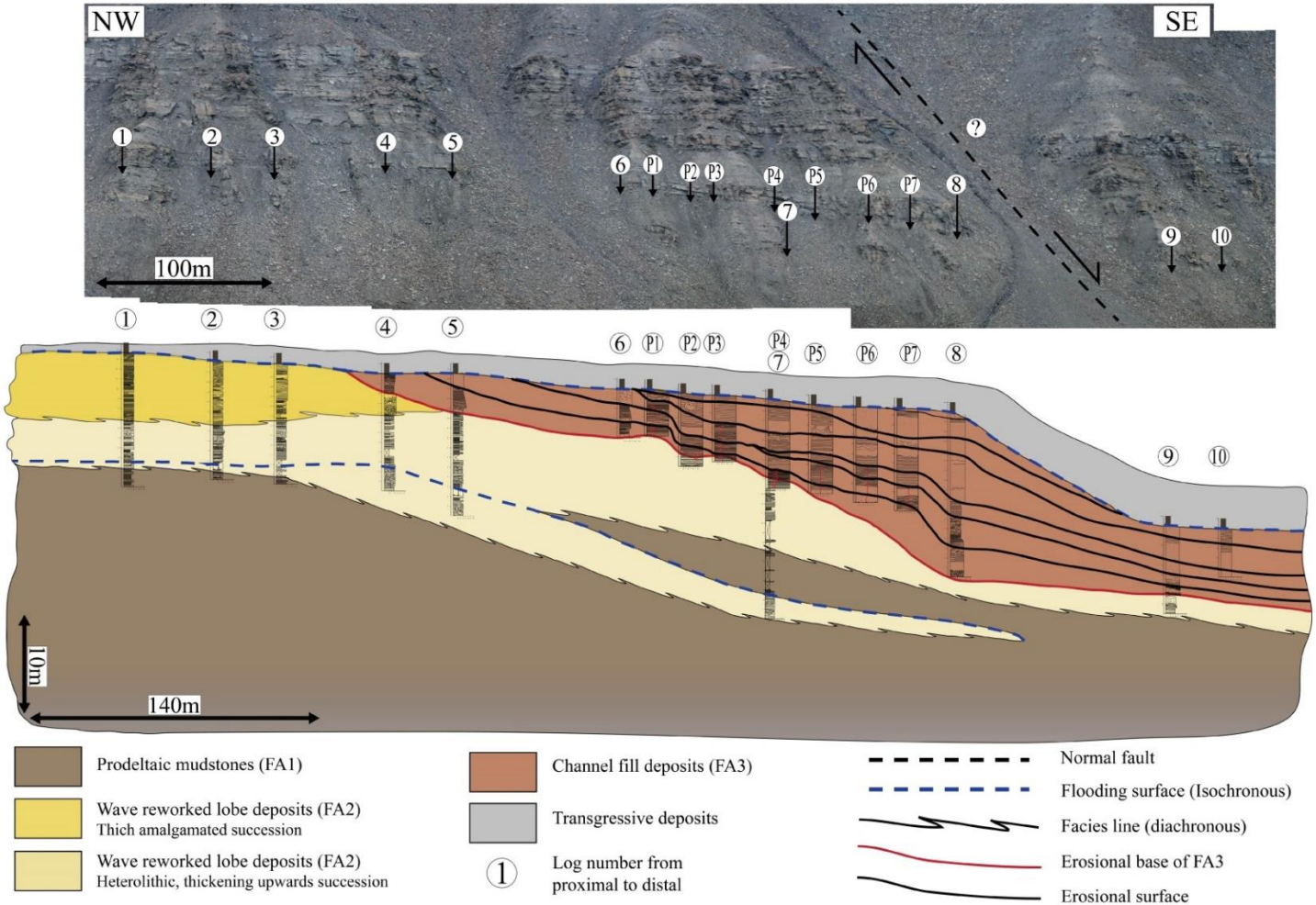

Figure 5.2: Interpreted correlation panel of the studied succession. The facies association boundaries have been correlated as diachronous lines, while the erosional surfaces have been drawn as isochronous lines. The yellow units present prograding wave reworked delta fronts. Laterally FA2 are eroded by the subaqueous channel deposits of FA3. The base of the subaqueous channelized deposits are represented with the red line. The upper boundary represents the drowning and the subsequent transgressive shelf-deposits. The erosional surfaces have been laterally traced across the possible normal fault , which is marked on the photo. For complete legend, see Appendix.

Temporal and spatial development of the system (Figure 5.2)

1. Prodelta deposits (FA1) originating from a prograding delta system positioned proximal to the study area, represents the lower part of the clinothem. The relative sea-level was high, which predominantly lead to deep water deposition of mudstones at this location. The intercalations of fine-grained sandstones of plane parallel-stratified sandstone (S_{PPS}) and asymmetrical rippled cross-laminated sandstone (S_{ARCL}) suggest deposition from unidirectional currents, possibly by hyperpycnal flows or waning turbidite currents. The prodelta deposits of FA1 are assigned to a highstand system tract. The deposits display a coarsening upward profile which is associated with the southeastern facies shift. The prodelta deposits represent marine portion of the highstand system and represents low-rate prograding normal regressive strata.
2. The delta remained progradational implying a steady input of supplied sediments from the tectonically uplifted hinterland. Mudstones and very fine- to fine-grained sandstones was laid down from the prograding delta front. Wave and storm-generated structures dominate the delta front succession, reflecting deposition in a wave agitated basin. The delta front deposits are separated by a flooding surface which points to a temporary abandonment of the sediment input. The abrupt deepening and the succeeding deposition of marine mudstones are probably a result of autogenic lobe switching (Gjelberg, 2010; Naurstad, 2014). The lobe deposits were accumulated within the forced regressive system tract. The interpretation of progradational deltaic lobes supports the notion of a delta front which gradually prograded basinward in concert with the high rates in sediment supply fed by landward positioned distributary channels.
3. Shelf-edge instability increased in concert with high rates of sediment supply and continuous relative sea-level fall. The dumping of sediments onto the shelf-edge and the fall in relative sea-level represent ideal conditions for igniting mass-flow deposits. The flute marks (Figure 4.25F) and the thick accumulations of rip-up mud conglomerates in the lowermost part of the wedging unit (Figure 4.25G) are interpreted to represent the product of the initial turbidity infill. The presence of multiple erosional surfaces succeeded by Bouma's T_{ab} division throughout the unit implies continued infill of scoured channels. The ability to ignite turbidity currents were possibly aided by retrogressive slumping. The presence of multiple erosional

surfaces, the average channel infill thickness of 2m and the regional notion of a small-scale system is in concert with an understanding of a delta dominated by frequent lobe switching. These settings suggest relative short-lived turbidites dumping sediments on the upper slope. The deposits are interpreted to represent deposition during relative sea-level fall (within the forced regression to lowstand wedge system tracts).

4. Transgressive marine mudstones mark up the upper boundary of the studied clinothem. The delta retreated towards the northwest, creating accommodation for marine deposition. The deposits were laid down in the transgressive system tract. The transgressive mudstones are overlain by tidally influenced shallow marine deposits of parasequence 9a (Mellere et al., 2003), which represents deposition in a succeeding sea-level highstands.

The vertical and lateral stacking of the clinothems at Brogniartfjella (especially characterizing the middle to the eastern part of the mountainside) suggests that the delta front faced deep waters forcing a decline in the rate of delta progradation (Helland-Hansen, 2009). The decline in the rate of advancement of the system induced repeated up building of shelf-edge deltas, slope systems and in some sites basin-floor fans. Eventually, the water depth was shallow enough for the fronting depositional foundation to advance further into the basin at a faster rate (Helland-Hansen, 2009). The interpretation supports the notion of an asymmetric basin with the studied clinothem positioned close to the axis of the syncline (Figure 1.1 and 3.3), also explaining the deeper waters dominating the studied succession. The vertically thickening and coarsening upward trend of the tabular unit comprising prodelta mudstones and wave reworked delta front deposits represent sedimentation during a shallowing upwards succession, following Walther's law.

Violations of Walther's law

Three major breaks were identified (Figure 5.2). The heterolithic lobe deposits of FA2 are abruptly overlain by prodelta mudstones of FA1. This is interpreted as a minor flooding surface within clinothem 8C, (Figure 5.2). Subaqueous channelized deposits are erosively cutting into the lobe and the prodetaic deposits (FA2 and FA1). This is marked by the lower erosional surface in figure 5.2. The surface is interpreted to represent the base of the channel infill deposits of FA3. Based on the dominance of plane parallel-stratified sandstone (S_{PPS}), low angle cross-stratified sandstone (S_{LACS}), soft-sediment deformed sandstone (S_{SSD}),

normal graded sandstone (S_{NG}), the multiple erosional surfaces marked with rip-up mud conglomerates, the identification of flutes and the abundant vertical shift from normal graded sandstone (S_{NG}) to plane parallel-stratified sandstone (S_{PPS}) / low angle cross-stratified sandstone (S_{LACS}) suggest event sedimentation from turbidites. Each event reflects the conditions at a certain time, expressed by the different characteristics of the turbidite infills. Offshore mudstones are covering the deposits of FA1, FA2 and FA3. The surface is interpreted to present a major flooding surface. Van Wagoner et al. (1988) defined the maximum flooding surface as; "a surface across which there is evidence of an abrupt increase in water depth. The surface has been used as a datum for the correlation panel (Figure 5.2 and 5.3).

Relationship between slope channels and lobes

Based on the observed thickening, slightly coarsening upwards trend, the sandbody geometry and the dominating lithofacies the tabular element is interpreted to present delta front lobes laid down on the shelf. The wedging element which is characterized by a wedged shaped geometry. The thickening from ~6-20m and the angle of the upper boundary which is ~5° confirms the statement. Based on these observations the wedging element is interpreted to represent the upper part of the slope. The investigated parasequence 8C was deposited within the shelf-edge-to-upper slope settings or also described as the topset and foreset segment of a clinoform (Porebski and Steel, 2006; Helland-Hansen, 2009).

According to Johannessen and Steel (2005) classification system, the tabular unit is part of a fourth-order clinoform, while the wedging unit is part of a fifth-order clinoform. Fourth order clinoforms form during hundreds of thousands of years, while the fifth-order clinoforms form over tens of thousands years. The fifth ordered clinoforms are normally observed as "peeled off" from the proximal fourth ordered clinoforms, forming wedged shaped sandy tongues at the slope.

Wave and storm-generated structures are extensive along the studied succession, especially in the tabular element (Figure 4.22C and 4.22G), although wave generated structures are also observed in the lower reaches of the wedging element (Figure 4.25D), indicated by the prevalence of symmetrical rippled cross-laminated sandstone (S_{SRCL}) and hummocky cross-stratified sandstone (S_{HCS}). The abundance of current generated structures, as plane parallel-

stratified sandstone (S_{PPS}), asymmetrical rippled cross-laminated sandstone (S_{ARCL}) and low angle cross-stratified sandstone (S_{LACS}) increases distally and are dominating the wedging element (Figure 4.25). The shift implies an increasing impact of hyperpycnal and turbiditic currents distally within the studied clinothem 8C. However, the channelized deposits also display evidence of oscillatory currents. Wright et al. (1988); Nemec (1995) suggested that it could be related to internal waves which develop near the density boundaries. Mutti (1992); Mutti et al. (1996) postulated that "sloshing" of sea-water might be a factor intensifying the oscillatory element of a flow within shallow depths of tectonically restricted basins (Mutti, 1992; Mutti et al., 1996). The boundary between the lobe deposits of FA2 and the channelized deposits of FA3 are occasionally exposed along the wedging unit. The initial channel infill deposits along the wedging element is characterized by an erosive base with rip-up mud conglomerates (Figure 4.25G). The sandstone unit is thick bedded (> 1m) and displays a high degree of amalgamation.

Multiple stacking of channelized turbidites dominate the wedging element (Figure 4.24B). The relief of the wedging element is produced by the scouring from turbidity currents, which later became infilled by younger turbidite deposits (Figure 5.2 and 5.3). The units are separated by rip-up mud conglomerates (Figure 4.25G) and organic fragment bearing surfaces, which possibly represents by-pass surfaces. The geometric connection between strata and the stratigraphic surface against which they terminate against are defined as stratal terminations (Catuneanu, 2002). Stratal terminations enable to interpret the type of shoreline shifts as well as changes of the base level at the shoreline (Catuneanu, 2002). An offlapping stacking pattern has been suggested based on the lateral correlation of the channelized deposits (Figure 5.3). Offlap is diagnostic for base level fall; thereof it is connected to forced regressions (Catuneanu, 2002). The erosional surfaces are characterized by internal onlap within the wedging unit (Figure 5.3). Based on the interpretation of scouring subaqueous channels the startal terminations are defined as marine onlap which was first defined by Galloway (1989). According to Embry (2001) forced regressive systems develop a regressive slope onlap surface as a result of gravity processes. The base of the channelized deposits could possibly represent a regressive slope onlap surface (Figure 5.2 and Figure 5.3).

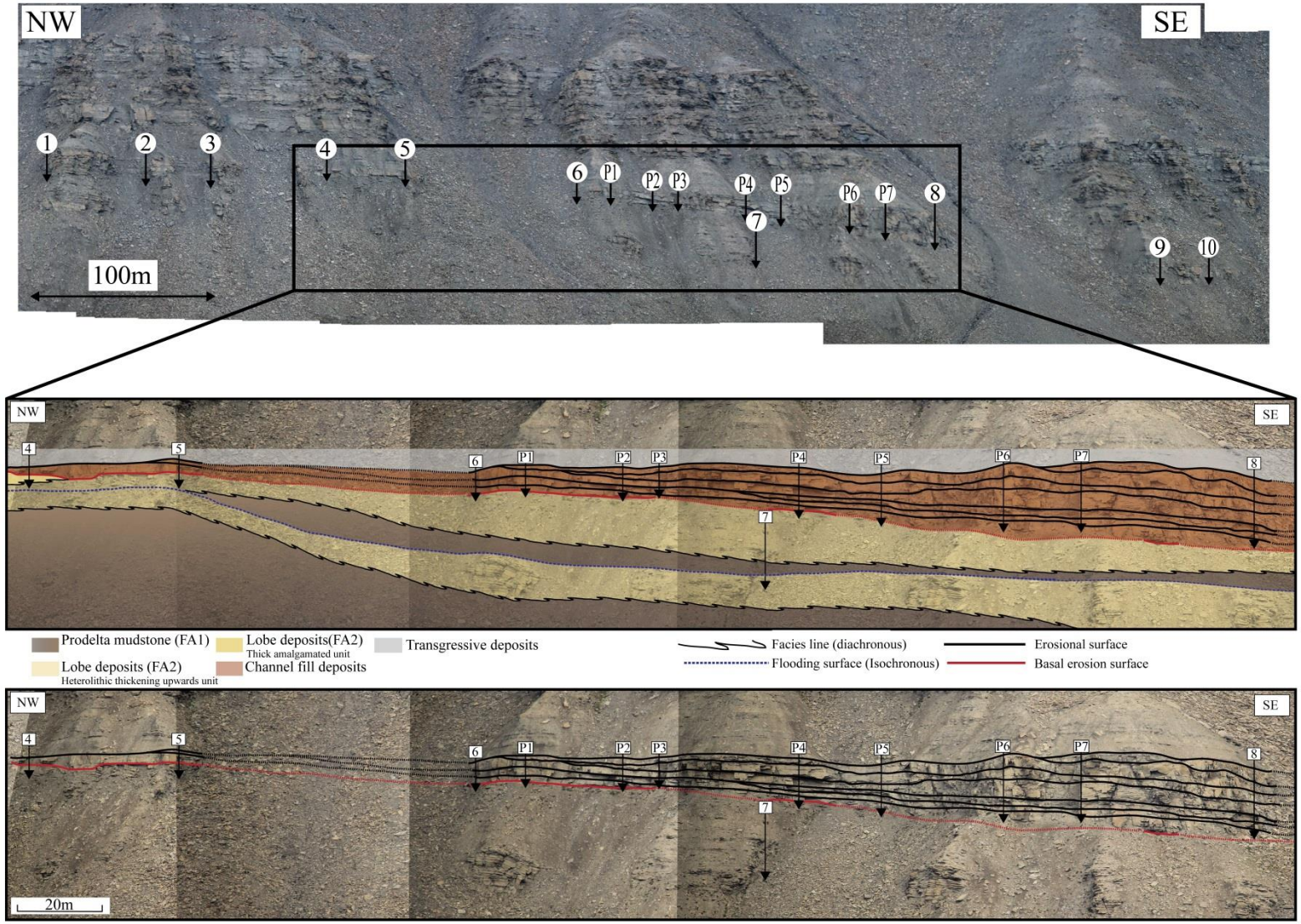

Figure 5.3: Correlation of erosive contacts from log 4-8. The illustration displays a complex cut and fills history of the studied succession. The lower surface presents the base of the channel. The channel was then filled with turbidite deposits within the forced regression to lowstand wedge system tracts. The upper surface indicates the following transgressive deposits comprising offshore mudstones, while the red line indicates the lower base of the channel infill complex.

6 Depositional environment and palaeogeography

6.1 Tanqua Karoo Basin as analouge

The Permian Tanqua Karoo Basin (Figure 6.1) in South Africa has been documented as a possible analogue to the sedimentary system in the Central Basin by different workers (Dixon, 2013; Grundvåg et al., 2014b). As with the Central Basin, the Tanqua Karoo Basin is classified as a foreland basin (Johnson et al., 2001). Both systems present an infill succession characterized by shallowing upwards successions. Common for both systems is the architectural stacking of beds forming lobes derivated from river dominated wave-influenced deltas (Figure 6.3).

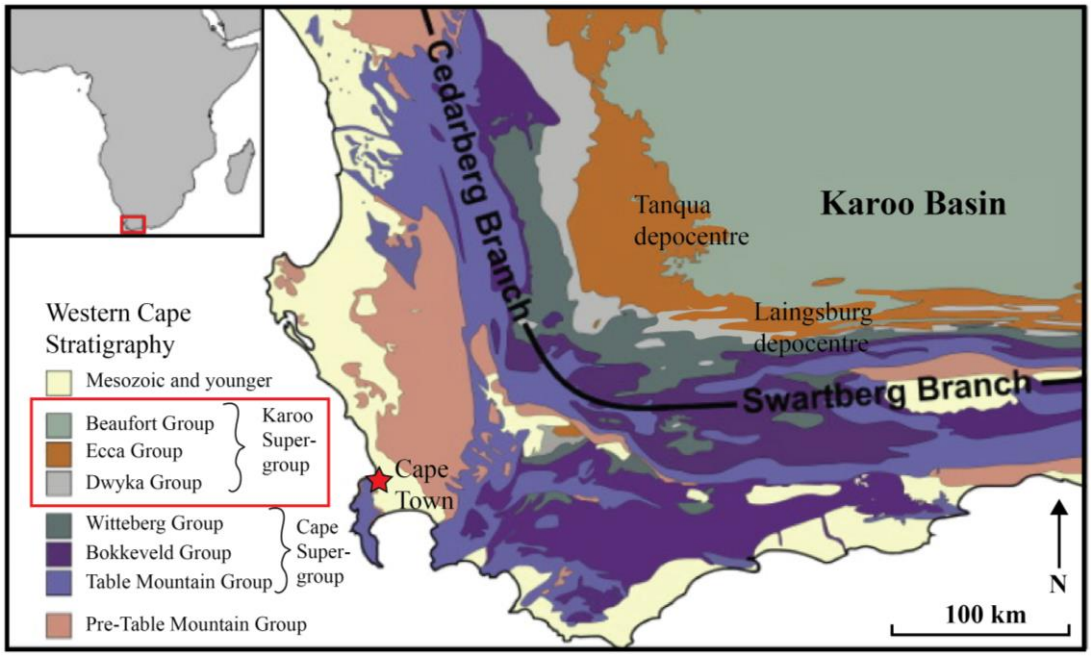

Figure 6.1: Map of Karoo Basin in South Africa, location is shown by the red rectangle in the upper left map. The Karoo Supergroup with the Permian infill succession is marked with a red rectangle, Figure modified from Flint et al. (2011).

Clinoforms with low (0.3°) shelf gradients, low (0.5°) slope gradients, and heights of 25-30 meters were identified by Wild et al. (2009) in the Tanqua Karoo Basin. The clinoforms along the Van Keulenfjorden transect display steeper shelf gradient of approximately 1° and an average slope gradient of 3-4° (Mellere et al., 2002). Mellere et al. (2002) estimated the shelf-break water depths to be 50m, while the depth to the basin-floor during sea-level higstands are estimated to be 250-300m in the Central Basin, indicating relatively shallow depths of the Central Basin. The Karoo Basin is a deep water basin with depths estimated from the basin-floor fans to the first deltaic deposits to 1800 m (Flint et al., 2011).

The infill succession of the Central Basin is deposited during a warm climate, in contrast to the sediments of Tanqua Karoo Basin representing infill during icehouse climate conditions in the upper Permian (Flint et al., 2011).

6.2 Depositional environment

Delta classification

The facies associations and their lateral geometry and distribution imply that the clinothems of the Battfjellet Formation were deposited in a deltaic shoreline depositional environment. The contention is consistent with several other previous studies from the area (Helland-Hansen, 1990; Steel et al., 2000; Plink-Björklund et al., 2001; Uroza and Steel, 2008; Helland-Hansen, 2009; Grundvåg, 2012).

In the present study, clinothem 8C within the Battfjellet Formation is interpreted in terms of a fluvial-driven environment agitated by wave and storm currents. The sedimentary environment displays a distinct dichotomy, where the tabular unit is dominated by wave reworked lobe deposits (FA2) intercalated with prodelta deposits (FA1) in the lower reaches, commonly thickening upwards into amalgamated sandstones, and occasionally (from log 4 and downslope) into channel infill deposits (FA3) (Figure 5.2). The wedging unit is dominated by the channel fill deposits (FA3). Furtermore, an interpretation of frequent lobe switching of the anastomosing fluvial system of the succeeding Apelintoppen Formation has been established by Naurstad (2014), which could imply a fluvial dominated environment also for the Battfjellet Formation. The fine-grained sandstones which are texturally immature suggest an effective dilution of the sand through the system. The facies assemblages within the tabular element are dominated by wave and storm currents, while the delta lobe morphology, the texturally immature sandstones, the abundance of soft-sediment deformed units imply dumping of sediments at the delta front from the distributaries. The affluence of identified turbidite, storm, flood and the possibly slump deposits reflect a delta front which frequently shifted between wave and fluvial dominance. The mismatch between the internal wave dominated lithofacies and the overall delta morphology controlled by frequent lobe switching has been highlighted in several publications (cf. Helland-Hansen, 2009; Gjelberg, 2010; Grundvåg, 2012). Hence, an interpretation in terms of a steady source of relatively fine-grained sediments and high rates of sediment accumulated are favored. Stable, slowly

prograding deltas with long distances to their fluvial entry points would not display such internal immaturity within the sediments (Helland-Hansen, 2009).

Scale of depositional system

Helland-Hansen (2009) illuminated the significance of the scale of the studied deltaic system. The study suggested sandbodies ranging from a few kilometers up to 10km in any direction, implying that the delta front can be classified in the same order of magnitude. According to Wright (1978), the short distance from the source implies a small drainage basin with minimal tributary linking, promoting the development of small deltas. Mellere et al. (2002) estimated the basin to be 90-100km wide with shelf-widths ranging from 15-20km which is consistent with the notion of the development of small-scale deltas.

According to Burgess and Hovius (1998); Muto and Steel (2002) it normally takes less than 100 000 years to form a delta and for the delta to regressively transit the entire shelf-width. By comparison, the shelves of the Central Basin deltas are postulated to be as narrow as 15-20km (Mellere et al., 2002). Consequently, the tectonic influence is assumed to be of less significance for the investigated succession. Clinothems develop over 100-300kyr, while tectonics normally operate on time scales of 100s to 1000s of million years (Grundvåg et al., 2014a). Notably, the studied succession is situated in the center of the synclinal axis of the Central Basin. The local tectonic control on the parasequence stacking pattern and the clinothem architecture is therefore interpreted to be minimal within the study area. Although, the upper slope has probably been prone to some degree of faulting (Figure 5.2).The observed offset of the wedging element may be a result of normal faulting. Another suggestion that operates on a local scale is that the offset is a result of a slide-plane parallel to the Brogniartfjella. The sliding develops a local scour creating a displacement. Normal faulting is not abundant in compressional regimes as a foreland basin system represents. The latter suggestion with a slide-plane is therefore more likely to cause the observed displacement within the studied succession. The sliding may be the result of glasi-isostatic uplift. Similar displacements are common at Spitsbergen (Helland-Hansen, 2017, personal communication).

The Eocene-Early Oligocene is characterized as a transitional period between the Pliocene-Pleistocene icehouse conditions and the greenhouse conditions of Late Cretaceous-Early Palaeocene (Sømme et al., 2009a).The eustatic amplitudes are suggested to be lower during greenhouse periods compared to icehouse periods, causing low shelf accommodation (Sømme et al., 2009a). The influence from tectonics and sediment supply are consequently larger permitting deltas to prograde across the shelf, developing shelf-edge deltas capable of delivering sediments to the slope and basin floor, even during sea-level highstands. (Sømme et al., 2009a). Warm climate with high precipitation rates presents ideal conditions for high rates of delta progradation.

The flat to descending shelf-edge trajectory of the clinoforms along Brogniartfjella is a result of a relative sea-level fall (Figure 6.2). The basinward scree-covered section of clinothem 8C makes it impossible to trace the deposits further downslope. Several clinoforms along the section (with ascending, flat and descending shelf-edge trajectories) constitutes basin-floor sand deposits (Figure 6.2) (Steel and Olsen, 2002; Johannessen and Steel, 2005). Basin-floor deposition is directly related to the fluvial run-off, suggesting that governing factors of the river systems also impact and possibly control basin-floor deposition (e.g., Blum and Hattier-Womack, 2009; Sømme et al., 2009b; Grundvåg et al., 2014b). Climate is the superior factor controlling the prevalence and the extent of river floods of a system. High discharge during potential flooding can generate hyperpycnal flows (Mulder et al., 2003), which are suggested to present an important process in the ignition of turbidity currents in ancient foreland basins (Mutti et al., 1996; Mutti et al., 2003). The mentioned factors in concert with the slope gradients which are up to 5° (e.g., Petter and Steel, 2006) suggest by-pass of sand-rich turbidites through the slope and into the deep water basin-floor. Vegetation and the run-off rates of a system are controlled by climate (Grundvåg et al., 2014b). A warm climate with high rates of precipitation and erosion significantly increase the sediment supply (Grundvåg et al., 2014b). According to Naurstad (2014), the palaeoenvironmental setting of the succeeding Aspelintoppen Formation could be compared to the modern day western Canada arctic, temperate climate. This included extensive swamps, ephemeral lakes and lowland vegetation. The temperate climate together with the rising hinterland would provide significant amounts of sediments which is optimal for deltas to reach the shelf-edge and possibly bypass sand to the basin-floor (Grundvåg et al., 2014b). Additional governing factors of a fluvial system to induce hyperpycnal flows are (1) shelf-width, (2) relief and

distance to source area, (3) flow concentration, (4) salinity of the water, (5) duration and flood magnitude (Mulder and Syvitski, 1995; Mutti et al., 1996; Mulder et al., 2003).

The majority of the papers written based on the Central Basin outcrops claim the system to be sediment driven (Henriksen et al., 2010; Grundvåg et al., 2014b). Burgess and Hovius (1998) studies of modern river systems validated that deltas can establish at the shelf-edge in less than 100Kyr independent of sea-level, although the system is dependent on high rates of sediment supply. This indicates that the studied clinoform could present a fourth order shelf transit as described by Steel and Olsen (2002); Johannessen and Steel (2005), though on a shorter time scale than the calculated 300Kyr (Grundvåg et al., 2014b). Several studies have emphasized hyperpycnal discharge (Figure 4.20) as the essential trigger of the high sedimentation rates resulting in accumulation at the shelf-edge and deep water (e.g., Plink-Björklund et al., 2001; Mellere et al., 2002; Petter and Steel, 2006; Henriksen et al., 2010). The hyperpycnals was competent to incise the slope and to generate channels. Wherever the channels located on the upper slope of the clinoforms are classified as channels, canyons or incised valleys have been a debated subject (C.f. Steel et al., 2000; Mellere et al., 2002; Plink-Björklund and Steel, 2002; Mellere et al., 2003; Johannessen and Steel, 2005; Plink-Björklund, 2005; Grundvåg et al., 2014b). Henriksen et al. (2010) suggested that the hypepycnal discharge was a result of catastrophic river floods in concert with headwall slumping generated the incisions. Henriksen et al. (2010), illuminated arguments were; (1) The transition from the offshore mudstones of the Frysjaodden Formation to the continental deposits of the Aspelintoppen Formation, demonstrates that sedimentation rates outpaced subsidence rates in the Central Basin, (2) The absence of regional erosive unconformities, which would verify lowstand shelf erosion and shelf-edge incision. Plink-Björklund (2005) demonstrated local erosional unconformities in the coastal plain succession at Brogniartfjella and Storvola with reliefs recorded between ~5-15m. However, several studies have postulated that the unconformities demonstrated in the upper slope to shelf-edge reach of some clinoforms, including clinoform 8C, represent subaqueous reaches of the upslope incised fluvial systems (Steel et al., 2000; Mellere et al., 2002; Plink-Björklund and Steel, 2002; Mellere et al., 2003; Johannessen and Steel, 2005). However, the erosional reliefs recorded by Plink-Björklund (2005) are associated with several uncertainties: the outcrops are dominantly dip-parallel, displaying a 2D-view of the unconformities and the minimal valley depth is calculated with the assumption that each valley was filled during one

lowstand-transgressive-highstand sequence (cf. Rahmani, 1988; Zaitlin et al., 1994). In contrast, Henriksen et al. (2010) suggested the incisions of being a result of hyperpycnal flows ignited from catastrophic flooding of rivers with high sediment load in concert with shelf-edge collapse succeeded by slumping. The collapse produced scars at the shelf-edge allowing bypass of hyperpycnites. According to Piper and Normark (2009), hyperpycnal flows and mud plume fallout (Figure 4.20) can result in erosive slope channels, which concentrate and foster sediment transfer to deep waters. The prevalence of scree limits the lateral extent of the outcrop along the studied succession. It might be argued that these restrictions prevent the possibility to map potential regional unconformities connected to possibly incised valleys and the continuity of sand bodies downslope. Henriksen et al. (2010) interpretation contradicts several other publications based on the outcropping clinoforms of the Central Basin, proposing the relative sea-level fall as the forcing mechanism generating shelf-edge incision and the associated basin-floor fans (Steel et al., 2000; Plink-Björklund et al., 2001; Mellere et al., 2002; Clark and Steel, 2006; Petter and Steel, 2006; Carvajal and Steel, 2009).

Clinothem 8C in the context of the Van Keulenfjorden transect

Clinothem 8C has been the main focus of this thesis, although in total there are 20 outcropping clinothems along the Van Keulenfjorden transect (Figure 6.2) (Steel and Olsen, 2002). The scale, the prevalence and the accessibility make the area perfect to perform shelf-edge trajectory analyses and system tract examinations. The studied succession form parts of a parasequence, which corresponds to an overall falling shelf-edge trajectory. Mellere et al. (2003) performed an extensive study of the linkage between the fluvial incised shelf-edge deltas and the upper slope channels at the Brogniartfjella. They classified the trajectory for the shelf-edge on the Brogniartfjella to be of very low-angle ascending. Bathymetry, sediment supply, eustatic sea-level changes and subsidence, which includes subsidence from compaction and loading are the controlling functions for the shelf-edge trajectory (Helland-Hansen and Hampson, 2009). Steel and Olsen (2002) made a transect over the clinothems exposed along the northern side of Van Keulenfjorden (Figure 1.2 and 6.2). They performed an extensive study of the clinothems in the area with focus on clinoform trajectory and deep water sands. Clinothem 8C is seen in the detailed in figure 6.2 which also includes the succeeding 9-10 clinothems at the Brogniartfjella. The big black arrows indicate the overall shelf-edge trajectory interpreted by Steel and Olsen (2002). The clinoforms at the

Brogniartfjella corresponds to an overall falling trajectory located between the rising trajectory of the shelf-edge at Pallfjellet and Storvola. Aggrading shelf-margin growth dominates the clinoforms along the transect. Nevertheless, the clinoforms at the Brogniartfjella presents prograding flat to falling trajectories.

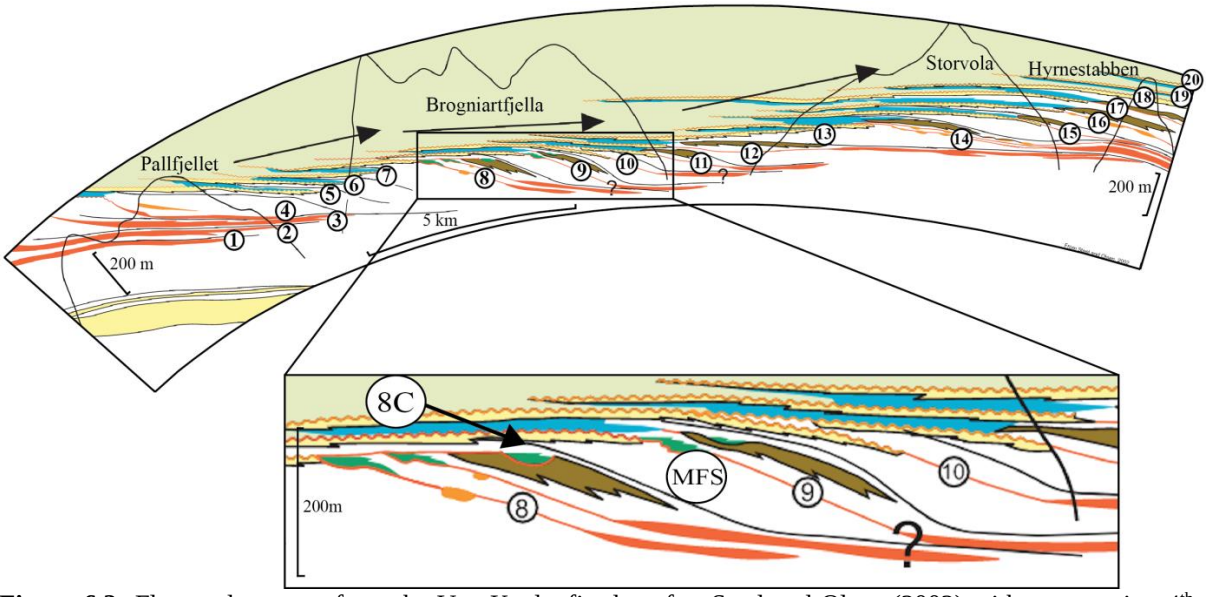

Figure 6.2: Flattened transect from the Van Keulenfjorden after Steel and Olsen (2002) with outcropping 4th-order clinoforms at Pallfjellet, Brogniartfjella, Storvola and Hyrnestabben. The Brogniartfjella with the studied clinothem 8C seen in the middle of the transect marked with the rectangle. The black arrows indicate the overall shelf-edge trajectory movement. Green=coastal plain, yellow/blue = shelf, brown/white = slope, white/red = basin floor. The lower image presents a close up of clinoforms 8-10 at the Braogniartfjella. Clinoform 8C is marked with the black arrow. The orange line (marked up by the black arrow) cutting into the military green deposits represent fluvial incision of the prograding lobes at the shelf-edge.

The 20 clinoforms can be subdivided based on the transiting of the shoreline across the shelf. Clinoform 5-7, 13 and 15 (all located in the Van Keulenfjorden transect at figure 6.2) represent shorelines that reached the shelf-edge and which subsequently retreated to the inner shelf (Steel and Olsen, 2002; Johannessen and Steel, 2005; Petter and Steel, 2006). Clinoform 1-4, 8-12 and 14 are clinoforms produced from shorelines which dropped below the shelf-edge with following erosion of the shelf-edge and bypassing of significant volumes of sand to the clinoform slopes and also to the basin-floor (Steel and Olsen, 2002). The studied clinoform of this thesis belongs to the latter group. Due to the south-eastwards shallowing of the Central Basin, the shelves widens with the increasing distance from the foredeep (Helland-Hansen, 1990). Steel and Olsen (2002) claimed that the shelves in the Central Basin were generally less than 15km wide. Clinoform 8C is characterized by a falling shelf-margin, dominated by lobes, channelized deposits and local erosional surfaces. In comparison, clinoform 14A at Storvola has a flat to falling shelf-margin trajectory, an upper slope dominated by slope channels and lobes and attached basin-floor fan approximately 4km

southeast of the slope-channel complex (Petter and Steel, 2006). This unit has similarities with clinoform 8C at Brogniartfjella. On the other hand, the trajectory of the succeeding clinoforms at Storvola (15-18) (Figure 6.2) are continuously rising (Crabaugh and Steel, 2004; Petter and Steel, 2006; Uroza and Steel, 2008), whereas the following clinoforms at the Brogniartfjella display a falling trajectory. Petter and Steel (2006) suggested that the distributaries were dumping sand directly into the upper-slope channels, creating a streamlined contact between the fluvial distributaries and the basin-floor fans. Mellere et al. (2002) also studied sand-prone type 1 and 2 clinoforms at Høgsnyta and Litledalsfjellet (Figure 6.3). They highlighted the frequent alternation between type 1 and 2 clinoforms (Figure 3.5) in the Central Basin, which imply a dynamic and fluctuating environment. They also studied sand delivery across the shelf-edge onto non-canyoned slopes. The sands were generally maintained as wedges (Figure 6.3) without sands being transported to the basin-floor (Mellere et al., 2002). However, the clinothems at Högsnyta which are traceable from the shelf-edge-to the lower slope are 10 meters thick (Steel et al., 2000), which is about half of the thickness of the investigated clinothem at Brogniartfjella. Plink-Björklund and Steel (2002) also stressed the absence of basin-floor fans connected to the forced regressive systems tract at Högsnyta. They concluded that the sediment volume generated by erosion of the shelf, shelf-edge and the upper slope was laid down at the slope and not at the basin-floor. The preservation of sediments on the slope in high sediment supply systems is typical for slopes which have not been prone to incision by canyons (Plink-Björklund and Steel, 2002). The Högsnyta clinoform complex presents a classical model of how siliciclastic shelf-margins propagate into a basin (Plink-Björklund and Steel, 2002). Similar conditions with thick sands accumulated at the slope preventing sand deposition at the basin-floor could be applicable for clinothem 8C at Brogniartfjella.

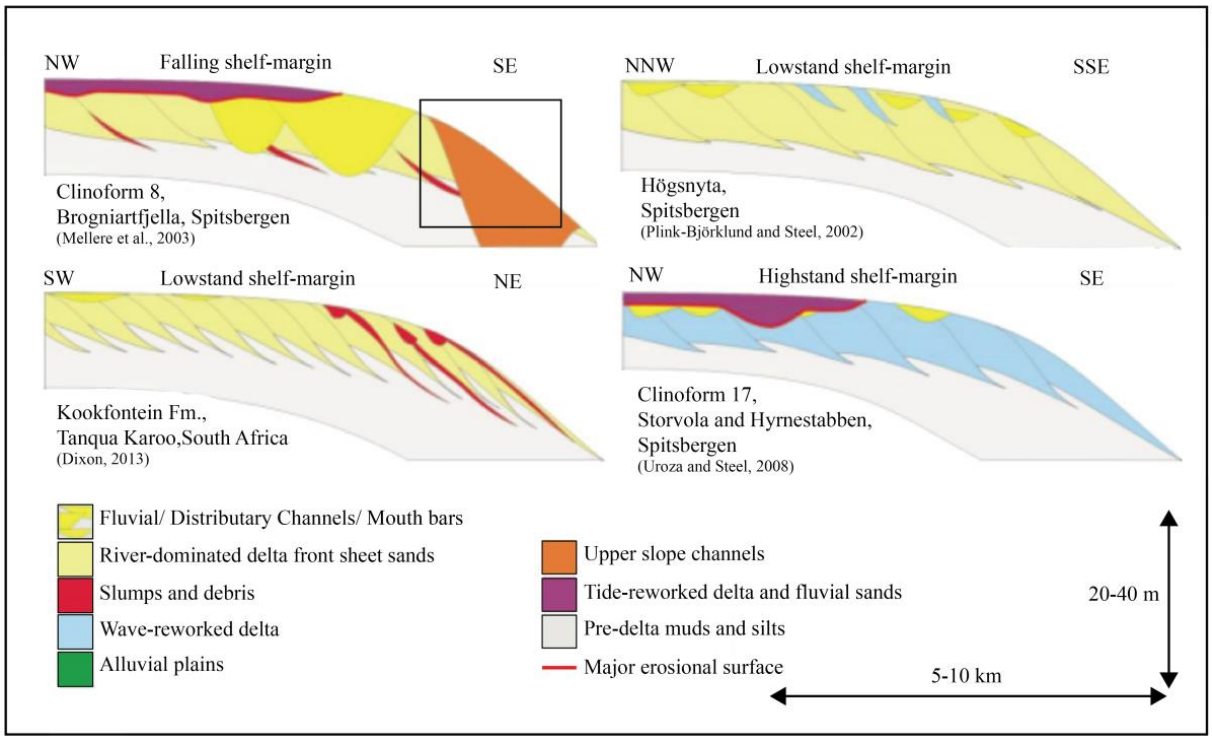

Figure 6.3: Cartoons of the shelf-edge delta with corresponding clinoforms from the Van Keulenfjorden transect including Högsnyta, Storvola and Hyrnestabben and clinoform 8 (the upper left cartoon). The lowstand shelf-margin of the Tanqua Karoo Basin is illustrated in the lower left cartoon (Chapter 6.1). The black square indicates the study area of this thesis. The dimensions and gradients are adjusted which allows us to compare the different systems. The channel incisions at the shelf-edge in Kookfontein Formation; Tanqua Karoo Basin is < 3 m deep, which is approximately an order of magnitude smaller than the incision observed within clinoform 8C. Slightly modified from (Dixon, 2013). As the cartoons illustrate Högsnyta and Kookfontein Formation are deposited during lowstand time, while the studied clinoform 8C is deposited during falling to lowstand time (forced regressive deposition). Clinoform 17 is deposited during sea-level highstands.

6.3 Palaeography:

Palaeocurrent data have been applied to reconstruct the palaeogeography of the Battfjellet Formation. The number of measurements is limited due to the accessibility of the clinothem; the data are therefore used as an implication for the palaeogeography. Palaeocurrent data of symmetrical ripple crests, obtained from the tabular unit of the succession, indicated a general flow direction towards the south-southeast (Figure 6.4 and 6.5). Few (2) palaeocurrent data were obtained along the wedging element. Consequently, not much weight should be put in these data. The flutes (Figure 4.25F) identified under the base of the mass-flow deposits were aligned east west. Helland-Hansen (1990) performed an extensive study with wide palaeocurrent data from the Central Basin. Symmetrical ripple crests measurements from this study were oriented preferentially north south, which is parallel to the approximately north-south oriented shoreline. Sole marks along the base of mass-flow deposits were measured in the same study to being aligned east west. The measurements coincide well with the documented notion of an easterly prograding deltaic system feed by

fluvial channels from the uplifted hinterland west of the basin (e.g., Helland-Hansen, 1990; Crabaugh and Steel, 2004; Plink-Björklund, 2005; Uroza and Steel, 2008).

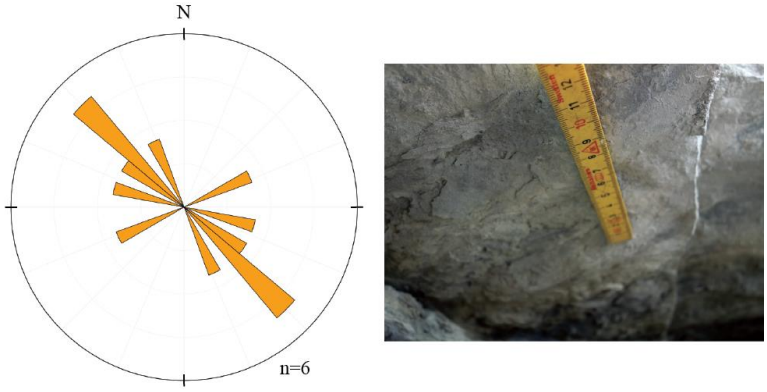

Figure 6.4: Rose diagram of symmetrical ripple crests from the tabular element. Photo of measurable symmetrical ripple crests from log 1 (Figure 5.2).

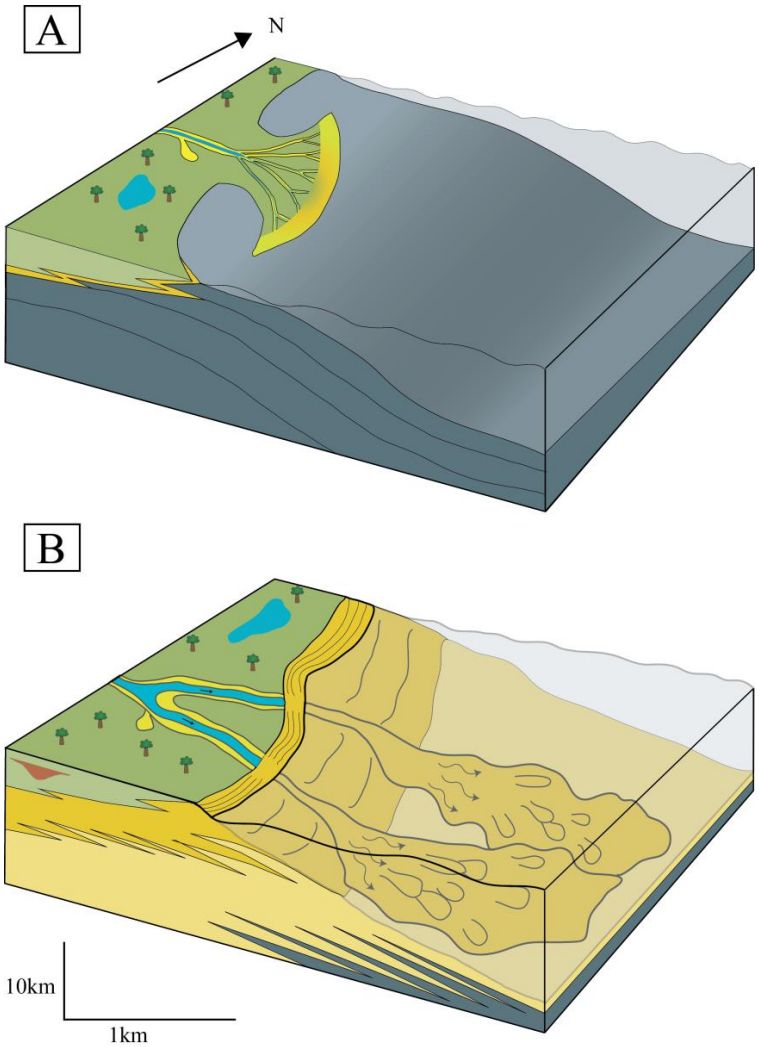

Figure 6.5: A Simplified regional palaeogeographic model for the evolution of the prograding delta of Battfjellet Formation. **A:** Delta front located on the middle shelf. The active delta front is fluvial dominated and wave influenced, while the abandoned areas are wave-dominated. The delta front progrades at the front due to high sediment supply. The abandonment areas are simultaneously transgressed as a result of the cut off in sediment supply. **B:** As progradation continued the delta front reaches the shelf-edge. High rates of sediment supply in concert with the relative sea-level fall ignited hyperpycnal flows and turbidity currents.

7 Summary and conclusions

Clinothem 8C within the Battfjellet Formation, Brogniartfjella has been studied on the basis of sedimentological field work. Facies distribution, their boundaries, the masterbedding architecture and the sandbody geometry have been the focus of this study. The obtained data were used to reconstruct the palaeogeography and to develop a depositional model for clinothem 8C.

The shelf-edge-to-slope system and the excellently preserved outcropping clinothems within the Van Keulenfjorden transect have been thoroughly investigated for several years. Previous work at Brogniartfjella has predominantly focused on the large-scale picture of the shelf-edge-to-slope system (Steel et al., 2000; Mellere et al., 2003; Grundvåg et al., 2014). This study comprises a more detailed study of clinothem 8C. The sedimentological investigation of clinothem 8C has leas to the following main conclusions:

- The studied succession has been subdivided into two different elements on the basis of the external sandbody geometry. The proximal package is characterized by a tabular geometry, while it develops into a sloping and wedging package in the distal part. The sudden shift in geometry from tabular to sloping is in concordance with a shelf-edge-to-slope system. The tabular element has been interpreted as being a part of the shelf, while the wedging element is interpreted as a part of the upper slope.
- Clinothem 8C have been divided into facies associations based on landward to basinal shift in facies characteristics. Two lobes separated by minor flooding surfaces were identified in the proximal reaches of the studied succession. A gradual transition from prodeltaic mudstones (FA1), to transition zone heterolithic, thickening upwards units, to thick amalgamated delta front deposits (FA2) characterizes the upper lobe (log 1-3). Hence, this upper delta lobe consists of a conformable succession of progressively more proximal strata, in agreement with Walther's law.
- An abrupt vertical and lateral shift from the wave reworked delta front lobe deposits (FA2) to the channel infill deposits (FA3) were identified from log 4 and basinward. The vertical and lateral shift in facies associations represents a violation of Walther's law and an increasing fluvial influence basinward.

- The channel deposits are interpreted to represent infill from hyperpycnal flows and turbidity currents during relative sea-level fall (within the forced regressive to lowstand wedge system tracts). The infill deposits are typically characterized by repeated vertical shifts from normal graded sandstone (S_{NG}) to plane parallel-stratified sandstone (S_{PPS}) and to low angle cross-stratified sandstone. These beds are interpreted as a Bouma-division T_{ab}. Subordinate, in the lower proximal reaches of the wedging element vertical shifts from normal graded sandstone (S_{NG}) to asymmetrical rippled cross-laminated sandstone (S_{ARCL}). These beds are interpreted as a Bouma-division T_{ac}. The identification of multiple erosive horizons with abundant rip-up mud conglomerates and coal fragments in the basal parts, the high rate of amalgamation, the identification of sole marks and the overall sandbody geometry supports the notion of an upper slope dominated by deposition from gravity flows. The gravity flows scoured the slope producing channels. The channels were later filled by younger turbidite deposits. The ignition of gravity flows was possibly aided by retrogressive slumping, representing an additional incensement of sediment supplied to the slope.
- The studied succession can be summarized as deposition within the highstand, forced regressive, lowstand wedge and transgressive system tracts.
- The palaeocurrent data obtained in this study coincides with the general understanding of an eastward progradational delta system.
- The tectonically active hinterland with a warm climate provided high rates of sediment supply. This, in concert with the narrow shelf (10-30km), represents ultimate conditions for deltas to reach the shelf-edge.

Suggestions for further work

The present study contributes to the understanding of the interacting processes of shelf-edge to-slope clinoforms. A “selfiestick” was used to document the impassable areas of the wedging element. The method was satisfactory in perfect weather conditions. For security reasons, to streamline the data collection and to obtain a more complete documentation a drone would be ideal. A drone would be able to provide a lateral continuous panorama view of the studied clinothem. This would also simplify the identification and lateral tracing of the facies associations and architecture, their boundaries, including internal architecture,

particularly within the wedging element. A drone could therefore improve and make the lateral correlation panel more accurate.

Furthermore, a petrographic analysis of the different elements of the clinothem may reveal contrasts in the textural and mineralogical properties of the different elements.

8 References:

Allen, J. R. L., 1970, Sediments of the modern Niger delta: a summary and review: Deltaic sedimentation, Modern and Ancient: SEPM Special pubication, v. 15, p. 138–151.

Allen, J. R. L., 1982, Sedimentary Structures: Their Character and Physical Basis. Developments in Sedimentology, 30A. Elsevier, Amsterdam, 593 p.

Allison, M. A., and Neill, C. F., 2003, Development of a modern subaqueous mud delta on the Atchafalaya Shelf, Louisiana. In: Scott, E.D , Bouma, A. H., and Bryant, W.R. (eds.), Siltstones, Mudstones and Shales: Depositional Processes and Characteristics: SEPM, CD-ROM, p. 23–34.

Augustinus, P. G. E. F., 1989, Cheniers and chenier plains: a general introduction: Marine Geology, v. 90, p. 219–229.

Bergh, S. G., and Andresen, A., 1990, Structural development of the Tertiary fold-and-thrust belt in east Oscar II Land, Spitsbergen: Polar Research, v. 8, p. 217–236.

Bergh, S. G., Braathen, A., and Andresen, A., 1997, Interaction of basement-involved and thin-skinned tectonism in the Tertiary fold-thrust belt of central Spitsbergen, Svalbard: AAPG Bulletin, v. 81, p. 637–661.

Bhattacharya, J. P., 2010, Deltas In: Dalrymple, R.W., James, N. P. (eds.), Facies Models 4. GEOtext 6: Geological Association of Canada, St. John`s, Newfoundland, p. 233–264.

Bhattacharya, J. P., and MacEachern, J. A., 2009, Hyperpycnal rivers and prodeltaic shelves in the Cretaceous seaway of North America: Journal of Sedimentary Research, v. 79, p. 184-209.

Bhattacharya, J. P., and Walker, R. G., 1992, Deltas. In: Walker, R. G and James, N.P. (eds.), Facies Models: Response to Sea-Level Change: Geological Association of Canada, St. John's, Newfoundland, 454 p.

Birkenmajer, K., 1975, Caledonides of Svalbard and plate tectonics: The Geological Society of Denmark, v. 24, p. 1–19.

Birkenmajer, K., 1981, The geology of Svalbard, the western part of the Barents Sea, and the continental margin of Scandinavia. In: Nairn, A.E.M., Churkin, M. and Stehli, F.G. (eds.), The ocean basins and margins, v. 5: The Arctic Ocean, Plenum Press, New York/London, p. 265–329.

Blinova, M., Faleide, J. I., Gabrielsen, R. H., and Mjelde, R., 2012, Seafloor expression and shallow structure of a fold-and-thrust system, Isfjorden, west Spitsbergen: Polar Research, v. 31, p. 1–13.

Blum, M. D., and Hattier-Womack, J., 2009, Climate change, sea-level change, and fluvial sediment supply to deepwater depositional systems: a review. In: Kneller, B., Martinsen, O. J., McCaffrey, W. D. (eds.), External controls on deepwater depositional systems: SEPM, Special Publication, v. 92, p. 15–39.

Blythe, A. E., and Kleinspehn, K. L., 1998, Tectonically versus climatically driven Cenozoic exhumation of the Eurasian plate margin, Svalbard: Fission track analyses: Tectonics, v. 17, p. 621–639.

Boggs, S. J., 2006, Principles of Sedimentology and Stratigraphy, 4th edn.: Upper Saddle River, New Jersey, Pearson Education, Ltd., 676 p.

Boggs, S. J., 2012, Principles of Sedimentology and Stratigraphy, 5th edn.: Upper Saddle River, New Jersey, Pearson Education, Ltd., 585 p.

Bouma, A. H., 1962, Sedimentology of some flysch deposits; a graphic approach to facies interpretation, Amsterdam, Elsevier, Amsterdam, 168 p.

Bouma, A. H., and Brower A. H., 1964, Turbidites. Developments in sedimentology, Elsevier, Amsterdam, 264 p.

Braathen, A., Bergh, S. G., and Maher, H. D., 1999, Application of a critical wedge taper model to the Tertiary transpressional fold-thrust belt on Spitsbergen, Svalbard: Geological Society of America Bulletin, v. 111, p. 1468–1485.

Bruhn, R., and Steel, R., 2003, High-resolution sequence stratigraphy of a clastic foredeep succession (Paleocene, Spitsbergen): An example of peripheral-bulge-controlled depositional architecture: Journal of Sedimentary Research, v. 73, p. 745–755.

Burgess, P. M., and Hovius, N., 1998, Rates of delta progradation during highstands: consequences for timing of deposition in deep-marine systems: Journal of the Geological Society of London, v. 155, p. 217–222.

Carmona, N. B., Buatois, L. A., Ponce, J. J., and Mángano, M. G., 2009, Ichnology and sedimentology of a tide-influenced delta, Lower Miocene Chenque Formation, Patagonia, Argentina: trace-fossil distribution and response to environmental stresses: Palaeogeography, Palaeoclimatology, Palaeoecology, v. 273, p. 75–86.

Carmona, N. B., Mángano, M. G., Buatois, L. A., and Ponce, J. J., 2010, Taphonomy and Paleoecology of the Bivalve Trace Fossil Protovirgularia in Deltaic Heterolithic Facies of the Miocene Chenque Formation, Patagonia, Argentina: Journal of Paleontology, v. 84, p. 730-738.

Carvajal, C., and Steel, R., 2009, Shelf-edge architecture and bypass of sand to deep water: influence of shelf-edge processes, sea level, and sediment supply: Journal of Sedimentary Research, v. 79, p. 652–672.

Cattaneo, A., Correggiari, A., Langone, L., and Trincardi, F., 2003, The late-Holocene Gargano subaqueous delta, Adriatic shelf: sediment pathways and supply fluctuations: Marine Geology, v. 193, p. 61–91.

Cattaneo, A., Trincardi, F., Asioli, A., and Correggiari, A., 2007, The Western Adriatic shelf clinoform: energy-limited bottomset: Continental Shelf Research, v. 27, p. 506–525.

Catuneanu, O., 2002, Sequence stratigraphy of clastic systems: concepts, merits and pitfalls.: Journal of African Earth Sciences, v. 35, p. 1–43.

Chamberlain, C. K., 1971, Morphology and ethology of trace fossils from the Ouachita Mountains, southeast Oklahoma: Journal of Paleontology, v. 45, p. 212–246.

Clark, B. E., and Steel, R. J., 2006, Eocene turbidite-population statistics from shelf edge to basin floor, Spitsbergen, Svalbard: Journal of Sedimentary Research, v. 76, p. 903–918.

Collinson, J. D., 1969, The sedimentology of the Grindslow Shales and the Kinderscout Grit: a deltaic complex in the Namurian of northern England: Journal of Sedimentary Research, v. 39, p. 194–221.

Collinson, J. D., Thompson, D. B., and Mountney, N., 2006, Sedimentary structures, 3rd, Terra Publishing, Hertfordshire, England, 292 p.

Crabaugh, J. P., and Steel, R. J., 2004, Basin-floor fans of the Central Tertiary Basin, Spitsbergen: relationship of basin-floor sand-bodies to prograding clinoforms in a structurally active basin: Geological Society, London, Special Publications, v. 222, p. 187–208.

Cummings, D. I., Dumas, S., and Dalrymple, R. W., 2009, Fine-grained versus coarse-grained wave ripples generated experimentally under large-scale oscillatory flow: Journal of Sedimentary Research, v. 79, p. 83–93.

Curray, J. R., and Moore, D. G., 1964, Pleistocene deltaic progradation of continental terrace, Costa de Nayarit, Mexico. In: Van Straaten, L. M. J. U. (ed.), Deltaic and Shallow Marine Deposits, Elsevier, Amsterdam p. 193–214.

Dalland, A., 1976, Erratic clasts in the lower Tertiary deposits of Svalbard—evidence of transport by winter ice: Norsk Polarinstitutt, Årbok 1976, p. 151–165.

Dallmann, W. K., 1999, Lithostratigraphic lexicon of Svalbard: review and recommendations for nomenclature use: Upper Palaeozoic to Quaternary bedrock. Norsk Polarinstitut, Tromsø, 318 p.

Dallmann, W. K., and Elvevold, S., 2015, Geoscience Atlas of Svalbard. In Dallmann, W. K., (ed.) Chapter 7: Bedrock geology: Nork Polarinstitutt, Tromsø, Norway, Report Series 148, p. 133–174.

Deibert, J., Benda, T., Løseth, T., Schellpeper, M., and Steel, R., 2003, Eocene clinoform growth in front of a storm-wave-dominated shelf, Central Basin, Spitsbergen: no significant sand delivery to deepwater areas: Journal of Sedimentary Research, v. 73, p. 546–558.

Dickinson, W. R., and Yarborough, H., 1979, Plate tectonics and hydrocarbon accumulation: AAPG, Continuing Education Course Note Series, Tulsa, Oklahoma, p. 1–62.

Dixon, J. F., 2013, Shelf to slope sediment partitioning on basin-margin scale clinoforms, Karoo Basin, South Africa [PhD dissertation], The Univeristy of Texas at Austin, p. 8–144.

Dumas, S., and Arnott, R., 2006, Origin of hummocky and swaley cross-stratification—the controlling influence of unidirectional current strength and aggradation rate: Geology, v. 34, p. 1073–1076.

Dumas, S., Arnott, R., and Southard, J. B., 2005, Experiments on oscillatory-flow and combined-flow bed forms: implications for interpreting parts of the shallow-marine sedimentary record: Journal of Sedimentary Research, v. 75, p. 501–513.

Dzulynsky, S., and Walton, E., 1965, Sedimentary features of flysch and greywackes. Elsevier, Amsterdam, 274 p.

Eldholm, O., Sundvor, E., Myhre, A. M., and Faleide, J. I., 1984, Cenozoic evolution of the continental margin off Norway and western Svalbard. In: Spencer, A. M (ed.), Petroleum Geology of the North European Margin, Graham and Trotman, London, p. 3–18.

Embry, A. F., 2001, The six surfaces of sequence stratigraphy: AAPG, Hedberg Research Conference on Sequence Stratigraphic and Allostratigraphic Principles and Concepts, p. 26–27.

Faleide, J. I., Tsikalas, F., Breivik, A. J., Mjelde, R., Ritzmann, O., Engen, O., Wilson, J., and Eldholm, O., 2008, Structure and evolution of the continental margin off Norway and the Barents Sea: Episodes, v. 31, p. 82–91.

Flint, S. S., Hodgson, D. M., Sprague, A. R., Brunt, R. L., Van der Merwe, W. C., Figueiredo, J., Prélat, A., Box, D., Di Celma, C., and Kavanagh, J. P., 2011, Depositional architecture and sequence stratigraphy of the Karoo basin floor to shelf edge succession, Laingsburg depocentre, South Africa: Marine and Petroleum Geology, v. 28, p. 658–674.

Friend, P., Harland, W., Rogers, D., Snape, I., and Thornley, R., 1997, Late Silurian and Early Devonian stratigraphy and probable strike-slip tectonics in northwestern Spitsbergen: Geological Magazine, v. 134, p. 459–479.

Friend, P. F., and Moody-Stuart, M., 1972, Sedimentation of the Wood Bay Formation (Devonian) of Spitsbergen: Norsk Polarinstitutt, Årbok 1972, p. 157-237.

Galloway, W. E., 1989, Genetic stratigraphic sequences in basin analysis 1: architecture and genesis of flooding-surface bounded depositional units: AAPG Bulletin, v. 73, p. 125–142.

Gingras, M. K., Dashtgard, S. E., MacEachern, J. A., and Pemberton, S. G., 2008, Biology of shallow marine ichnology: a modern perspective: Aquatic Biology, v. 2, p. 255–268.

Gjelberg, H. K., 2010, Facies Analysis and Sandbody Geometry of the Paleogene Battfjellet Formation, Central Western Nordenskiöld Land, Spitsbergen [Master thesis]: The University of Bergen, 172 p.

Gjelberg, J., and Steel, R. J., 1995, Helvetiafjellet Formation (Barremian-Aptian), Spitsbergen: characteristics of a transgressive succession: Norwegian Petroleum Society, Special Publications, v. 5, p. 571–593.

Gjelberg, J. G., and Steel, R. J., 1981, An outline of Lower-Middle Carboniferous sedimentation on Svalbard: effects of climatic, tectonic and sea level changes in rift basin sequences: Canadian Society of Petroleum Geologists, v. 7, p. 543–561.

Greenwood, B., and Sherman, D. J., 1986, Hummocky cross-stratification in the surf zone: flow parameters and bedding genesis: Sedimentology, v. 33, p. 33–45.

Gressly, A., 1838, Observations géologiques sur le Jura Soleurois: Nouveaux Mémoires de la Société Helvétique des Sciences Naturelles, v. 2, p. 1–112.

Grundvåg, S.-A., 2012, Outcrop and subsurface characterization of shelf-margin clinoform systems [PhD dissertation]: University of Bergen, p. 252.

Grundvåg, S. A., Helland-Hansen, W., Johannessen, E. P., Olsen, A. H., and Stene, S. A. K., 2014a, The depositional architecture and facies variability of shelf deltas in the Eocene Battfjellet Formation, Nathorst Land, Spitsbergen: Sedimentology, v. 61, p. 2172–2204.

Grundvåg, S. A., Johannessen, E. P., Helland-Hansen, W., and Plink-Björklund, P., 2014b, Depositional architecture and evolution of progradationally stacked lobe complexes in the Eocene Central Basin of Spitsbergen: Sedimentology, v. 61, p. 535–569.

Harland, W. B., 1969, Contribution of Spitsbergen to Understanding of Tectonic Evolution of North Atlantic Region. In: Kay, M. (ed.), North Atlantic: Geology and Continental Drift: AAPG Memoir 12, p. 817–851.

Harland, W. B., Anderson, L. M., Manasrah, D., Butterfield, N. J., Challinor, A., Doubleday, P. A., Dowdeswell, E. K., Dowdeswell, J. A., Geddes, I., and Kelly, S. R., 1997, The geology of Svalbard: Geological Society of London, Memoir 17, 521 p.

Hart, B. S., Sibley, D. M., and Flemings, P. B., 1997, Seismic stratigraphy, facies architecture, and reservoir character of a Pleistocene shelf-margin delta complex, Eugene Island Block 330 Field, offshore Louisiana: AAPG Bulletin, v. 81, p. 380–397.

Helland-Hansen, W., 1985, Sedimentology of the Battfjellet Formation (Palaeogene) in Nordenskiöld Land, Spitsbergen: Unpublished Cand. Scient. thesis, University of Bergen, 322 p.

Helland-Hansen, W., 1990, Sedimentation in Paleogene Foreland Basin, Spitsbergen (1): AAPG Bulletin, v. 74, p. 260–272.

Helland-Hansen, W., 1992, Geometry and facies of Tertiary clinothems, Spitsbergen: Sedimentology, v. 39, p. 1013–1029.

Helland-Hansen, W., 2009, Facies and stacking patterns of shelf-deltas within the Palaeogene Battfjellet Formation, Nordenskiöld Land, Svalbard: implications for subsurface reservoir prediction: Sedimentology, v. 57, p. 190–208.

Helland-Hansen, W., and Hampson, G. J., 2009, Trajectory analysis: concepts and applications: Basin Research, v. 21, p. 454–483.

Helland-Hansen, W., and Martinsen, O. J., 1996, Shoreline trajectories and sequences: description of variable depositional-dip scenarios: Journal of Sedimentary Research, v. 66, p. 670–688.

Helland-Hansen, W., Steel, R. J., and Sømme, T. O., 2012, Shelf genesis revisited: Journal of Sedimentary Research, v. 82, p. 133–148.

Henriksen, S., Ponten, A., Janbu, N., and Paasch, B., 2010, The importance of sediment supply and sequence-stacking pattern in creating hyperpycnal flows. In: Slatt, R.M and Zavala, C (eds.), Sediment transfer from shelf to deep water-Revisiting the delivery system: AAPG Studies in Geology, v. 61, p. 1–24.

Hodgson, D. M., Flint, S. S., Hodgetts, D., Drinkwater, N. J., Johannessen, E. P., and Luthi, S. M., 2006, Stratigraphic evolution of fine-grained submarine fan systems, Tanqua depocenter, Karoo Basin, South Africa: Journal of Sedimentary Research, v. 76, p. 20–40.

Howard, J. D., 1966, Characteristic trace fossils in Upper Cretaceous sandstones of the Book Cliffs and Wasatch Plateau: Utah Geological Survey, Bulletin 80, p. 35–53.

Hunt, D., and Tucker, M. E., 1992, Stranded parasequences and the forced regressive wedge systems tract: deposition during base-level fall.: Sedimentary Geology v. 81, p. 1–9.

Johannessen, E., and Steel, R., 2005, Clinoforms and their exploration significance for deepwater sands: Basin Research, v. 17, p. 521–550.

Johnson, S. D., Flint, S., Hinds, D., and De Ville Wickens, H., 2001, Anatomy, geometry and sequence stratigraphy of basin floor to slope turbidite systems, Tanqua Karoo, South Africa: Sedimentology, v. 48, p. 987–1023.

Kellogg, H. E., 1975, Tertiary stratigraphy and tectonism in Svalbard and continental drift: AAPG Bulletin, v. 59, p. 465–485.

Khan, S. M., Imran, J., Bradford, S., and Syvitski, J., 2005, Numerical modeling of hyperpycnal plume: Marine Geology, v. 222, p. 193–211.

Kim, W., Paola, C., Voller, V. R., and Swenson, J. B., 2006, Experimental measurement of the relative importance of controls on shoreline migration: Journal of Sedimentary Research, v. 76, p. 270–283.

Knaust, D., 2015, Siphonichnidae (new ichnofamily) attributed to the burrowing activity of bivalves: Ichnotaxonomy, behaviour and palaeoenvironmental implications: Earth-Science Reviews, v. 150, p. 497–519.

Knaust, D., 2017, Atlas of Trace Fossils in Well Core: Appearance, Taxonomy and Interpretation. Springer International Publishing, 208 p.

Knaust, D., Curran, H. A., and Dronov, A. V., 2012, Shallow-marine carbonates: Trace Fossils as Indicators of Sedimentary Environments: Developments in Sedimentology, v. 64, p. 703–750.

Kneller, B., 1995, Beyond the turbidite paradigm: physical models for deposition of turbidites and their implications for reservoir prediction: Geological Society, London, Special Publications, v. 94, p. 31–49.

Komar, P. D., and Miller, M. C., 1975, The initiation of oscillatory ripple marks and the development of plane-bed at high shear stresses under waves: Journal of Sedimentary Petrology, v. 45, p. 697–703.

Li, W., Bhattacharya, J. P., Zhu, Y., Garza, D., and Blankenship, E., 2011, Evaluating delta asymmetry using three-dimensional facies architecture and ichnological analysis, Ferron 'Notom Delta', Capital Reef, Utah, USA: Sedimentology, v. 58, p. 478–507.

Ljutkevic, E. M., 1937, Geologiceskij ocerk i problem uglenosnosti gory Piramidy ostrova Spicbergena. (Geological survey and problems of the coal fields of mount Pyramiden, Spitsbergen.): Trudy Arktieeskogo Instituta Leningrad, v. 76, p. 25–38.

Lowe, D. R., 1975, Water escape structures in coarse-grained sediments: Sedimentology, v. 22, p. 157–204.

Lowe, D. R., 1982, Sediment gravity flows: II Depositional models with special reference to the deposits of high-density turbidity currents: Journal of Sedimentary Petrology, v. 52, p. 279–297.

M'Coy, F., 1850, On some genera and species of Silurian Radiata in the collection of the University of Cambridge: Annals and Magazine of Natural History, v. 2, p. 270–290.

Maceachern, J. A., Bann, K. L., Bhattacharya, J. P., and Howell Jr, C. D., 2005, Ichnology of deltas: organism responses to the dynamic interplay of rivers, waves, storms, and tides. In: Giosan, L., and Bhattacharya, J., P. (eds.), River Deltas-Concepts, Models and examples: SEPM Special Pubication, v. 83, p. 49–85.

Major, H., and Nagy, J., 1964, (Cartographer), Adventdalen. Geologisk kart.

Major, H., and Nagy, J., 1972, Geology of the Adventdalen map area: Norsk Polarinstitutt Skrifter, v, 138, p. 1-58.

Mattern, F., 2002, Amalgamation surfaces, bed thicknesses, and dish structures in sand-rich submarine fans: numeric differences in channelized and unchannelized deposits and their diagnostic value: Sedimentary-Geology, v. 150, p. 203–228.

Mayall, M. J., Yeilding, C. A., Oldroyd, J. D., A.J. Pulham, A. J., and Sakurai, S., 1992, Facies in a shelf-edge delta—an example from the subsurface of the Gulf of Mexico, middle Pliocene, Mississippi Canyon, Block 109: AAPG bulletin, v. 76, p. 435–448.

Mellere, D., Breda, A., and Steel, R. J., 2003, Fluvially-incised shelf-edge deltas and linkage to upper-slope channels (Central Tertiary Basin, Spitsbergen): Global significance and future exploration potential: Gulf Coast Section: SEPM Special Publication, v. 23, p. 231–266.

Mellere, D., Plink‐Björklund, P., and Steel, R. J., 2002, Anatomy of shelf deltas at the edge of a prograding Eocene shelf margin, Spitsbergen: Sedimentology, v. 49, p. 1181–1206.

Middleton, G. V., 1993, Sediment deposition from turbidity currents: Annual Review of Earth and Planetary Sciences, v. 21, p. 89–114.

Middleton, G. V., Church, M. J., Coniglio, M., Hardie, L. A., and Longstaffe, F. J., 2003, Encyclopedia of Sediments and Sedimentary Rocks, Geoscience Canada, v. 32.

Mortimer, E., Gupta, S., and Cowie, P., 2005, Clinoform nucleation and growth in coarse-grained deltas, Loreto basin, Baja California Sur, Mexico: a response to episodic accelerations in fault displacement: Basin Research, v. 17, p. 337–359.

Morton, R. A., and Suter, J. R., 1996, Sequence stratigraphy and composition of Late Quaternary shelf-margin deltas, Northern Gulf of Mexico: AAPG Bulletin, v. 80, p. 505–530.

Mulder, T., and Syvitski, J. P., 1995, Turbidity currents generated at river mouths during exceptional discharges to the world oceans: The Journal of Geology, v. 103, p. 285–299.

Mulder, T., Syvitski, J. P., Migeon, S., Faugères, J.C., and Savoye, B., 2003, Marine hyperpycnal flows: initiation, behavior and related deposits. A review: Marine and Petroleum Geology, v. 20, p. 861–882.

Müller, R. D., and Spielhagen, R. F., 1990, Evolution of the Central Tertiary Basin of Spitsbergen: towards a synthesis of sediment and plate tectonic history: Palaeogeography, Palaeoclimatology, Palaeoecology, v. 80, p. 153–172.

Muto, T., and Steel, R. J., 2002, In defence of shelf-edge delta development during falling and lowstand of relative sea level: Journal of Geology, v. 110, p. 421–436.

Mutti, E., 1992, Facies con Hummocky Cross-Stratification Prodotte da Flussi Gravitativi in Sistemi Confinati di Fan Delta di Acque Basse (Shelf-Type Fan Deltas): Società Geologica Italiana, v. 76, p. 102–105.

Mutti, E., Davoli, G., Tinterri, R., and Zavala, C., 1996, The importance of ancient fluvio-deltaic systems dominated by catastrophic flooding in tectonically active basins: Memorie di Scienze Geologiche, v. 48, p. 233–291.

Mutti, E., Tinterri, R., Benevelli, G., di Biase, D., and Cavanna, G., 2003, Deltaic, mixed and turbidite sedimentation of ancient foreland basins: Marine and Petroleum Geology, v. 20, p. 733–755.

Myhre, A. M., Eldholm, O., and Sundvor, E., 1982, The margin between Senja and Spitsbergen fracture zones: implications from plate tectonics: Tectonophysics, v. 89, p. 33–50.

Nagy, J., Kaminski, M. A., and Kuhnt, W., 2000, Agglutinated Foraminifera from Neritic to Bathyal Facies in the Paleogene of Spitsbergen and the Barents Sean. In: Hart, M. B., Kaminski M. A. and Smart C. W. (eds.), Proceedings of the Fifth International Workshop on Agglutinated Foraminifera: Grzybowski Foundation Special Publication, v. 7, p. 333–361.

Nathorst, A. G., 1910, Beiträge zur Geologie der Bäreninsel, Spitzbergens und des König-Karl-Landes: Bulletin Geologiska Institutionen Univeritetet i Uppsala, (1910-1911), v. 10 p. 261–416.

Naurstad, O. A., 2014, Sedimentology of the Aspelintoppen Formation (Eocene-Oligocene), Brogniartfjella, Svalbard [Master thesis]: The University of Bergen, 128 p.

Nemec, W., 1995, The dynamics of deltaic suspension plumes In: Oti, M.N., Postma, G. (eds.), Geology of Deltas: AA Balkema, Rotterdam, p. 31–93.

Nichols, G., 2009, Sedimentology and stratigraphy, John Wiley & Sons, London, Blackwell, 355 p.

Nichols, R. J., Sparks, R. S. J., and Wilson, C. J. N., 1994, Experimental studies of the fluidization of layered sediments and the formation of fluid escape structures: Sedimentology, v. 41, p. 233–253.

Nopsca, F. B., 1923, Die Familien der Reptilien, v. 2, p. 1–210 p.

Nøttvedt, A., 1982, Characteristics and evolution of the Askeladden Deltaic Sequence (Palaeocene) on Spitsbergen—with comparisons with the Ravenscar Group Deltaic Sequences (Bajocian) of Northeast England [PhD thesis]: University of Bergen, 146 p.

Nøttvedt, A., Livbjerg, F., Midbøe, P. S., and Rasmussen, E., 1992, Hydrocarbon potential of the Central Spitsbergen Basin: Norwegian Petroleum Society, Special Publication, v. 2, p. 333–361.

Orvin, A., 1940, Outline of the geological history of Spitsbergen. Skrifter om Svalbard og Ishavet, v. 78, (reprint 1969; 1961-1957).

Paech, H. J., 1999, The Tertiary and Cretaceous of Spitsbergen and North-Greenland: its Alpine signature: Alfred Wegener Institute for Polar and Marine Research & German Society of Polar Research, v. 69, p. 107–115.

Parsons, J. D., Bush, J. W., and Syvitski, J. P., 2001, Hyperpycnal plume formation from riverine outflows with small sediment concentrations: Sedimentology, v. 48, p. 465–478.

Petter, A. L., and Steel, R. J., 2006, Hyperpycnal flow variability and slope organization on an Eocene shelf margin, Central Basin, Spitsbergen: AAPG Bulletin, v. 90, p. 1451–1472.

Pettijohn, F. J., 1975, Sedimentary Rocks, 3rd edn., Harper & Row, New York, 628 p.

Piper, D. J. W., and Normark, W. R., 2009, Processes that initiate turbidity currents and their influence on turbidites: a marine geology perspective: Journal of Sedimentary Research, v. 79, p. 347–362.

Plink-Björklund, P., 2005, Stacked fluvial and tide-dominated estuarine deposits in high-frequency (fourth-order) sequences of the Eocene Central Basin, Spitsbergen: Sedimentology, v. 52, p. 391–428.

Plink-Björklund, P., Mellere, D., and Steel, R. J., 2001, Turbidite variability and architecture of sand-prone, deep-water slopes: Eocene clinoforms in the Central Basin, Spitsbergen: Journal of Sedimentary Research, v. 71, p. 895–912.

Plink-Björklund, P., and Steel, R. J., 2002, Sea-level fall below the shelf edge, without basin-floor fans: Geology, v. 30, p. 115–118.

Plink-Björklund, P., and Steel, R. J., 2004, Initiation of turbidity currents: outcrop evidence for Eocene hyperpycnal flow turbidites: Sedimentary Geology, v. 165, p. 29–52.

Plink-Björklund, P., and Steel, R. J., 2005, Deltas on falling-stage and lowstand shelf margins, the Eocene Central Basin of Spitsbergen: importance of sediment supply. In: Giosan, L., and Bhattacharya, J.P., eds., River Deltas: Concepts, Models, and Examples: SEPM, Special Publication, v. 83, p. 179–206.

Pontén, A., and Plink-Björklund, P., 2009, Process regime changes across a regressive to transgressive turnaround in a shelf–slope basin, Eocene central Basin of Spitsbergen: Journal of Sedimentary Research, v. 79, p. 2–23.

Porębski, S. J., and Steel, R. J., 2003, Shelf-margin deltas: their stratigraphic significance and relation to deepwater sands: Earth-Science Reviews, v. 62, p. 283–326.

Porębski, S. J., and Steel, R. J., 2006, Deltas and Sea-Level Change: Journal of Sedimentary Research, v. 76, p. 390–403.

Prothero, D. R., and Schwab, F., 2004, Sedimentary Geology: An Introduction to Sedimentary Rocks and Stratigraphy, 2nd edn, Freeman and Company, New York, W.H., 557 p.

Rahmani, R. A., 1988, Estuarine tidal channel and nearshore sedimentation of a Late Cretaceous epicontinental sea, Drumheller, Alberta, Canada. In: de Boer, P. L., van Gelder, A., and Nio, S .D. (eds.), Tide-influenced Sedimentary Environments and Facies: Boston, D. Reidel, p. 433–481.

Reineck, H.-E., and Singh, I. B., 1980, Depositional Sedimentary Environments, with Reference to Terrigenous Clastics. Springer-Verlag, Berlin, 549 p.

Rich, J. L., 1950, Flow markings, groovings, and intra-stratal crumplings as criteria for recognition of slope deposits, with illustrations from Silurian rocks of Wales: AAPG Bulletin, v. 34, p. 717–741.

Rich, J. L., 1951, Three critical environments of deposition, and criteria for recognition of rocks deposited in each of them: Geological Society of America Bulletin, v. 62, p. 1–20.

Rine, J. M., and Ginsburg, R. N., 1985, Depositional facies of a mud shoreface in Suriname, South America— a mud analogue to sandy, shallow-marine deposits: Journal of Sedimentary Research, v. 55, p. 633–652.

Roest, W., and Srivastava, S., 1989, Sea-floor spreading in the Labrador Sea: A new reconstruction: Geology, v. 17, p. 1000-1003.

Rotondo, K. A., and Bentley Sr, S. J., 2004, Marine dispersal of fluvial sediments as fluid muds: old concept, new significance. In: Scott, E. D., Bouma, A. H., and Bryant, W. R. (eds.), Siltstones, Mudstones and Shales: Depositional Processes and Characteristics: SEPM, CD-ROM, p. 24–49.

Rudloe, A., 1981, Aspects of the biology of juvenile horseshoe crabs, Limulus polyphemus: Bulletin of Marine Science, v. 31, p. 125–133.

Skorstad, A., Kolbjørnsen, O., Manzocchi, T., Carter, J. N., and Howell, J. A., 2008, Combined effects of structural, stratigraphic and well controls on production variability in faulted shallow-marine reservoirs: Petroleum Geoscience, v. 14, p. 45–54.

Sømme, T. O., Helland-Hansen, W., and Granjeon, D., 2009a, Impact of eustatic amplitude variations on shelf morphology, sediment dispersal, and sequence stratigraphic interpretation: Icehouse versus greenhouse systems: Geology, v. 37, p. 587–590.

Sømme, T. O., Helland-Hansen, W., Martinsen, O. J., and Thurmond, J. B., 2009b, Relationships between morphological and sedimentological parameters in source-to-sink systems: A basis for predicting semi-quantitative characteristics in subsurface systems: Basin Research, v. 21, p. 361–387.

Stanistreet, I. G., Le Blanc Smith, G., and Cadle, A. B., 1980, Trace fossils as sedimentological and palaeoenvironmental indices in the Ecca Group (Lower Permian) of the Transvaal: Transactions of the Geological Society of South Africa, v. 83, p. 333–344.

Stanley, D. C. A., and Pickerill, R. K., 1995, Arenituba, a new name for the trace fossil ichnogenus Micatuba Chamberlain, 1971: Journal of Paleontology, v. 69, p. 612–614.

Steel, R. J., 1977, Observations on some Cretaceous and Tertiary sandstone bodies in Nordenskiold Land, Svalbard: Norsk Polarinstitutt, Årbok 1976, p. 43–67.

Steel, R. J., Crabaugh, J., Schellpeper, M., Mellere, D., Plink-Björklund, P., Deibert, J., and Loeseth, T., 2000, Deltas vs. rivers on the shelf edge: their relative contributions to the growth of shelf-margins and basin-floor fans (Barremian and Eocene, Spitsbergen): Gulf Coast Section, SEPM Foundation, 20th Annual Research Conference, Deep-Water Reservoirs of the World, p. 981–1009.

Steel, R. J., Dalland, A., Kalgraff, K., and Larsen, V., 1981, The Central Tertiary Basin of Spitsbergen: sedimentary development of a sheared-margin basin: Canadian Society Petroleum Geology, v. 7, p. 647–664.

Steel, R. J., Gjelberg, J., Helland-Hansen, W., Kleinspehn, K., Nøttvedt, A., and Rye-Larsen, M., 1985, The Tertiary strike-slip basins and orogenic belt of Spitsbergen: SEPM Special Publication, v. 37, p. 339–360.

Steel, R. J., and Olsen, T., 2002, Clinoforms, clinoform trajectories and deepwater sands. In: Proceedings Sequence-stratigraphic models for exploration and production: Evolving methodology, emerging models and application histories: Gulf Coast Section SEPM 22nd Research Conference, Houston, Texas, p. 367–381.

Steel, R. J., and Worsley, D., 1984, Svalbard's post-Caledonian strata – an atlas of sedimentational patterns and palaeogeographic evolution. In: Spencer A. M., et al. (eds.), Petroleum geology of the north European margin: Graham & Trotman Ltd., London, p. 109–35.

Suter, J. R., and Berryhill, H. L., 1985, Late Quaternary shelf-margin deltas, northwest Gulf of Mexico: AAPG Bulletin, v. 69, p. 77–91.

Swift, D. J. P., and Thorne, J. A., 1991, Sedimentation on continental margins: a general model for shelf sedimentation In: Swift, D. J. P., Oertel, G. F., Tillman, R. W., and Thorne, J. A. (eds.), Shelf sand and sandstone bodies-Geometry, Facies and Sequnece Stratigraphy: International Association of Sedimentologists, Special Publication, v. 14, p. 3–31.

Sydow, J., and Roberts, H. H., 1994, Stratigraphic framework of a late Pleistocene shelf-edge delta, Northeast Gulf of Mexico. : AAPG Bulletin, v. 78, p. 1276–1312.

Ta, T. K. O., Nguyen, V. L., Tateishi, M., Kobayashi, I., and Saito, Y., 2005, Holocene delta evolution and depositional models of the Mekong River Delta, southern Vietnam. In: Giosan, L., and Bhattacharya, J.P., eds., River Deltas: Concepts, Models, and Examples: SEPM, Special Publication, v. 83, p. 453–466.

Torell, O., 1870, Petrificata Suecana Formationis Cambricae: Lunds Universitet, Årsskrift 6, p. 1–14.

Uroza, C. A., and Steel, R. J., 2008, A highstand shelf-margin delta system from the Eocene of West Spitsbergen, Norway: Sedimentary Geology, v. 203, p. 229–245.

Van Wagoner, J. C., Posamentier, H. W., Mitchum, R. M., Vail, P. R., Sarg, J. F., Loutit, T. S., and Hardenbol, J., 1988, An overview of sequence stratigraphy and key definitions. In: Wilgus, C. K., Hastings, B. S., Kendall, C. G. St .C., Posamentier, H. W., Ross, C. A., and Van Wagoner, J. C. (eds.), Sea-level Changes: an Integrated Approach: SEPM Special Pubication, v. 42, p. 39–45.

Walker, R. G., 1967, Turbidite Sedimentary Structures and their Relationship to Proximal and Distal Depositional Environments: Journal of Sedimentary Research, v. 37, p. 25–43.

Walker, R. G., 1984, Shelf and shallow marine sands. In: Walker, R., G. (ed.), Facies Models, 2nd edn. Geological Association of Canada, Geoscience Canada Reprint Series, v. 1, p. 141–170.

Wild, R., Flint, S. S., and Hodgson, D. M., 2009, Stratigraphic evolution of the upper slope and shelf edge in the Karoo Basin, South Africa. In: Henriksen, S., Hampson, G. J., Helland-Hansen, W., Johannessen, E. P., and Steel, R. J. (eds.), Trajectory Analyses in Stratigraphy: Basin Research, v. 21, p. 502–527.

Winker, C. D., and Edwards, M. B., 1983, Unstable progradational clastic shelf margins. In: Stanley, D. J., Moore, G. T. (eds.), The Shelfbreak, Critical Interface on Continental Margins: SEPM Special Pubication, v. 33, p. 139–157.

Worsley, D., 2008, The post-Caledonian development of Svalbard and the western Barents Sea: Polar Research, v. 27, p. 298–317.

Worsley, D., and Aga, O. J., 1984, The Geological History of Svalbard. Evolution of an arctic archipelago. Det norske stats oljeselskap a.s, Stavanger, 120 p.

Worsley, D., Aga, O. J., Dalland, A., Elverhøi, A., and Thon, A., 1986, The geological history of Svalbard—evolution of an Arctic archipelago: Statoil, Stavanger, 122 p.

Wright, L., 1978, River deltas, In: Davis, R. A. J., (ed.), In: Coastal Sedimentary Environments: Springer-Verlag, New York, p. 5–68.

Wright, L. D., Wiseman, W. J., Bornhold, B. D., Prior, D. B., Suhayda, J. N., Keller, G. H., Yang, Z. S., and Fan, Y. B., 1988, Marine dispersal and deposition of Yellow River silts by gravity-driven underflows: Nature, v. 332, p. 629–632.

Zaitlin, B. A., Dalrymple, R. W., and Boyd, R., 1994, The stratigraphic organization of incised-valley systems associated with relative sea-level change. In: Dalrymple, R. W., Boyd, R. and Zaitlin, B. A. (eds.), Incised valley Systems: Origin and Sedimentary Sequences, SEPM Special Pubication, v. 51, p. 45–60.

http://toposvalbard.npolar.no/ (downloaded 06.07.2016)

9 Appendix:

Lithostratigraphical logs, Clinoform 8C, Brogniartfjella, Svalbard

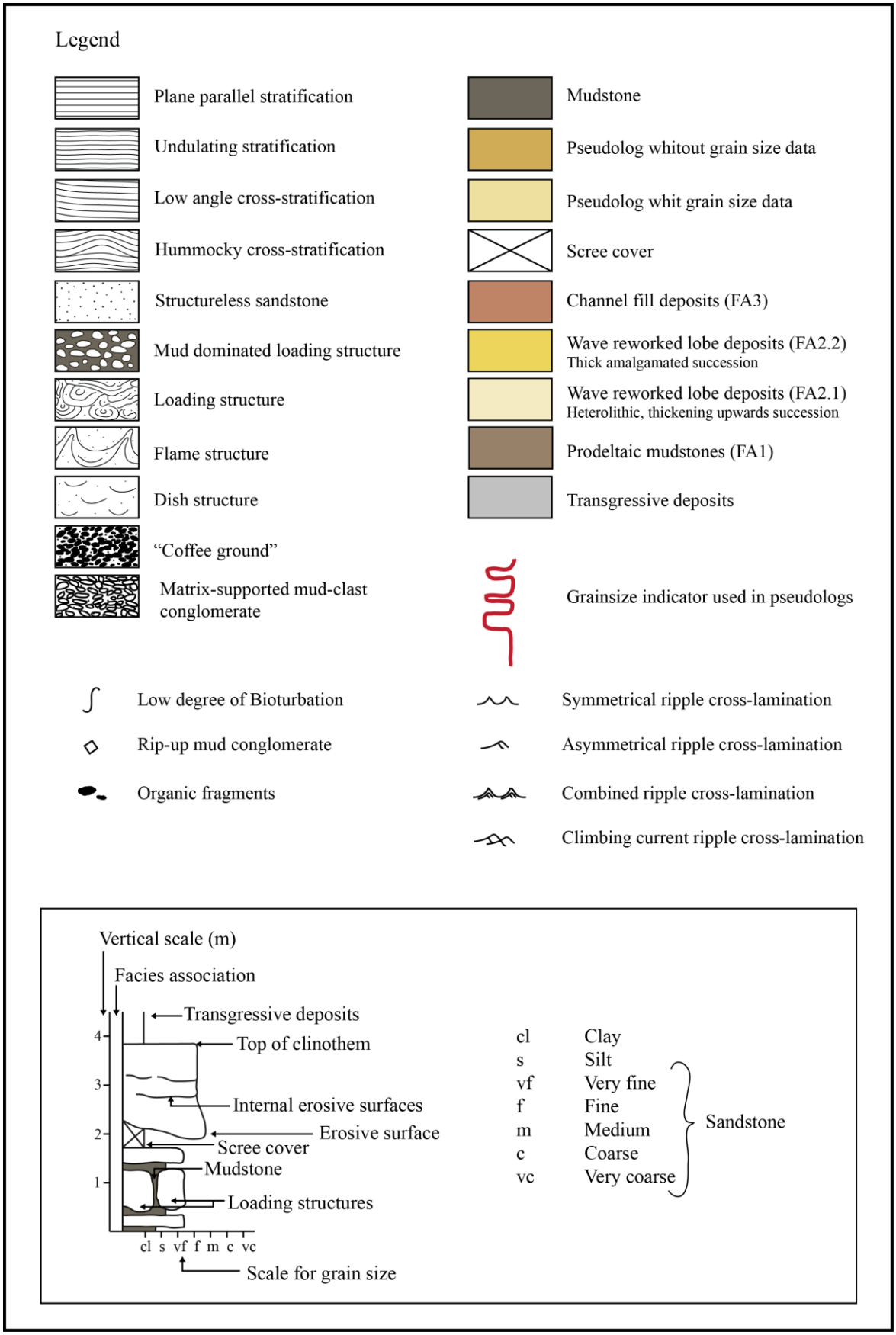

The logs are presented in a 1:50 scale. Due to challenges collecting the photos for the pseudologs, the pseudologs appears in different sizes. The meassurestick on the "photologs" are 1m.

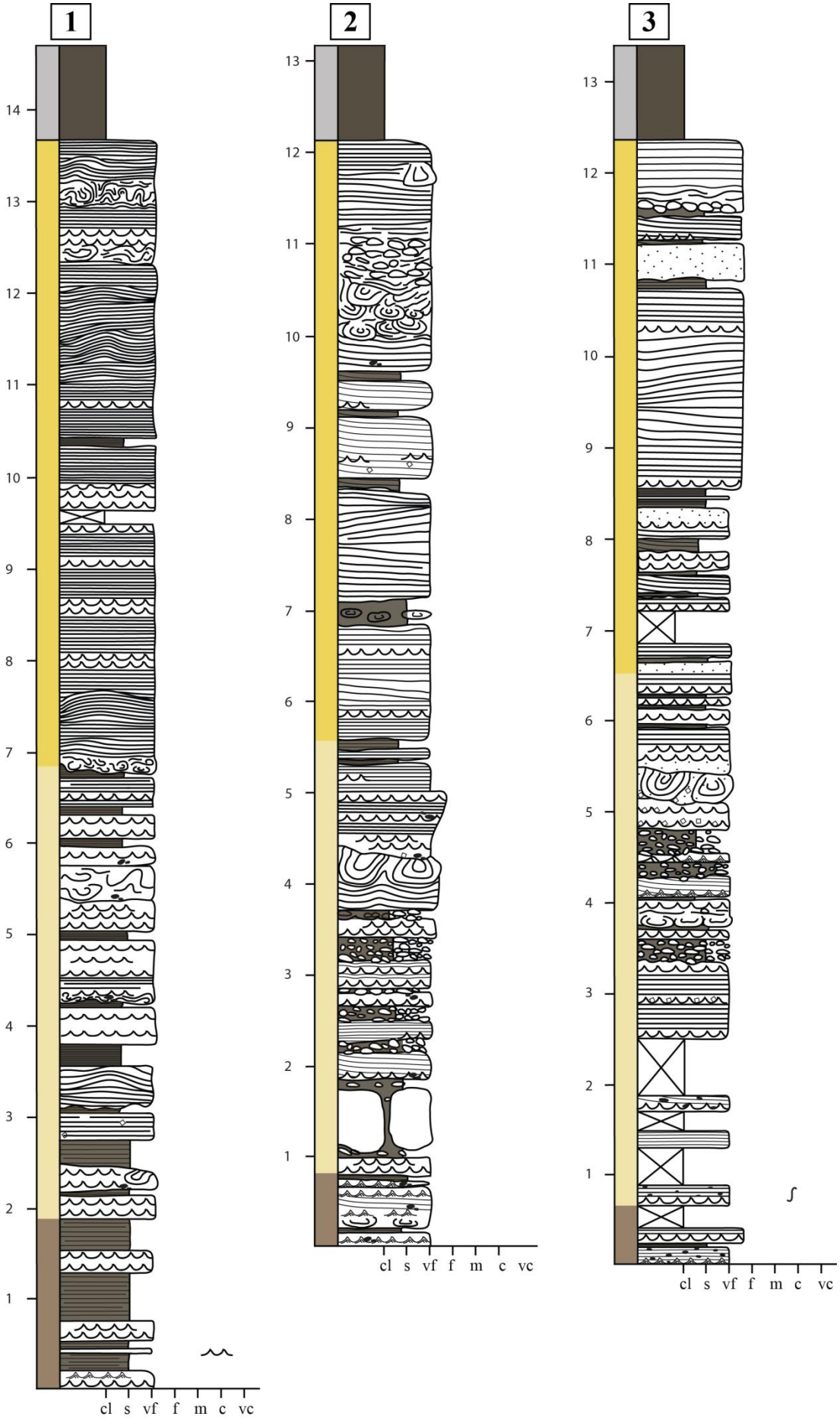
1
2
3
cl s vf f m c vc
cl s vf f m c vc
cl s vf f m c vc

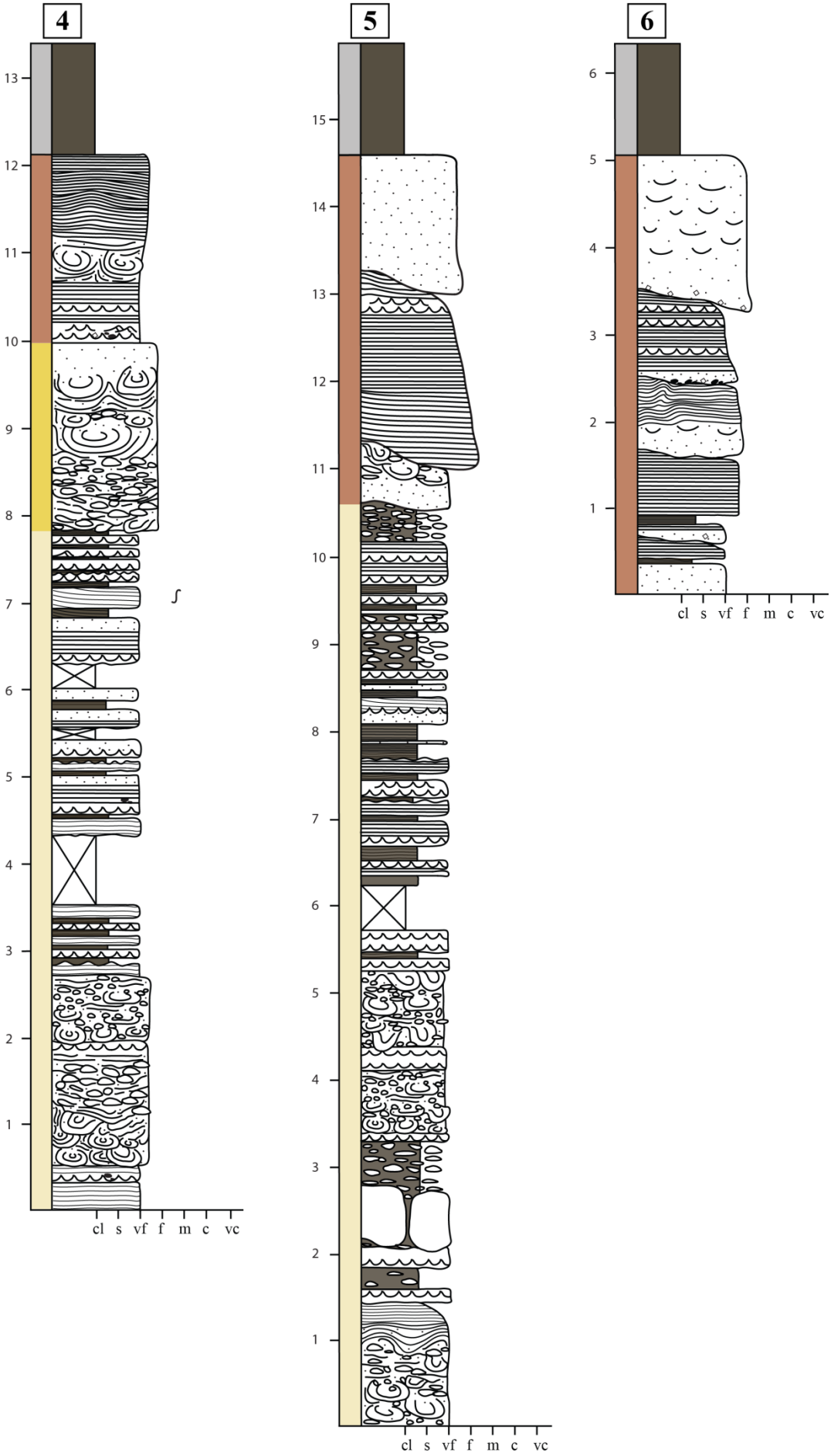
4
5
6
cl s vf f m c vc

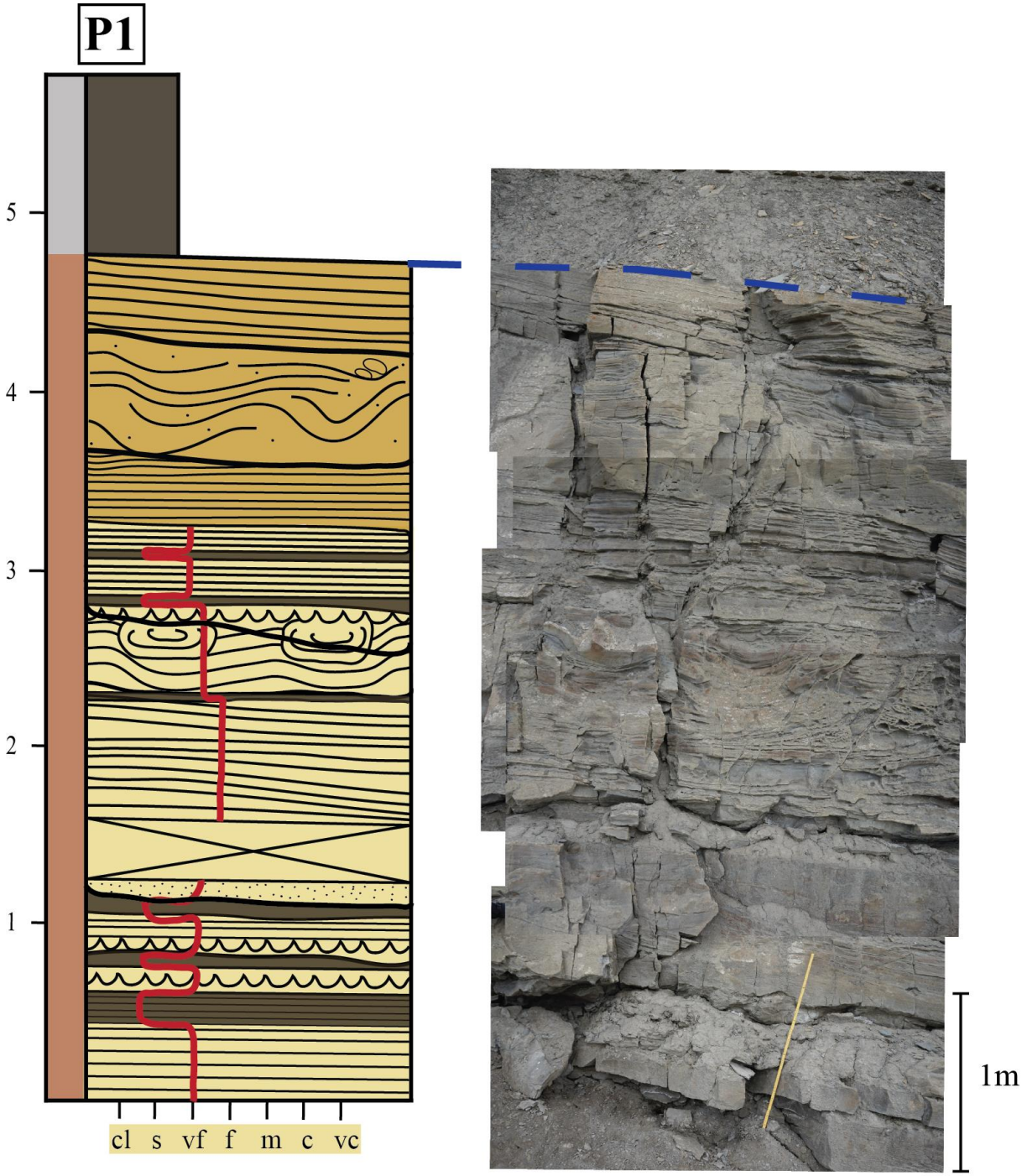
P1
5
4
3
2
1
cl s vf f m c vc
1m

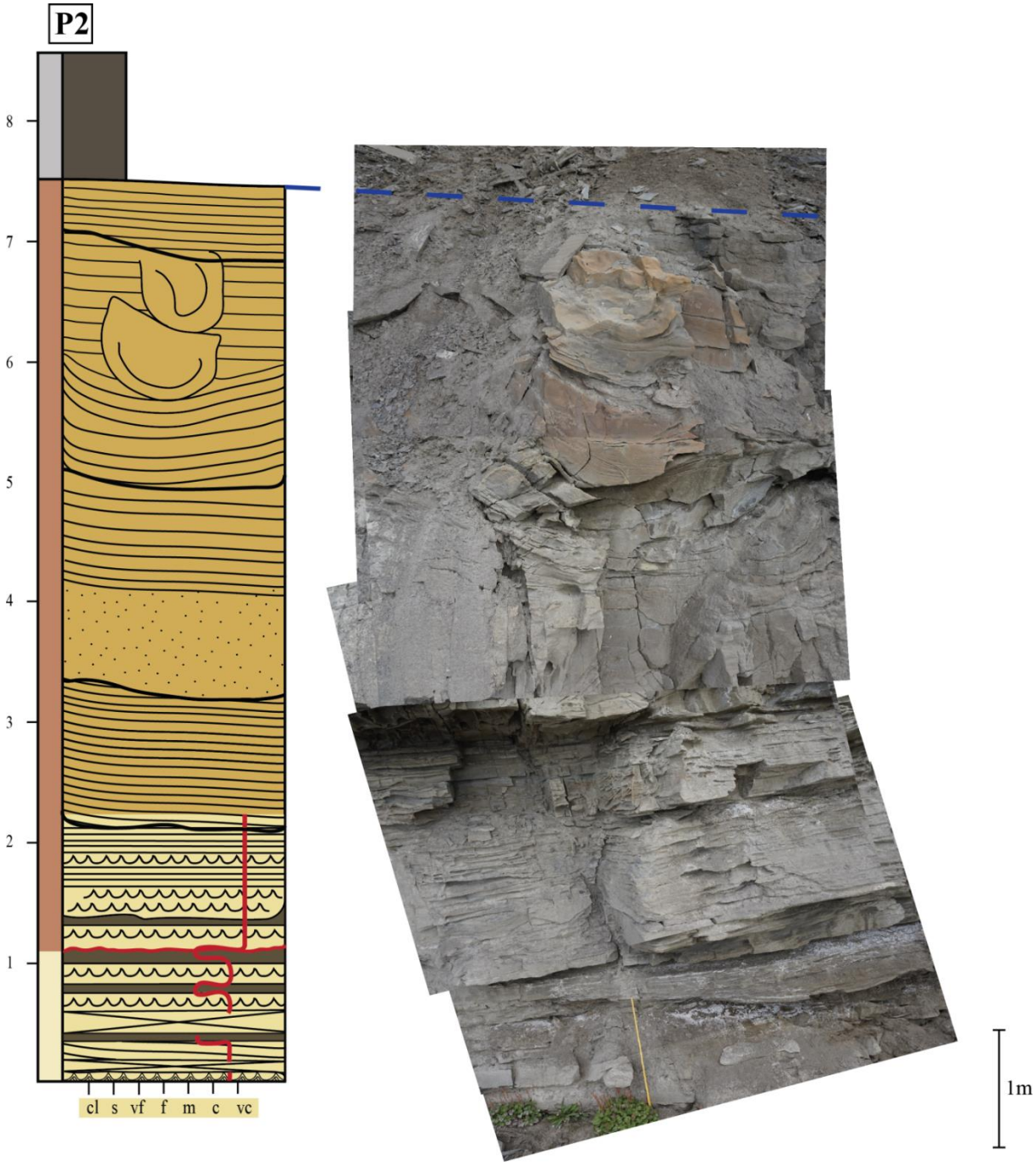
P2
8
7
6
5
4
3
2
1
cl s vf f m c vc
1m

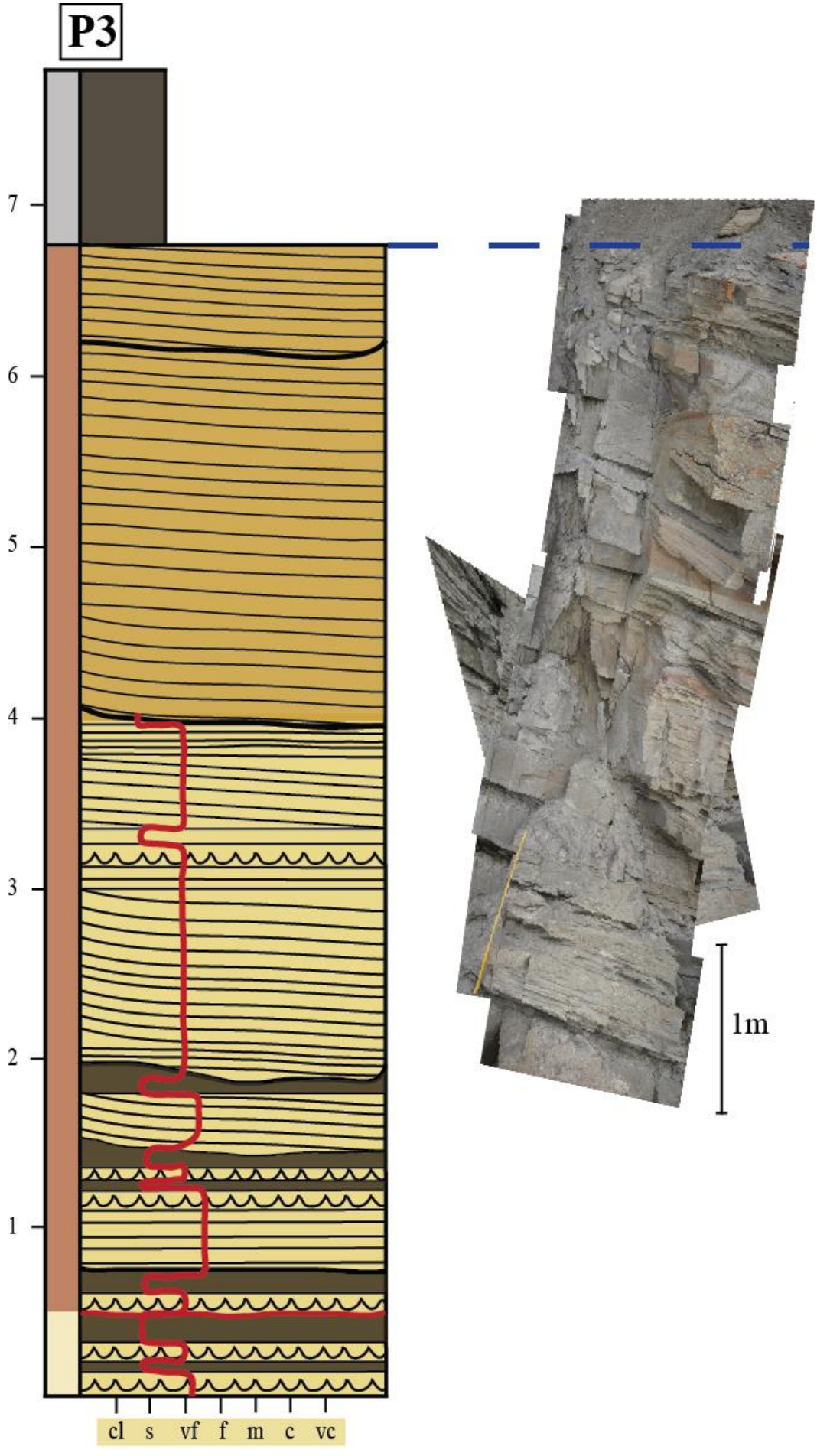
P3
7
6
5
4
3
2
1
cl
s
vf
f
m
c
vc
1m

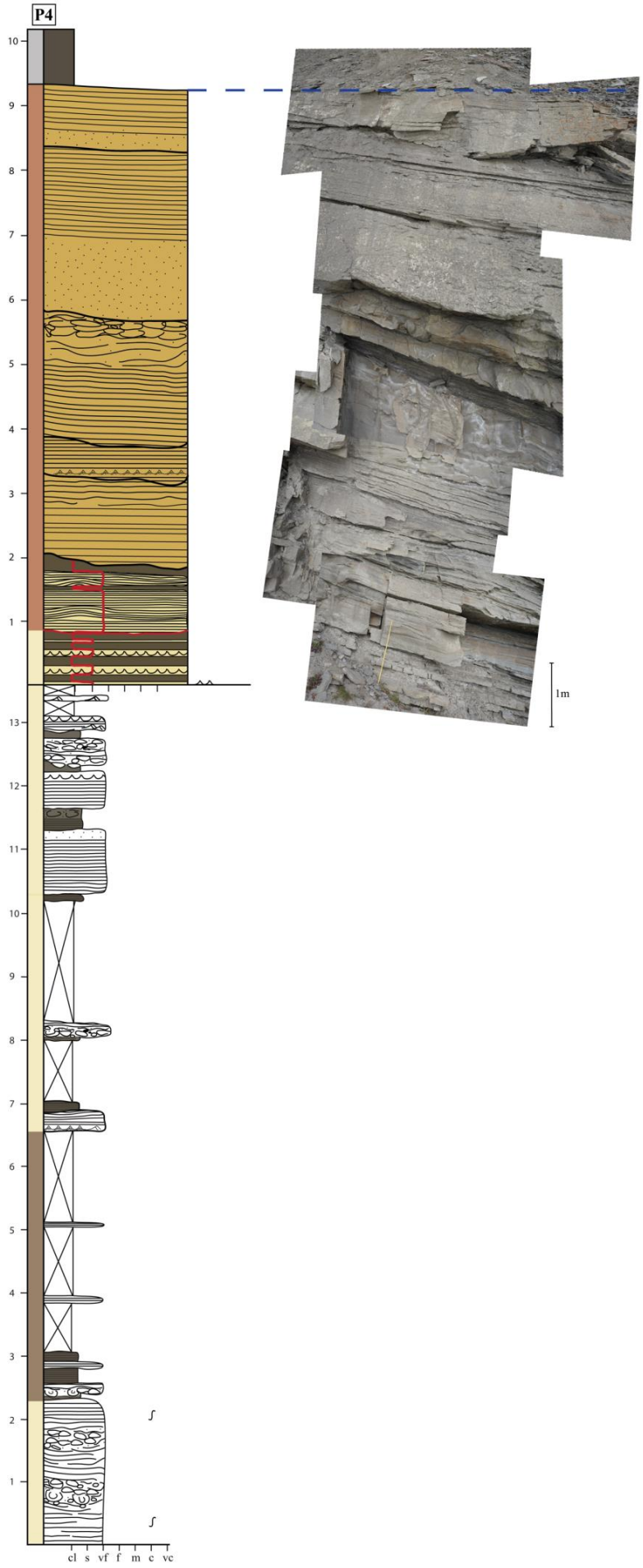
P4
1m
cl s vf f m c vc

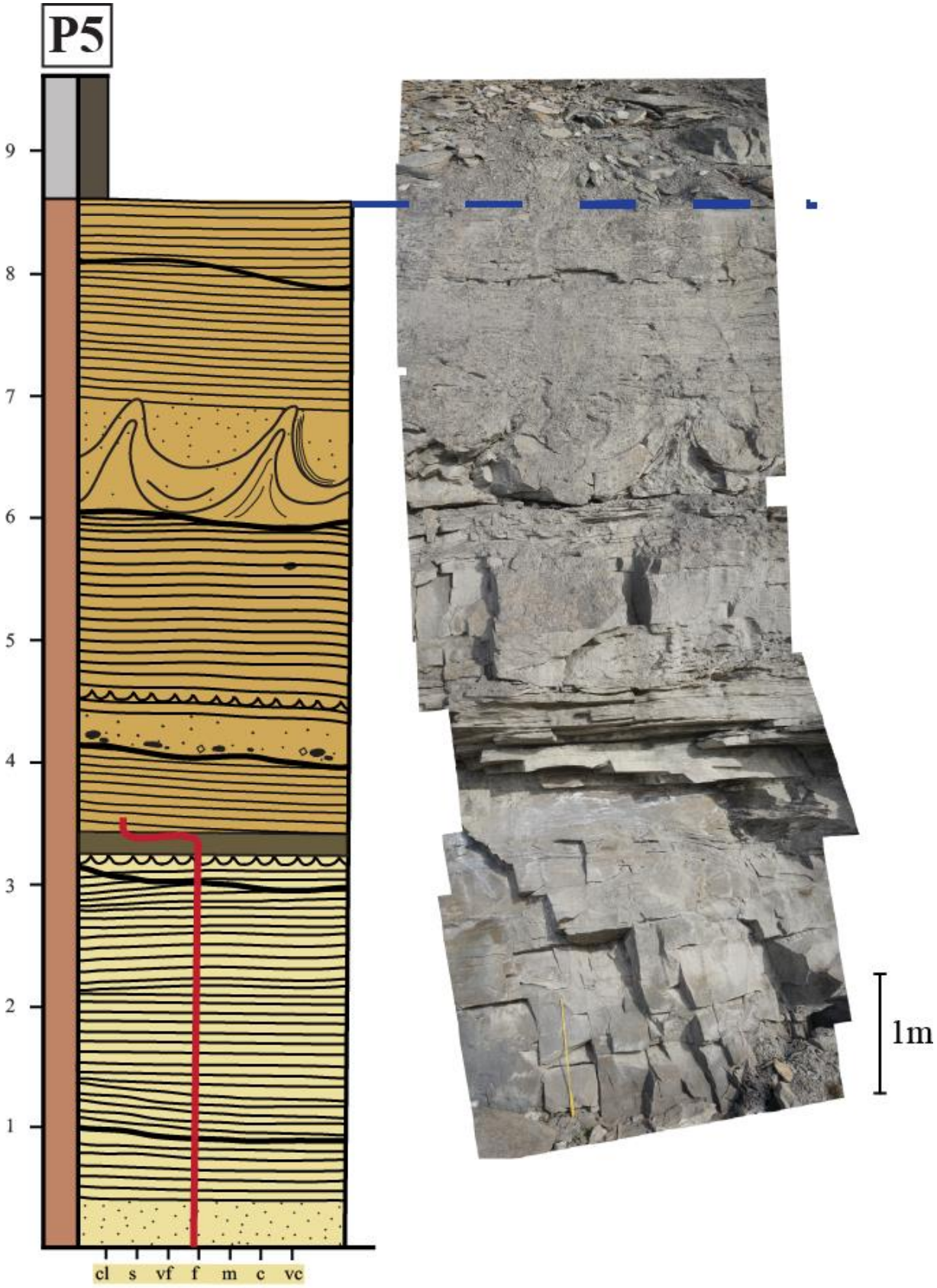
P5
9
8
7
6
5
4
3
2
1
cl
s
vf
f
m
c
vc
1m

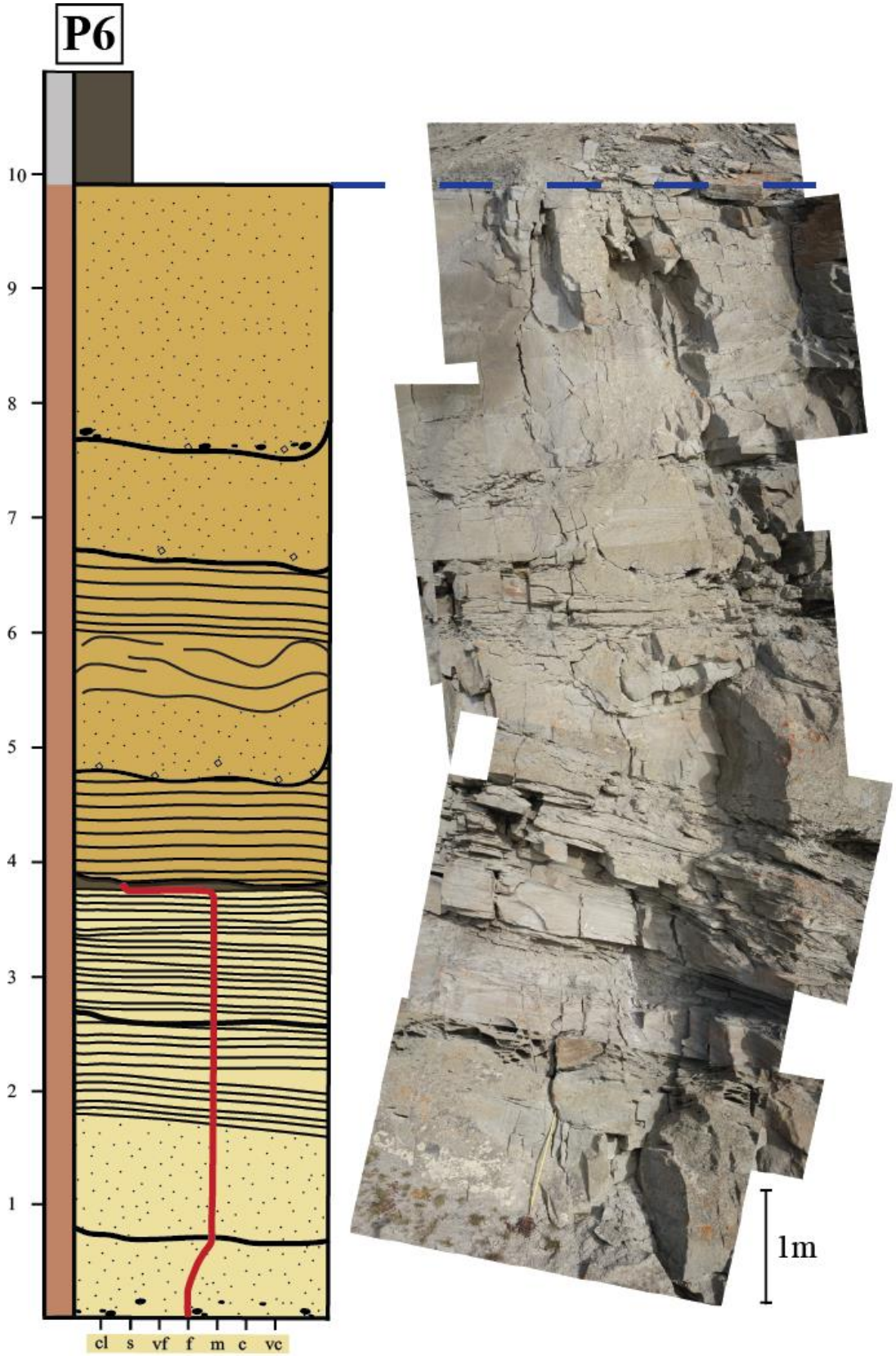
P6
10
9
8
7
6
5
4
3
2
1
cl
s
vf
f
m
c
vc
1m

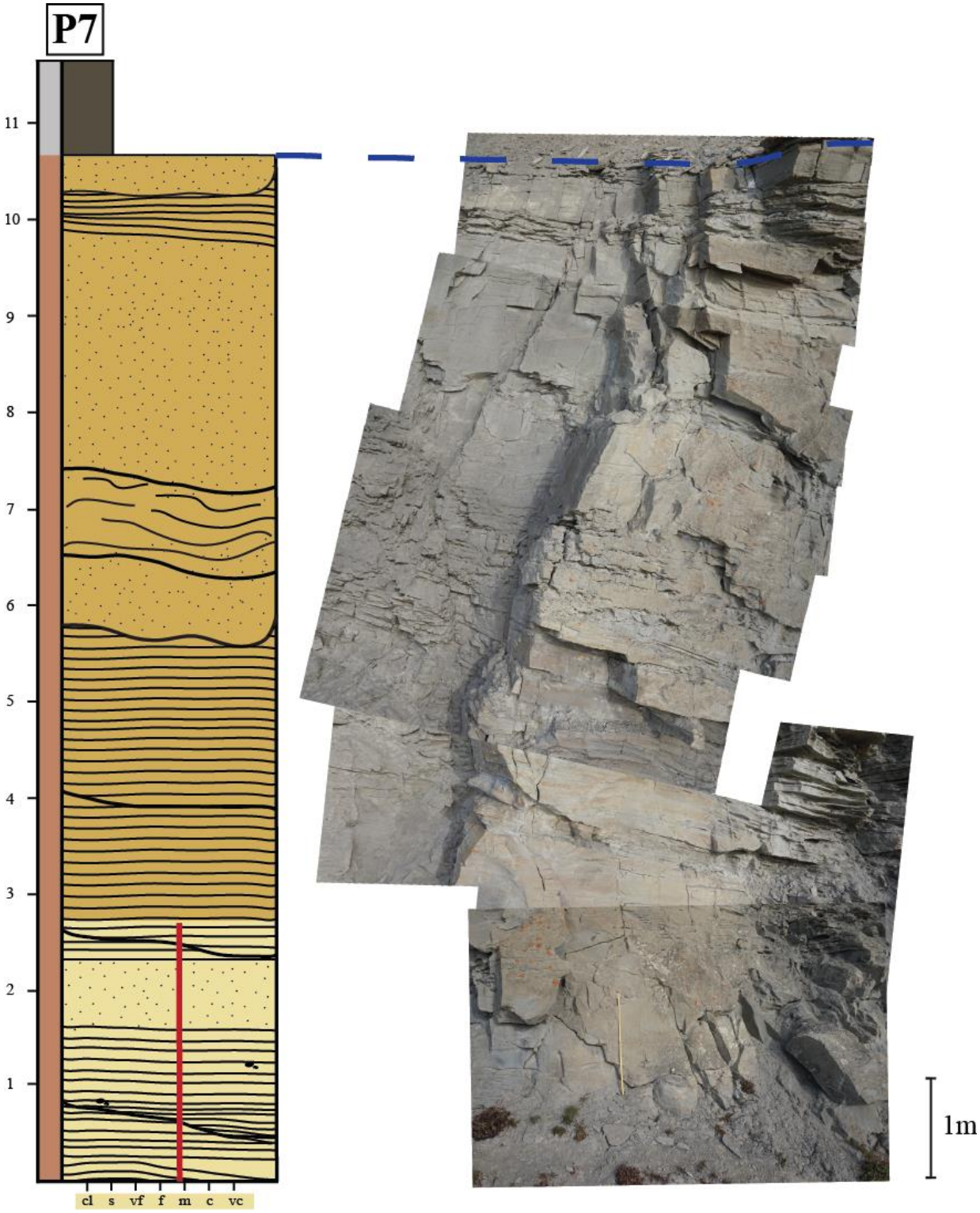
P7
11
10
9
8
7
6
5
4
3
2
1
cl s vf f m c vc
1m

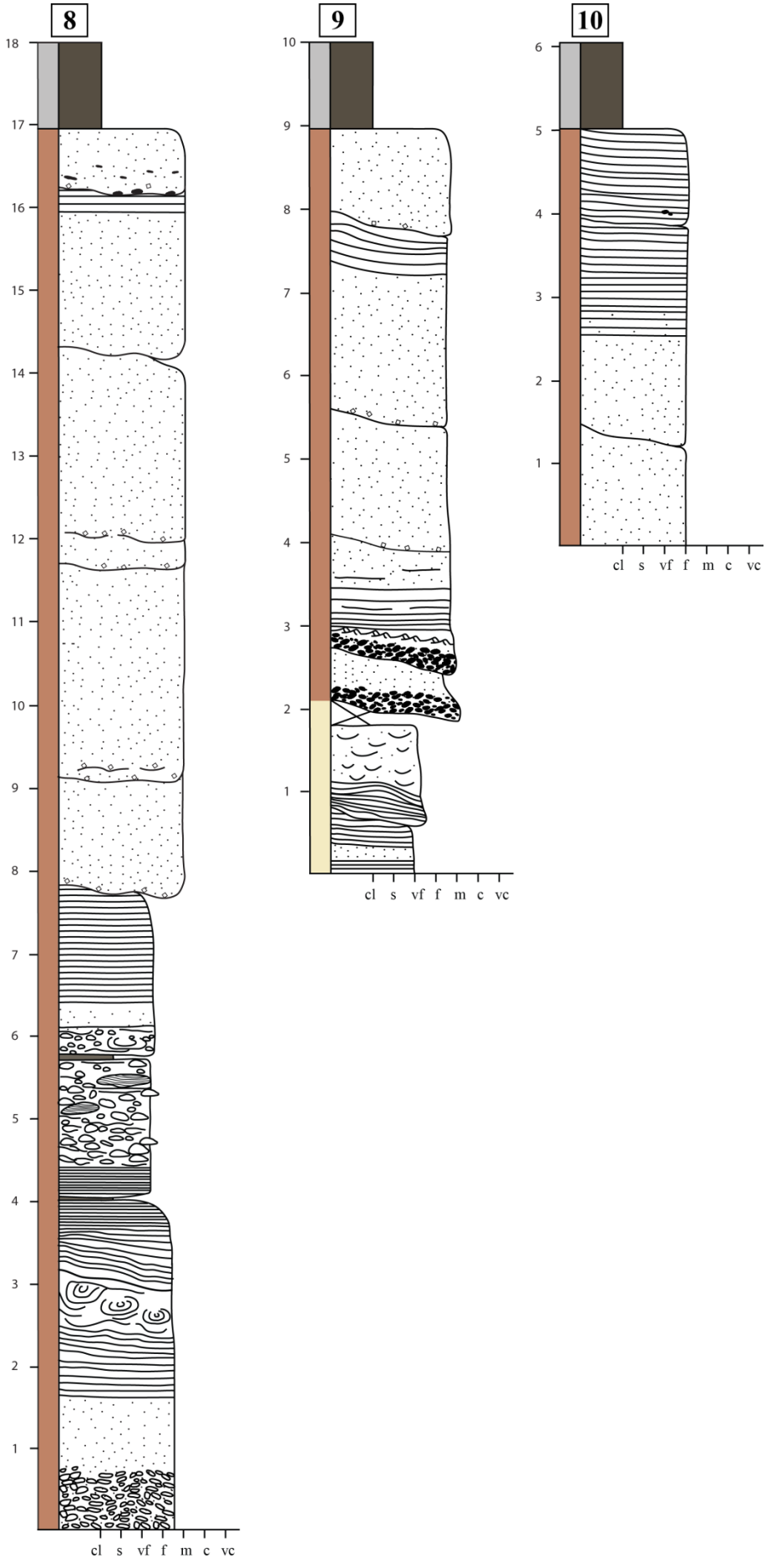
8
18
17
16
15
14
13
12
11
10
9
8
7
6
5
4
3
2
1
cl s vf f m c vc
9
10
9
8
7
6
5
4
3
2
1
cl s vf f m c vc
10
6
5
4
3
2
1
cl s vf f m c vc